NASA CR-72488
GE-RS 69SD420

MODIFICATION OF THE ONE-DIMENSIONAL REKAP PROGRAM TO ALLOW FOR CHARRING IN THREE MATERIAL LAYERS

by

R. E. Price and F. E. Schultz

prepared for

NATIONAL AERONAUTICS AND SPACE ADMINISTRATION

CONTRACT NAS 3-10285

GENERAL ELECTRIC

RE-ENTRY SYSTEMS
P.O. Box 8555 • Philadelphia, Penna. 19101

Requests for copies of this report should be referred to

National Aeronautics and Space Administration
Office of Scientific and Technical Information
Box 33
College Park, Md. 20740

NASA CR-72488
GE-RS 69SD420

FINAL REPORT

MODIFICATION OF THE ONE-DIMENSIONAL REKAP PROGRAM TO ALLOW FOR CHARRING IN THREE MATERIAL LAYERS

by

R. E. Price and F. E. Schultz

prepared for

NATIONAL AERONAUTICS AND SPACE ADMINISTRATION

January 2, 1969

CONTRACT NAS 3-10285

Technical Management
NASA Lewis Research Center
Cleveland, Ohio
Liquid Rocket Technology Branch
Erwin A. Edelman

GENERAL ELECTRIC
RE-ENTRY SYSTEMS
P. O. Box 8555 • Philadelphia, Penna. 19101

TABLE OF CONTENTS

LIST OF ILLUSTRATIONS

LIST OF TABLES

MODIFICATION OF THE ONE-DIMENSIONAL REKAP PROGRAM TO ALLOW FOR CHARRING IN THREE MATERIAL LAYERS

by

R. E. Price and F. E. Schultz

ABSTRACT

The one-dimensional Reaction Kinetics Ablation Program (REKAP) was modified in order to compute the thermal response of a ten layer body in which any or all of the first three layers may thermally degrade. The application of the modified program to one, two and three charring layer problems is described, with emphasis on a rocket nozzle throat insert case.

NOMENCLATURE

C_P	Specific heat, BTU/lb-deg. R.
C_T	Constant used in turbulent blocking-equation (Appendix A)
E	Activation energy, BTU/lb
F_{12}	Fraction of layer 2 degradation gases which flow into layer 1.
F_{23}	Fraction of layer 3 degradation gases which flow into layer 2.
H_{c_g}	Heat of gas phase chemical reaction, BTU/lb
H_{g_f}	Heat of decomposition, BTU/lb
H_r	Recovery enthalpy, BTU/lb
K	Thermal conductivity, BTU/sec ft^2deg. R./ft
K_1	Quantity used in the graphite diffusion regime mass loss equation, BTU/lb
K_2	Dimensionless quantity used in the graphite diffusion regime mass loss equation
ierfc	Integral of the complementary error function
M	Molecular weight, lb/lb-mole.
$\dot{m}_g$	Mass flux, lb/sec-ft^2
Pr	Prandtl number
$\dot{q}_c$	Convective heating rate, BTU/sec-ft^2
R	Universal gas constant, BTU/lb mole-deg. R.
T	Temperature, deg. R.
t	Time, sec.
X	Distance from front face, ft.
Z	Pre-exponential factor in equation (2)

NOMENCLATURE (Cont'd)

η	Order of thermal degradation reaction
ρ	Density, lb/ft^3

SUBSCRIPTS

AB	Ablative material
AMB	Ambient
BF	Back face
BL	Boundary layer
c	Char
FF	Front face
g	Gas
LN	Last node, i.e., node nearest back face
T	Total
VP	Virgin (un-degraded) material
W	Wall
1	First layer, i.e., layer adjacent to front face
2	Second layer
3	Third layer

1.0 INTRODUCTION

One of the dominating factors in the design of a rocket propulsion system is the ability of the exhaust nozzle wall to withstand an intense thermal environment. For some rocket missions of interest it is advantageous to employ an ablative nozzle and thereby avoid the complexity of a liquid cooled system. The design of ablative rocket nozzles is often based on empirical information drawn from rocket test firings. An experimental study of the thermal performance of a variety of ablative materials and nozzle configurations over a range of actual rocket operating conditions is a lengthy and costly process. If the physical and chemical processes which control the thermal response of an ablative rocket nozzle are adequately characterized, then such a parametric study can be performed primarily by means of high-speed computer systems. A relatively small amount of rocket test data can serve as boundary conditions for the computerized analytical solutions.

For several years the REKAP (Reaction Kinetics Ablation Program) computer program has been used by General Electric, Re-entry Systems to solve thermal design problems associated with ablative systems (for both rocket nozzles and re-entry vehicle heat shields). This program computes the temperature, density and surface recession history for a multi-layered slab of material. Charring (i.e., the in-depth gasification of the resin binder of a composite material) has been confined to the first layer, prior to the present work. For some rocket nozzle designs of interest a charring material is employed for sub-surface layers. Under the present contract, the capability of the REKAP program has been extended to allow for charring in three material layers.

2.0 SUMMARY

The one-dimensional Reaction Kinetics Ablation Program (REKAP) is modified to compute the thermal response of a ten layer rocket nozzle in which up to three layers may thermally degrade (char). The equation of conservation of energy in a charring material is re-written to allow for the flow of degradation gases from one charring layer through adjoining charring layers.

The application of the modified program to one, two and three charring layer problems is described, with emphasis on a rocket nozzle throat insert case.

Appendix A gives a detailed derivation of the equation of conservation of energy for three charring layers. Appendix B provides a program user's manual.

3.0 DISCUSSION

The primary function of the REKAP program is to compute finite-difference solutions of a conservation of energy equation which is used to describe the thermal response of an externally heated slab composed of up to ten layers of material (one of which may be a gas gap). Each layer is divided into nodal volumes ("nodes") across each of which all properties (e.g., temperature, density, chemical composition) are defined to be invariant with distance. In effect, an energy equation is solved for each node at every computation time step. A detailed derivation of the energy equation is presented in Appendix A. Reference 1 contains an analysis of the numerical techniques used in the Program.

The REKAP energy equation may be expressed as follows:

STORAGE | CONDUCTION | DECOMPOSITION | CONVECTION | GAS PHASE CHEMICAL REACTION

$$(1)\quad \rho C_P \frac{\partial T}{\partial t} = \frac{\partial}{\partial X}\left(K \frac{\partial T}{\partial X}\right) + H_{g_f} \frac{\partial \rho}{\rho t} + \overline{C}_{P_g} \dot{m}_{g_T} \frac{\partial T}{\partial X} + \overline{H}_{c_g} \dot{m}_{g_T} \frac{\partial T}{\partial X}.$$

ρ, C_P, K and T are the density, specific heat, thermal conductivity and temperature of the solid material, respectively. H_{g_f} is the heat required to decompose a unit mass of material from solid to gas. $\overline{C}_{P_g}$ is the mean specific heat of the degradation gases within a nodal volume. $\overline{H}_{c_g}$ is the heat which may be absorbed or released due to chemical reactions between the gases which may be present within a "node". $\dot{m}_{g_T}$ is the total mass flux of the degradation gases which flow through a node toward the front surface.

The thermal conductivity, K and the specific heat C_P, of a charring material are both temperature and density dependent so that the values of K and C_P within a node are determined by the instantaneous values of T and ρ for that node.

In order to evaluate the rate of heat conduction ($K\ \partial T/\partial X$) into a body at the front surface, an energy flux balance is performed. In other words, the total heat flux toward the surface is balanced against the total flux away from the surface. The REKAP program provides for surface heating due to convection, radiation and chemical reaction (e.g., combustion in an adjacent gaseous boundary layer). Surface cooling mechanisms include re-radiation, heat absorption due to melting or vaporization, the "blocking" of convective heating due to surface out-gassing and finally, heat conduction into the solid body ($K\ \partial T/\partial X$).

For a charring material REKAP computes the rate of change of material density by means of an Arrhenius relation of the form:

$$(2)\quad \frac{\partial \rho}{\partial t} = -\rho_{VP}\left(\frac{\rho-\rho_C}{\rho_{VP}}\right)^{\eta} \Sigma_i Z_i e^{-E_i/RT}$$

in which the subscripts "VP" and "C", respectively designate virgin (i.e., uncharred)

material and completely charred material. ρ and T are the instantaneous local values of solid material density and temperature. It was assumed that the degradation process within a particular layer is negligibly affected by the presence of gases which have originated in another layer. This assumption is judged to be reasonable because within any charring layer the degradation process is essentially complete, on a mass basis, prior to the entry of gases from a sub-layer. For example, gas cannot flow from layer two into layer one (the layer adjacent to the front surface) unless the intervening solid material is porous, which is the case only when the material near the backface of layer one is charred. Therefore, Z, E and η of equation (2) and H_{g_f} of equation (1) are functions only of the material within a given layer.

The gas mass flux $\dot{m}_{g_T}$ is the total mass flux of the gases which may flow through a node, regardless of their origin. Within their layer of origin, the mass flux of degradation gases evaluated at depth X is given by:

$$\dot{m}_g = -\int_{X_{FF}}^{X_{BF}} \left(\frac{\partial \rho}{\partial t}\right) dx, \tag{3}$$

in which "BF" denotes the backface of the layer and $\partial\rho/\partial t$ is computed according to equation (2). The minus sign in equation (3) is required because the degradation gases flow toward the surface (i.e., in the minus X direction). The total mass flux through a node is expressed as follows for layers one, two and three, respectively:

$$\left(\dot{m}_{g_T}\right)_1 = \dot{m}_{g_1} + F_{12} \cdot \dot{m}_{g_{2_{FF}}} + F_{12} \cdot F_{23} \cdot \dot{m}_{g_{3_{FF}}}, \tag{4}$$

$$\left(\dot{m}_{g_T}\right)_2 = \dot{m}_{g_2} + F_{23} \cdot \dot{m}_{g_{3_{FF}}} \quad \text{and} \tag{5}$$

$$\left(\dot{m}_{g_T}\right)_3 = \dot{m}_{g_3} . \tag{6}$$

F_{12} represents the fraction (by mass) of the gases generated within layer two which flow into layer one. Similarly, F_{23} is the fraction of layer three gases which flow into layer two. These fractions are computed as follows:

$$F_{12} = \frac{\rho_{VP_1} - \rho_{LN_1}}{\rho_{VP_2} - \rho_{c_1}} \quad \text{and} \tag{7}$$

$$F_{23} = -\frac{\rho_{VP_2} - \rho_{LN_2}}{\rho_{VP_2} - \rho_{c_2}} . \tag{8}$$

The subscripts 1 and 2 signify layers one and two, respectively. LN refers to the node at the back of a layer. A rapid change in the heat flux to the front face of layer one will cause a considerably slower change in the backface temperatures of layers one and two for typical charring materials and layer thicknesses. Since the time rates of change of F_{12} and F_{23} depend on $(\partial\rho/\partial t)_{LN_1}$ and $(\partial\rho/\partial t)_{LN_2}$ respectively (ρ_{VP} and ρ_c are constants), the rate of change of the flow rate of degradation gases from one layer into another is relatively insensitive to rather sudden changes in the heating rate from the external environment to the front face. Therefore, it is unlikely that time variations of F_{12} and F_{23} will significantly contribute to mathematical instability in the finite difference solution of the energy equation. Another section of the present report presents the results of a REKAP run which serves to confirm this conclusion.

In solving the energy equation (1) for a particular node and time step, the specific heat and the heat of chemical reaction, $\overline{C}_{P_g}$ and $\overline{H}_{c_g}$ respectively, must be evaluated for the mixture of layer one, two and three gases which may reside in the node over that time interval. $\overline{C}_{P_g}$ and $\overline{H}_{c_g}$ are calculated on a mass fraction basis as follows:

$$(9)\qquad \left(\overline{C}_{P_g}\right)_1 = \left(C_{P_{g_1}} \cdot \dot{m}_{g_1} + F_{12} \cdot C_{P_{g_2}} \cdot \dot{m}_{g_{2_{FF}}} + F_{12} \cdot F_{23} \cdot C_{P_{g_3}} \cdot \dot{m}_{g_{3_{FF}}}\right) \Big/ \left(\dot{m}_{g_T}\right)_1 ,$$

$$(10)\qquad \left(\overline{C}_{P_g}\right)_2 = \left(C_{P_{g_2}} \cdot \dot{m}_{g_2} + F_{23} \cdot C_{P_{g_3}} \cdot \dot{m}_{g_{3_{FF}}}\right) \Big/ \left(\dot{m}_{g_T}\right)_2 ,$$

$$(11)\qquad \left(\overline{C}_{P_g}\right)_3 = C_{P_{g_3}} ,$$

$$(12)\qquad \left(\overline{H}_{c_g}\right)_1 = \left(H_{c_{g_1}} \cdot \dot{m}_{g_1} + F_{12} \cdot H_{c_{g_2}} \cdot \dot{m}_{g_{2_{FF}}} + F_{12} \cdot F_{23} \cdot H_{c_{g_3}} \cdot \dot{m}_{g_{3_{FF}}}\right) \Big/ \left(\dot{m}_{g_T}\right)_2 ,$$

$$(13)\qquad \left(\overline{H}_{c_g}\right)_2 = \left(H_{c_{g_2}} \cdot \dot{m}_{g_2} + F_{23} \cdot H_{c_{g_3}} \cdot \dot{m}_{g_{3_{FF}}}\right) \Big/ \left(\dot{m}_{g_T}\right)_2 , \text{ and}$$

$$(14)\qquad \left(\overline{H}_{c_g}\right)_3 = H_{c_{g_3}} .$$

$H_{c_{g_1}}$ applies only to chemical reactions which may take place between gases which are generated in layer one. $H_{c_{g_2}}$ and $H_{c_{g_3}}$ have the analogous meanings for layers two and three. Therefore, the form of relations (12) and (13) implies that chemical reactions between the gaseous degradation products from any layer are negligibly affected by the presence of gaseous species which are generated within another layer. This assumption is considered to be valid because no gas can flow from layer two into layer one (or from layer three into layer two) until layer one is almost totally degraded. That is, no "foreign" gases are admitted to a layer until its back node chars (note the dependence of F_{12} and F_{23} on ρ_{LN_3} and ρ_{LN_2}, respectively). After they escape from a given layer, degradation gases may continue to react among themselves according the the H_{c_g} of their layer of origin. The H_{c_g} for each charring layer is input to the program in a temperature-dependent table to encompass the full range of temperature to which gaseous degradation products may be exposed (whether they remain in one layer or flow into other layers).

For some configurations of interest a non-charring (and hence non-porous) material may be sandwiched between charring layers or between a charring layer and the front surface of layer one. In these cases, degradation gases are impeded from flowing to the surface. It was assumed that these gases leave the system at the charring/non-charring interface. The corresponding rate of energy loss from the system can be expressed as follows for a charring layer:

$$\text{(15)} \qquad \text{Loss} = C_{P_g} \dot{m}_g (T_{FF} - T_{AMB})$$

where T_{AMB} is the temperature of the surroundings into which the gases escape. It can be conjectured that in these situations there may be a sub-surface pressure build-up sufficient to cause mechanical failure or to alter degradation kinetics. An analysis of these effects was outside the scope of the present contract requirements.

The recession rate due to mass removal at the surface is calculated according to any one of a variety of analytical models which are based on the aerothermochemical inter-action between the surface and its environment. Within the REKAP program a co-ordinate transformation is made so that the nodes in the first material layer (recession is limited to the first layer) shrink in size as the surface ablates (nodes are not "dropped").

3.1 Application of the Modified Program

In order to test the three-charring layer REKAP program, three sets of computer runs were made. The first group of (nine) test cases served to establish that the modified program and the previous program produce identical results for problems which do not involve charring past the first material layer. The second set of check runs is concerned with the prediction of the thermal response of a rocket nozzle throat insert

upon exposure to two different rocket engine firing cycles. The final group of (three) test computer runs deals with two and three charring layer problems. Copies of the computed results for all the test cases have been delivered to the NASA Lewis Research Center in Cleveland, Ohio.

3.1.1 Input Data for Rocket Throat Insert Cases

A description of the throat insert and of the pertinent rocket engine operating characteristics are presented in Table 1. It is noted that the conditions for Test 1 and Test 2 are identical except for the oxidizer/fuel ratio and the firing cycle. With respect to the REKAP program, Test 2 includes all the essential features of Test 1, in addition to a greater variation in heating environment. Therefore, with regard to the rocket insert computations it seems appropriate to concentrate discussion on the REKAP runs for Test Case 2.

TABLE 1. ROCKET THROAT INSERT TESTS

TEST 1	
Insert	JTA Graphite, 0.514 inch thick at nozzle throat
Backup Material	Fiberite MX2641 Ablative, 1.386 inch thick at throat
O/F	1.6
Pc	100 psia
Rocket Cycle	206 seconds firing, followed by cool-down to ambient
Propellant	N_2O_4/50% N_2H_4 - 50% UDMH
TEST 2	
Insert	*
Backup Material	*
O/F	2.0
Pc	*
Rocket Cycle	99 seconds firing, cool-down to ambient, followed by 170 seconds firing and cool-down to ambient
Propellant	*

*Same as for Test 1

As presented in Table 1, the rocket throat insert consists of a layer of JTA graphite over a layer of Fiberite MX2641 ablative material. The properties of JTA graphite are given in Figure 1. The thermal properties used for Fiberite MX2641 are presented in Table 2 and in Figure 2. The values given for Hg_f, Hc_g, Cp_g, Z_1, Z_2, Z_3, E_1, E_2 and E_3 apply to refrasil phenolic materials having a thirty percent resin content (to which class Fiberite MX2641 belongs). The Fiberite thermal conductivity for temperatures up to 750 degrees Fahrenheit is found in Reference 2. For higher temperatures it was assumed that the conductivity-temperature dependence is similar to that presented in Reference 3 for silica phenolic materials.

TABLE 2. REKAP PROPERTIES FOR FIBERITE MX2641

Item	Value	Reference
H_{g_f}	400 BTU/lb	4
C_{P_g}	0.6 BTU/lb deg. R	4
H_{c_g}	0	4
M^1	30 lb/lb mole	5
Z_1, Z_2, Z_3	10^{-4}, 1300, 10^6 sec^{-1}	4
E_1, E_2, E_3	1200, 33500, 56040 BTU/lb-mole	4
ρ_{VP}	112 lb/ft^3	6
ρ_c	94.3 lb/ft^3 (assumed that ρ_c/ρ_{VP} is the same as for 30% resin phenolic refrasil)	
η	2	4, 5
Chart (5)[2]	1	4
Chart (6)[2]	-0.4	4
Chart (7)[2]	1	4
Chart (8)[2]	0.4	4
$\frac{M_{BL}}{M_{ABL}}^1$	1	4
Pr^1	.7	
C_T^1	1	4

[1] See Appendix A

[2] See Appendix B

The rocket throat insert is initially at ambient temperature. Almost instantaneously after ignition of the oxidizer-fuel mixture, the throat insert is exposed to the hot (~ 5000 deg R) combustion gases. The insert temperature response for this starting transient was computed by the program using an approximate analytic solution of the equation of one-dimensional heat conduction in a semi-infinite slab having constant thermal properties and constant heat flux at the surface (References 7 and 8):

$$(16) \qquad \Delta T = \frac{2\dot{q}}{\sqrt{K\rho C_p}} \left[\sqrt{t}\ \text{ierfc} \left(\frac{X}{2\sqrt{\Delta t}} \sqrt{\frac{\rho C_p}{K}} \right) \right]$$

in which ΔT is the temperature rise at depth X for surface heating duration Δt. The applicability of equation (16) depends on the validity of the "semi-infinite slab" (i.e., $\Delta T_{BF} = 0$) and the "constant thermal properties" assumptions. For equation (16) the maximum backface temperature rise for the JTA layer would take place for the cold wall heat flux and the room temperature value of $\rho C_p/K$. Figure 3 shows the maximum backface ΔT plotted versus Δt. For the REKAP run a Δt of 0.15 seconds was chosen (maximum backface ΔT = 2.5 deg R). The error in surface temperature was less than 5 percent as a result of the "constant thermal properties" assumption. The full finite-difference energy equation solution could be used, but this would require initial computation time steps considerably smaller than 0.15 seconds and involve more computer operations to achieve essentially the same result as provided by the analytic solution.

The convective heat transfer coefficient at the rocket nozzle throat was calculated according to the formulation given in Reference 9. The thermal properties in the throat boundary layer were evaluated at the reference temperature stated by Summerfield (Reference 9) to give "the best correlation of experimental results":

$$(17) \qquad T_{REF} = T_W + 0.23\,(T_g - T_W) + 0.19\,(T_r - T_W), \text{ which approaches}$$

$$(18) \qquad T_{REF} = \frac{T_W + T_g}{2} \text{ as the Mach number approaches zero.}$$

A temperature recovery factor of 0.91 was used, according to Summerfield's experimentally based estimation for a compressible turbulent boundary layer in a rocket nozzle. The boundary layer edge conditions were determined by utilizing an equilibrium Mollier diagram for N_2O_4/50 percent hydrazine - 50 percent UDMH (Reference 10) and assuming an isentropic expansion process from the rocket combustion chamber to the throat. The thermodynamic and transport properties and the combustion chamber temperature were obtained from Reference 11. The final results of the heat transfer coefficient calculation are:

> For O/F = 2.0, $\dot{q}_c/(T_R - T_W)$ = 0.163 BTU/sec ft^2 deg R, which corresponds to $\dot{q}_c/(h_r - h_w)$ = 0.233 BTU/sec ft^2/BTU/lb. The heat transfer coefficient for O/F = 1.6 was taken to be essentially the same as for O/F = 2.0.

The heat transfer coefficient as calculated above is approximately 65 percent lower than that calculated using the simplified Bartz equation (Reference 12). In his derivation Bartz states: "If it is allowed that C_p and Pr do not vary appreciably with temperature, they can be assumed constant at stagnation temperature values...." In Bartz' equation the heat transfer coefficient is proportional to $(C_p/Pr)^{0.6}$. Figure 4 shows the variation of $(C_p/Pr)^{0.6}$ with temperature. If Bartz' equation (3) is used (variable C_p and Pr) the resulting value of the heat transfer coefficient differs by less than 10 percent from the value given above.

3.1.2 Computed Results for Rocket Throat Insert

Figures 5 and 6 show typical REKAP results for the in-depth temperature history of the rocket throat insert during firing and cool-down, respectively. Figure 7 presents the wall temperature history as well as the front and back face temperature history for the Fiberite back-up material. Figure 8 gives the density profile history for the Fiberite layer. The specifications for the REKAP test case (see Table 1) require that the throat insert thermal response be computed for "cool-down to ambient". Figure 8 shows that very little thermal degradation occurs after t = 300 seconds. The REKAP program predicts that there will be no further degradation after t = 700 seconds. Figure 9 presents the history of degradation gas flow rate at the front surface of the Fiberite sub-layer.

Experimental measurements of rocket throat surface recession are compared with REKAP results in Figure 10. In order to develop an adequate model for surface recession it is necessary to solve the chemistry problem at the surface between graphite and the N_2O_4/UDMH-hydrazine combustion gases. Such chemical analysis was outside the scope of the present contract. However, the REKAP model for the recession of graphite was adjusted to obtain an agreement with the experimental values. The REKAP surface temperature results (2000-5000 deg R) indicate that the process of diffusion of oxygen-bearing species to the surface would predominate for an <u>air</u> boundary layer. For this regime the REKAP equation of surface recession is:

$$(19) \qquad \dot{S}_m = \frac{1}{\rho_{surface}} \frac{\dot{q}_c}{(K_1 + K_2 (H_r - C_{P_{BL}} T_W)} \qquad \dot{}$$

in which, $\dot{S}_m$ is the surface recession rate, $\dot{q}_c$ is the convective heating rate, H_r is the recovery enthalpy, $C_{P_{BL}}$ is the mean specific heat of the boundary layer gases, T_W is the wall temperature, and K_1 and K_2 are quantities which depend upon the diffusion process. Equation (19) suggests that $K_1 + K_2 (H_r - C_{P_{BL}} TW)$ may be interpreted as a "hot wall effective heat of ablation". It was assumed that in the $(H_r - C_{P_{BL}} TW)$ range of interest $K_1 = 0$. Measurments of the slope of curves of experimental throat recession distance versus time and theoretical values of $\dot{q}_c$, H_r, $C_{P_{BL}}$ and TW (previous REKAP results) were employed with equation (19) to obtain effective values of K_2. This approach may be useful in predicting the recession of graphite in the N_2O_4/UDMH-hyrazine environment for other nozzles.

3.1.3 Computed Results for Two and Three Charring Layers

A group of two and three charring layer test cases was devised. No attempt was made to analyze multi-layer configurations of existing materials. Instead, material properties were tailored to provide a rigorous test of the present REKAP modifications. That is, the thermal conductivities and degradation coefficients (Z and E in equation 2) were chosen to allow a considerable degree of sub-layer charring and inter-layer flow of degradation gases.

Figures 11 and 14, respectively give the in-depth density profile history for a two and a three charring layer problem. Figures 12 and 15 present the corresponding histories of the inter-layer gas flow control factors F_{12} and F_{23} which are defined in equations (7) and (8) of this report. Figures 12 and 15 demonstrate that the admission of gases from one layer into another is accomplished smoothly with respect to time. Thus the finite difference solution of the energy equation is preserved from any sudden changes and a potential source of mathematical instability is suppressed. Figures 13 and 16 show the flow rates of degradation gases at the front face of their respective layers of origin. For example, the curve labeled "Layer 2" in Figure 13 gives the flow rate of the gases which are generated within layer 2, evaluated at the front face of layer 2. The "Total at the Front Face" curve shows the value of the gas mass flux at the front surface as given by equations (4), (5) and (6). This is the mass flux which is used in the calculation of the "blocking" of convective heating (see Appendix A).

4.0 CONCLUSIONS AND RECOMMENDATIONS

The Reaction Kinetics Ablation Program (REKAP) has been modified to account for simultaneous thermal degradation in any or all of the first three layers in a ten layer composite.

The modified program was used to predict the thermal response of a nozzle throat insert in an N_2O_4/UDMH-hydrazine rocket having a combustion chamber pressure of 100 psia and a throat diameter of 1.2 inches. The throat insert consists of a layer of JTA graphite backed by Fiberite MX2641 ablative material. The REKAP results indicate that the JTA graphite attains a steady-state surface temperature of approximately 5000 deg R after 30 seconds of rocket firing. After 99 seconds of firing the Fiberite temperature remains below 700 deg R at a depth of 0.5 inch (measured from the graphite back face) and the "char depth" (the depth at which the density equals 97 percent of the virgin material density) is approximately 0.25 inch. During 600 seconds of cool-down, the graphite temperature decreases from 5000 to 1000 deg R while the back face temperature of the Fiberite rises to approximately 600 deg R. Fiberite thermal degradation is essentially complete after 200 seconds of cool-down, when the char depth is 0.35 inch. After 600 seconds of cool-down the rate of degradation is approximately zero and the char depth is 0.36 inch.

The surface recession history of JTA graphite in an N_2O_4/UDMH-hydrazine environment can be adequately described if the proper surface chemistry constants are used in conjunction with the REKAP program. It is recommended that a boundary layer-surface chemistry computer program be used to develop surface recession models for rocket nozzle flow environments. A set of surface recession parameters for a range of pressure, temperature and O/F ratio could be derived for each surface material and oxidizer-fuel system of interest.

REFERENCES

1. Gordon, Paul, "Analysis of the One-Dimensional Heat Conduction Computer Program", General Electric Company Missile and Space Division Report R66SD10, March 1966.

2. Pears, C. D., Engelke, W. J., and Thornburgh, J. D., "The Thermal and Mechanical Properties of Five Ablative Reinforced Plastics from Room Temperature to 750 Degrees F.", Southern Research Institute Technical Report No. AFML-TR-65-133, April 1965.

3. Cline, P. B., and Schultz, F. E., "Investigation of the Effect of Material Properties on Composite Ablative Material Behavior",General Electric Company Re-entry Systems Department Final Report, NASA Lewis Research Center Contract NAS3-6291, NASA Report No. CR-72142, April 17, 1967.

4. Bueche, J., and LaMonaca, T., "Thermal Properties: Supplement V", General Electric Company PIR-TPSD-8151-799, May 1, 1967.

5. Bueche, J., "Thermal Properties: Supplement I", General Electric Company PIR-TPSD-8151-585, June 16, 1966.

6. Fiberite MX2641 Material Specification, Fiberite Corp., April 1, 1963.

7. Carslaw, H. S., and Jaeger, J. C., "Conduction of Heat in Solids", Oxford University Press, 1959.

8. Nolan, E. J., and Young, J. P., "Graphical and Analytical Solutions to Certain Transient Aerodynamic Heat Conduction Problems", General Electric Company Missile and Space Division Report R60SD310, February 1960.

9. Summerfield, Martin, "The Liquid Propellant Rocket Engine", in Liquid Propellant Rockets, ed. by C. DuP. Donaldson, Princeton Aeronautical Paperbacks, Princeton University Press, 1960.

10. Rindal, R. A., Flood, D. T., and Kendall, R. M., "Analytical and Experimental Study of Ablation Material for Rocket Engine Application", Vidya Report No. 136, March 17, 1964.

11. Private communication from L. D. Plewes (NASA Lewis Research Center).

12. Bartz, D. R., "A Simple Equation for Rapid Estimation of Rocket Nozzle Heat Transfer Coefficients", Jet Propulsion, January 1957.

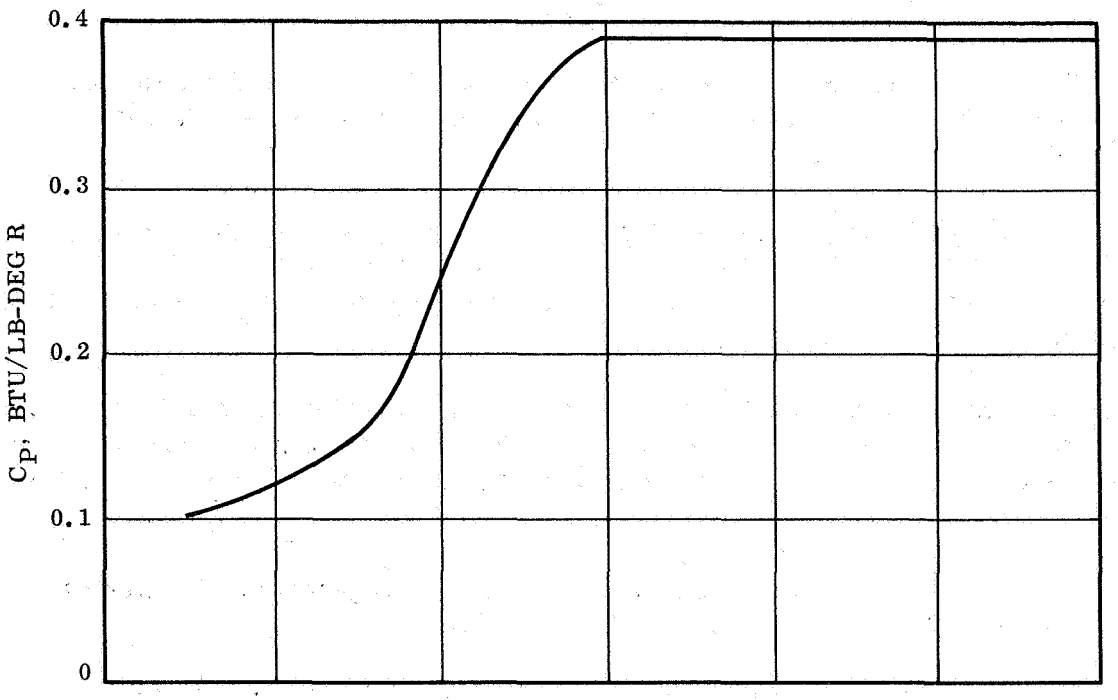

REFERENCE 5

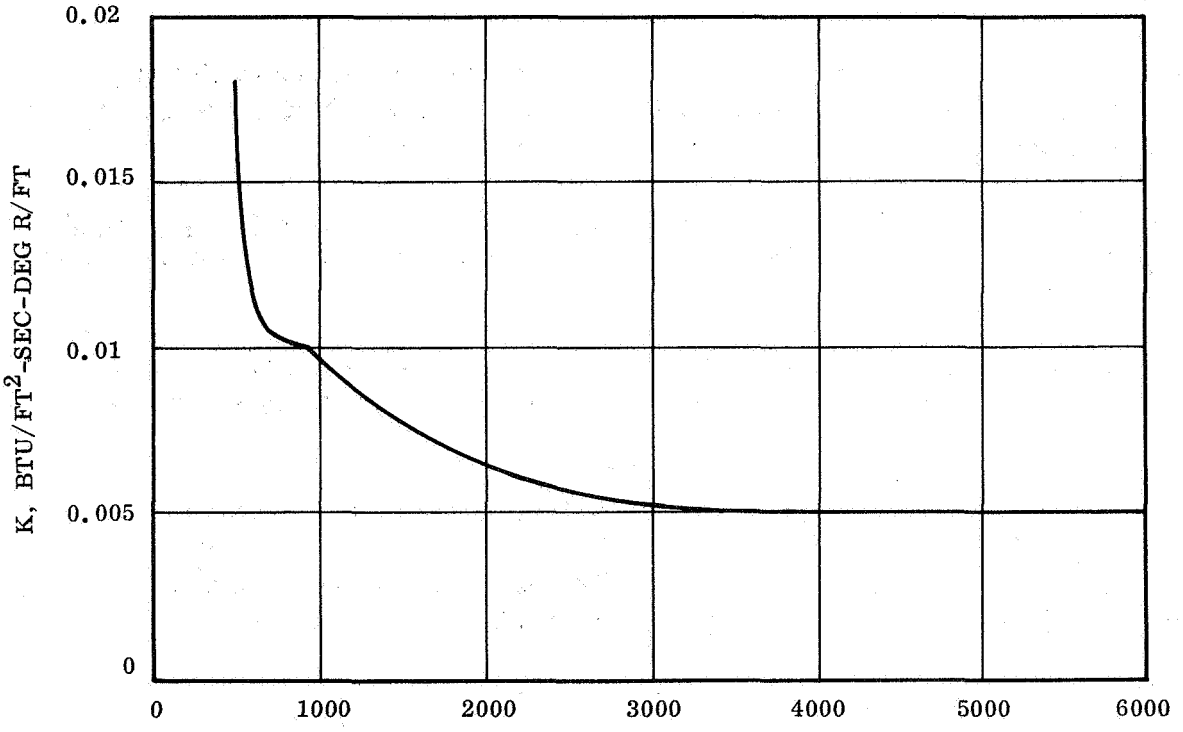

Figure 1. JTA Graphite Thermal Properties

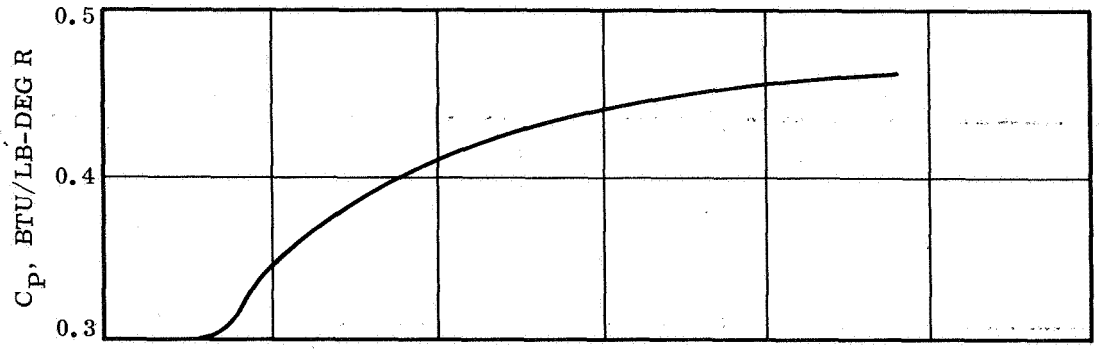

REFERENCES 2, 3 AND 4

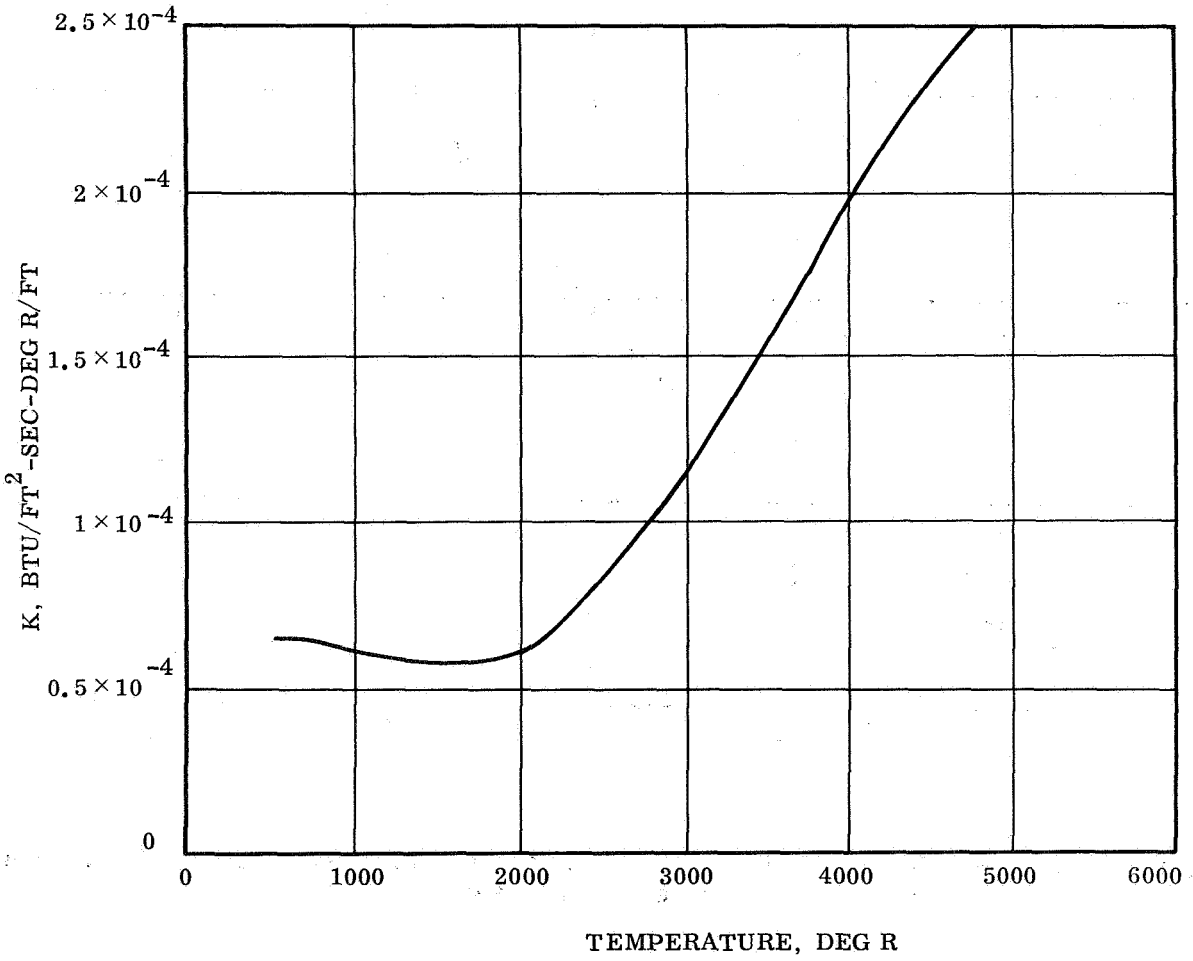

Figure 2. Fiberite MX2641 Thermal Properties

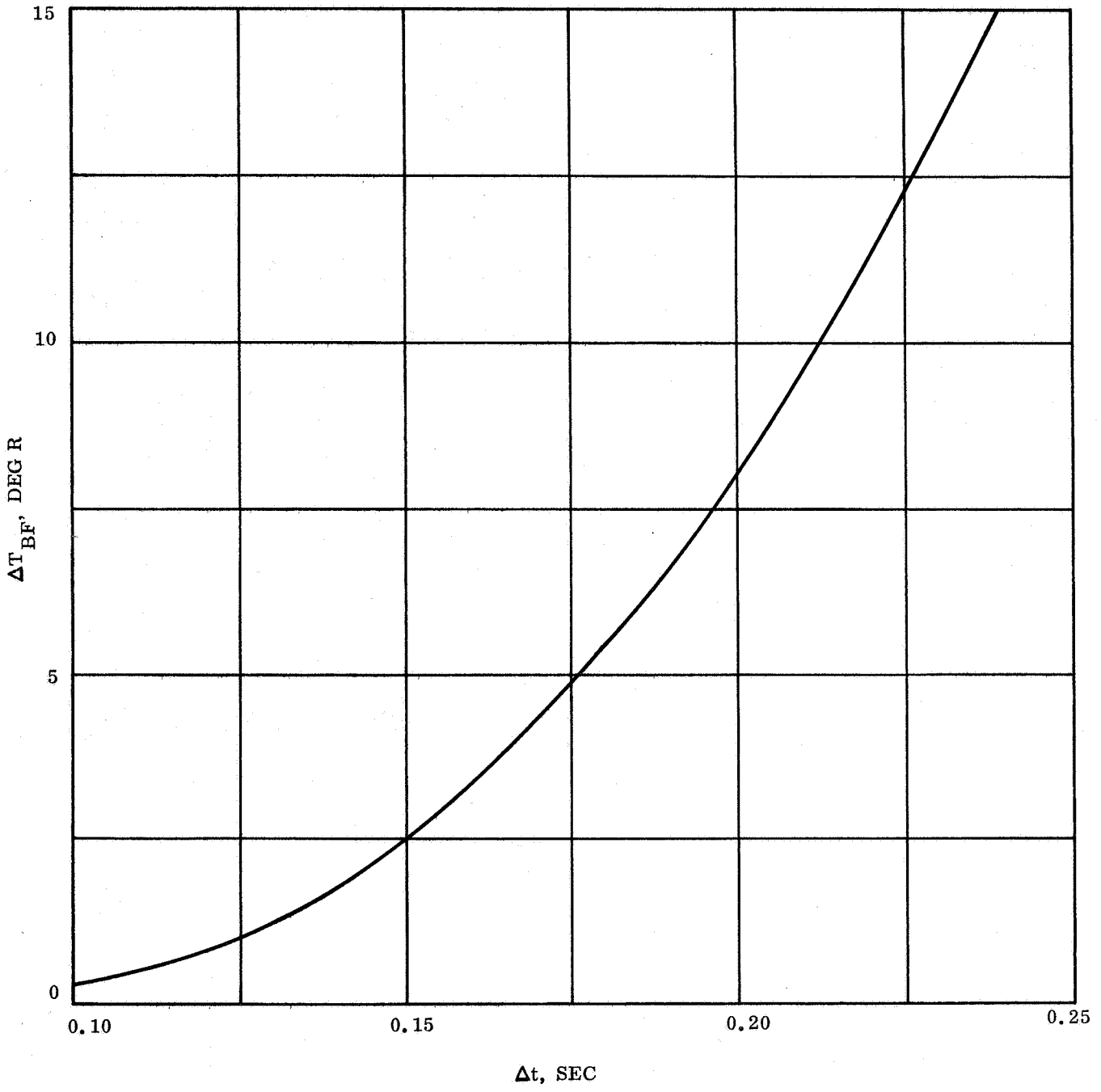

Figure 3. Validity of Semi-infinite Slab Assumption for Initial Heat Pulse to JTA Graphite Rocket Throat Insert

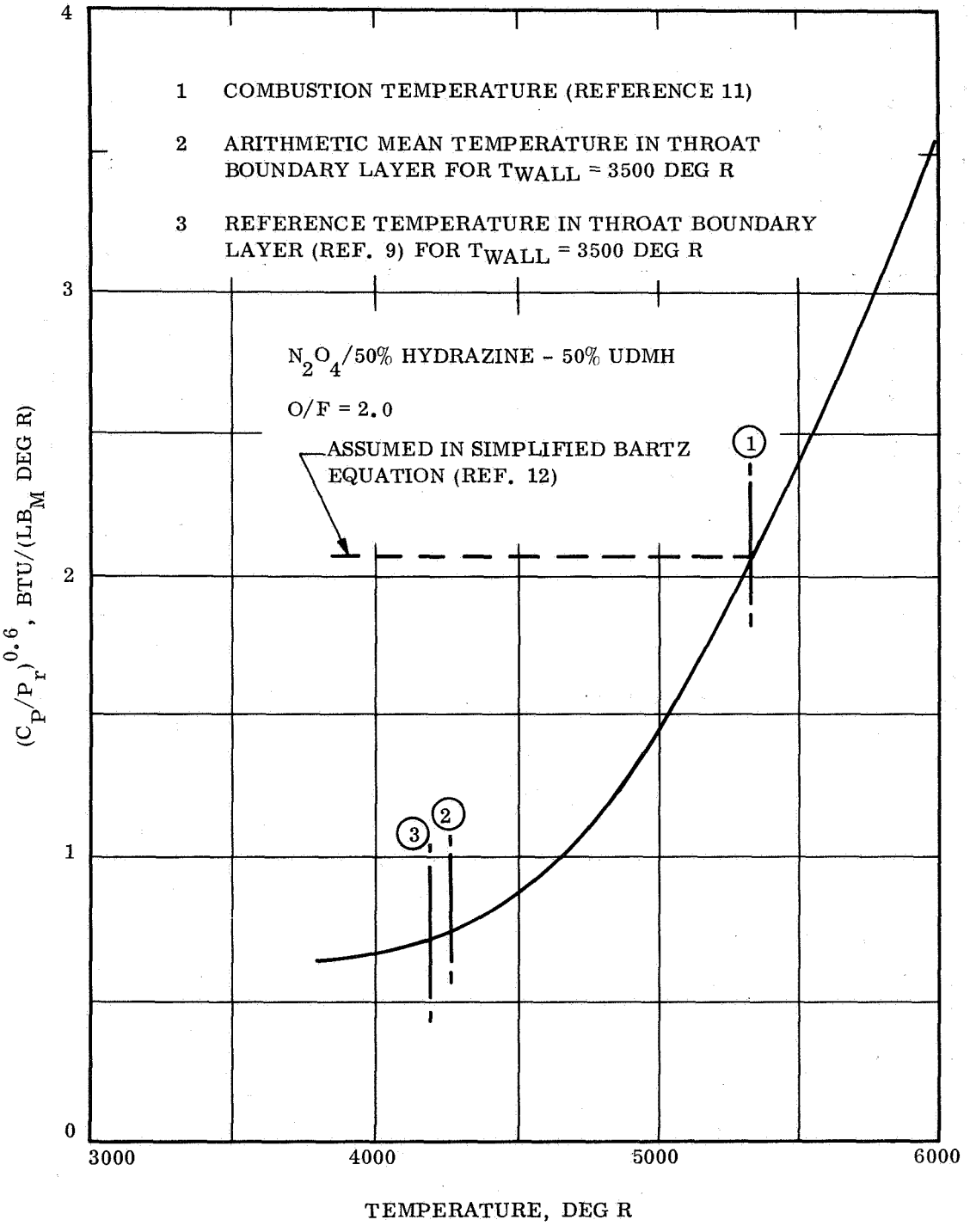

Figure 4. Variation of $(Cp/Pr)^{0.6}$ with Temperature for N_2O_4/50% Hydrazine - 50% UDMH

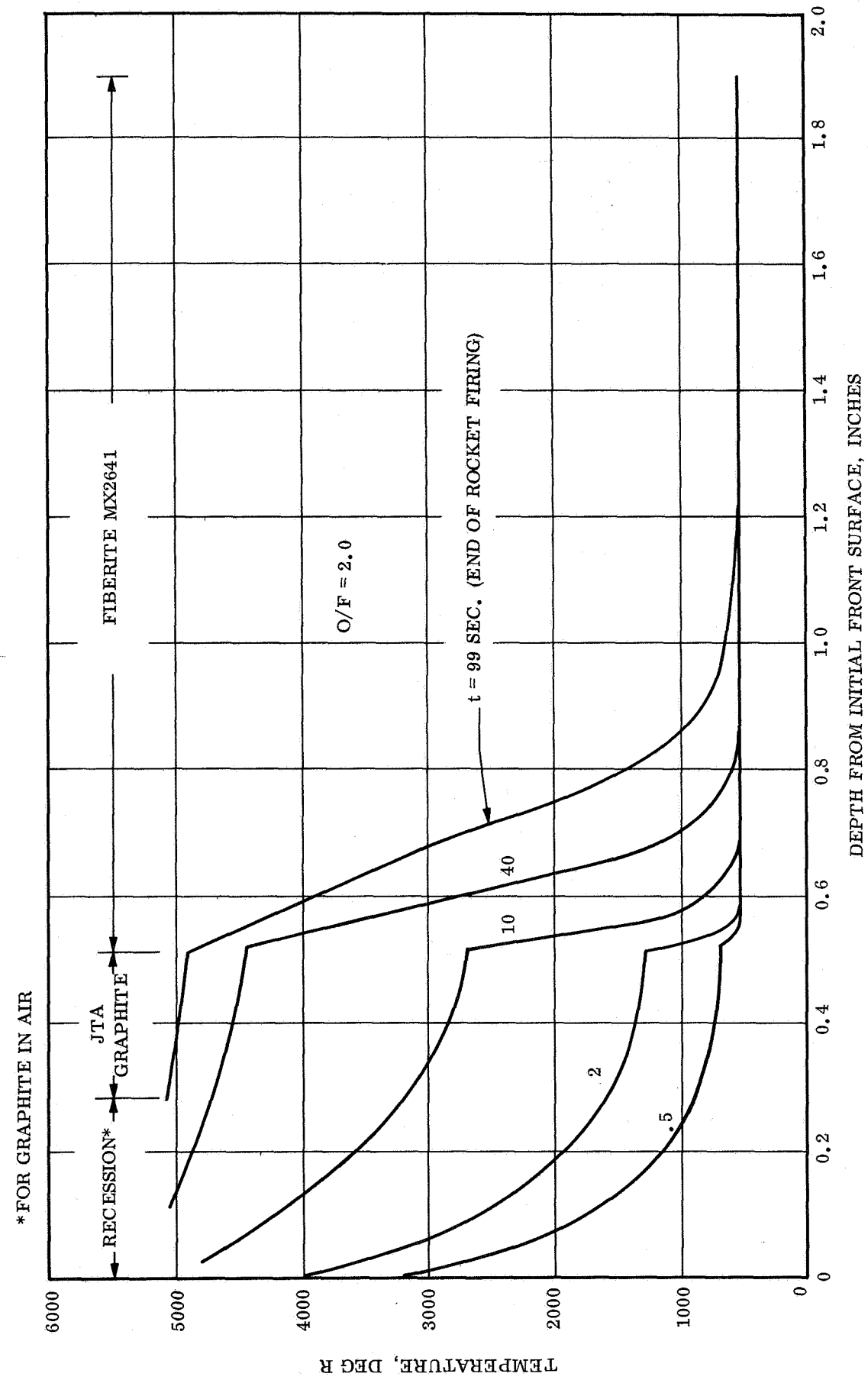

Figure 5. Throat Insert Temperature Profile - Firing

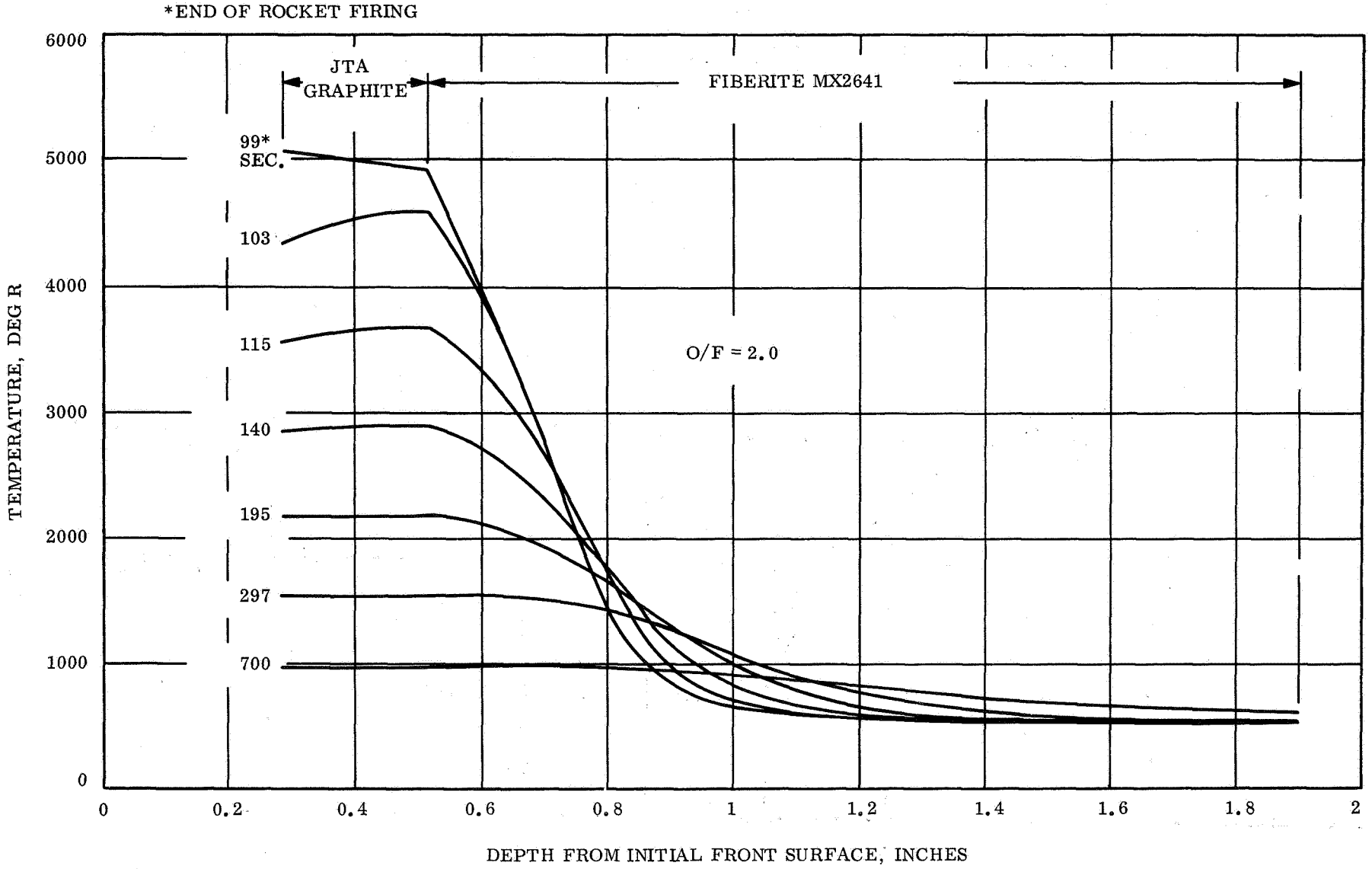

Figure 6. Throat Insert Temperature Profile - Cool-down

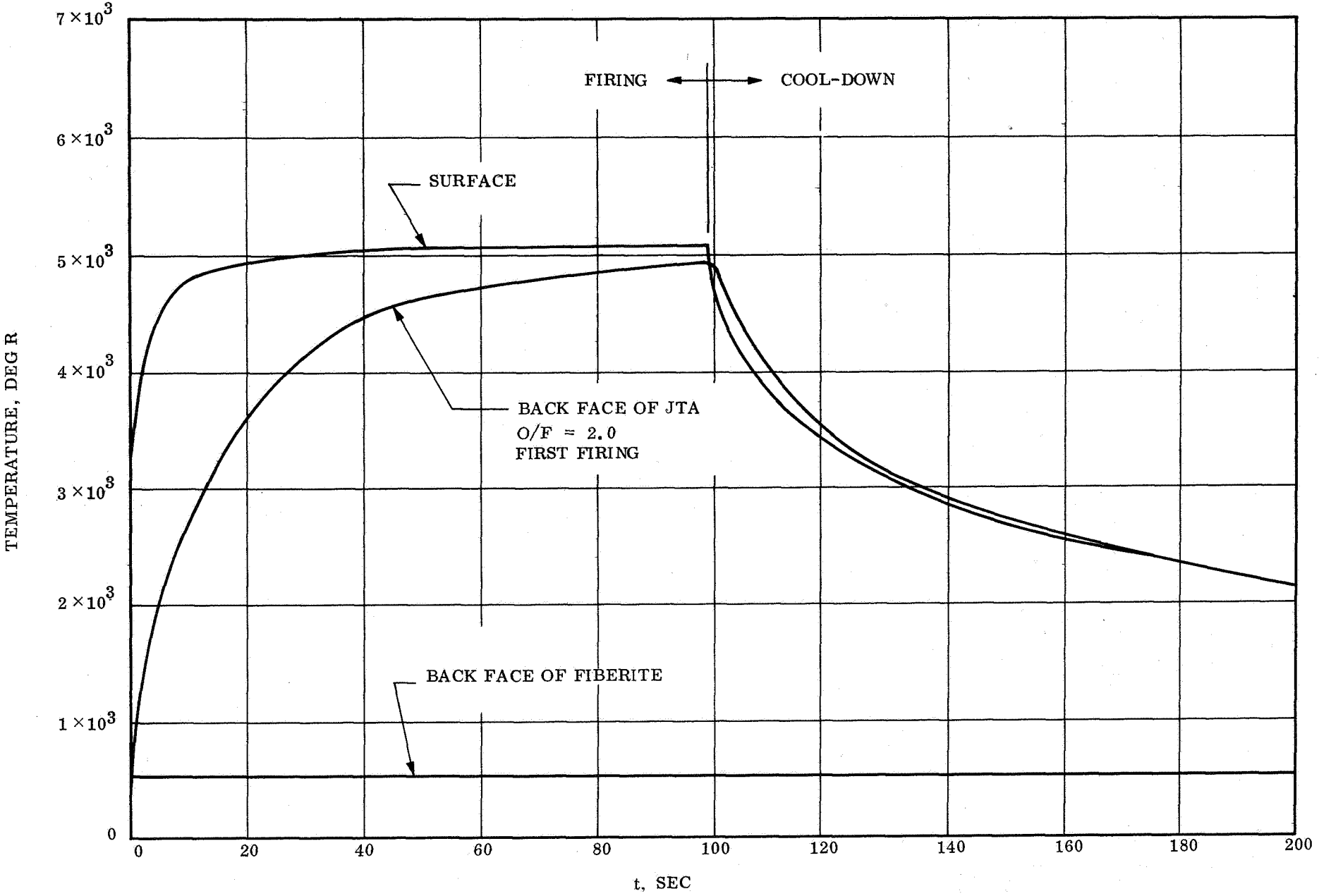

Figure 7. Rocket Throat Insert Temperature History

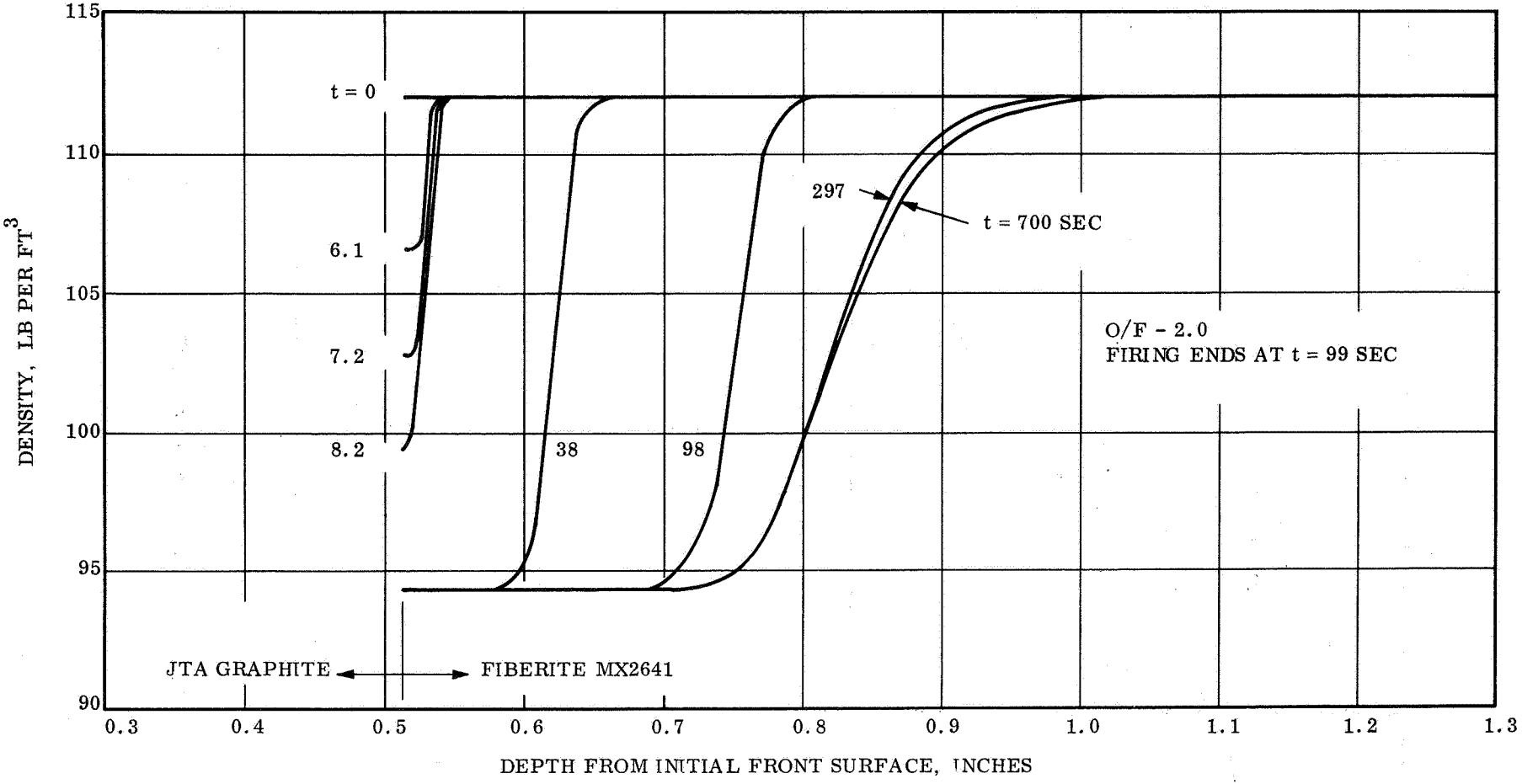

Figure 8. Rocket Throat Insert Sub-Layer Density History

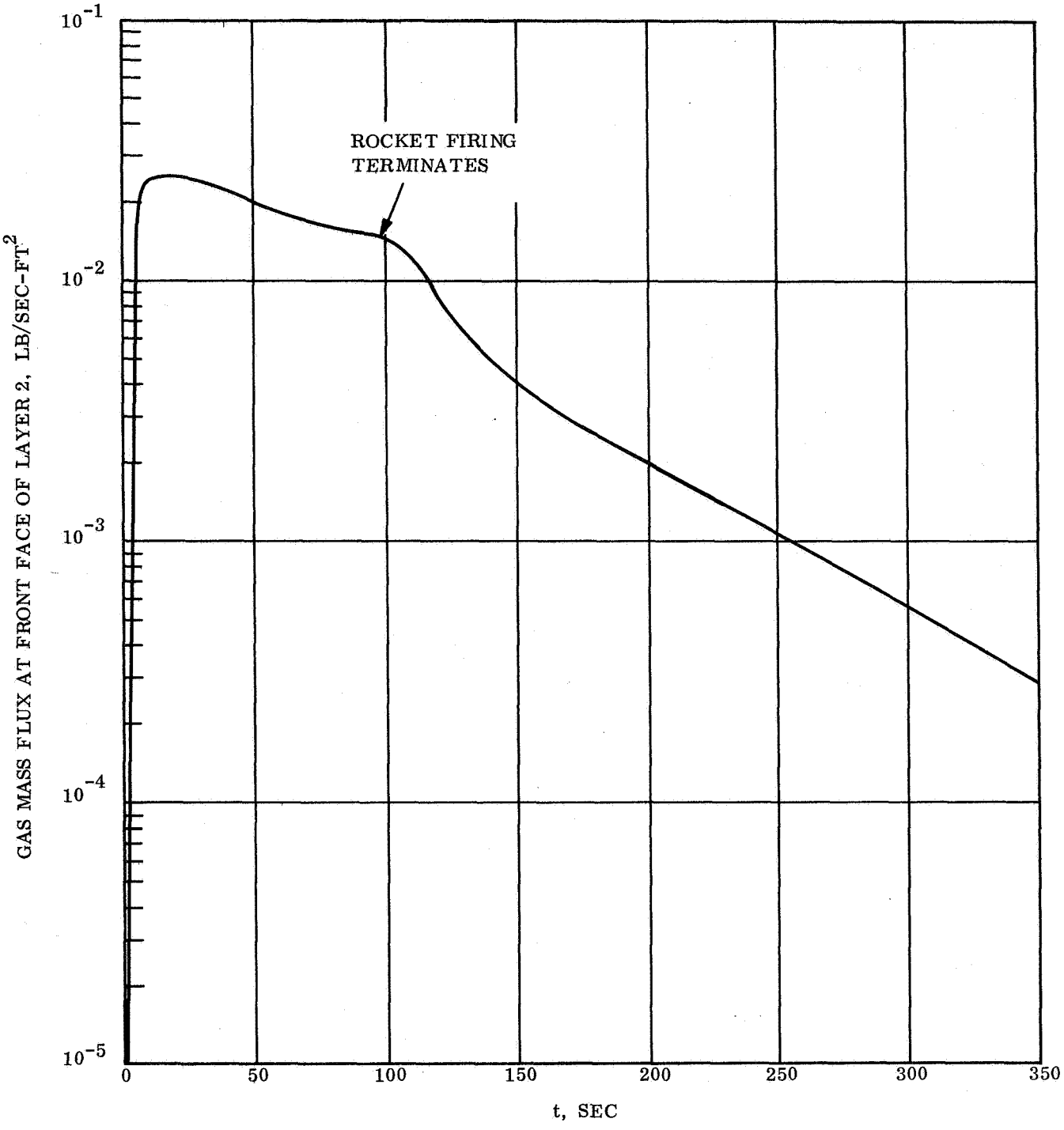

Figure 9. Gas Flow Rate for Throat Insert Sub-Layer

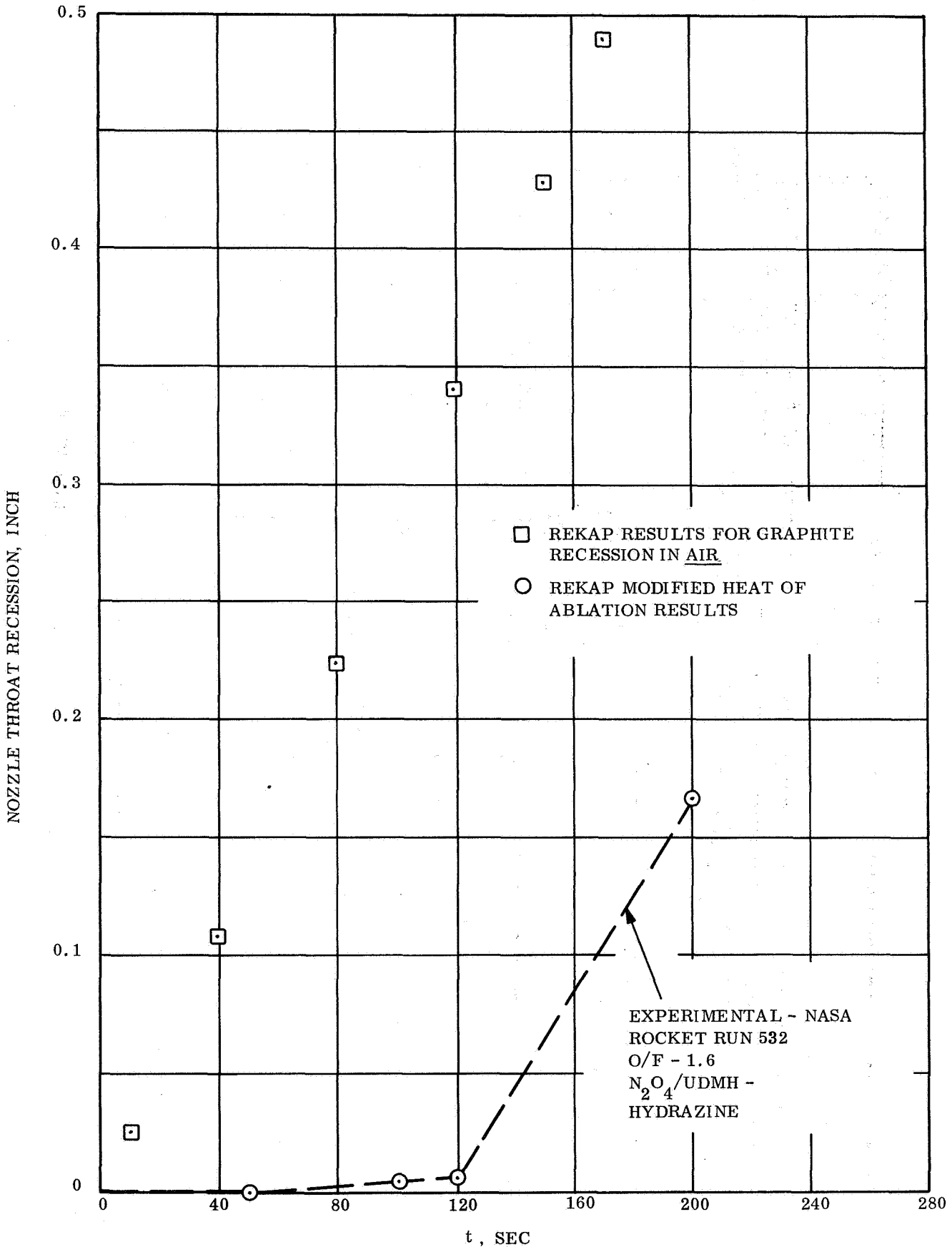

Figure 10. Measured Surface Recession Vs REKAP Results

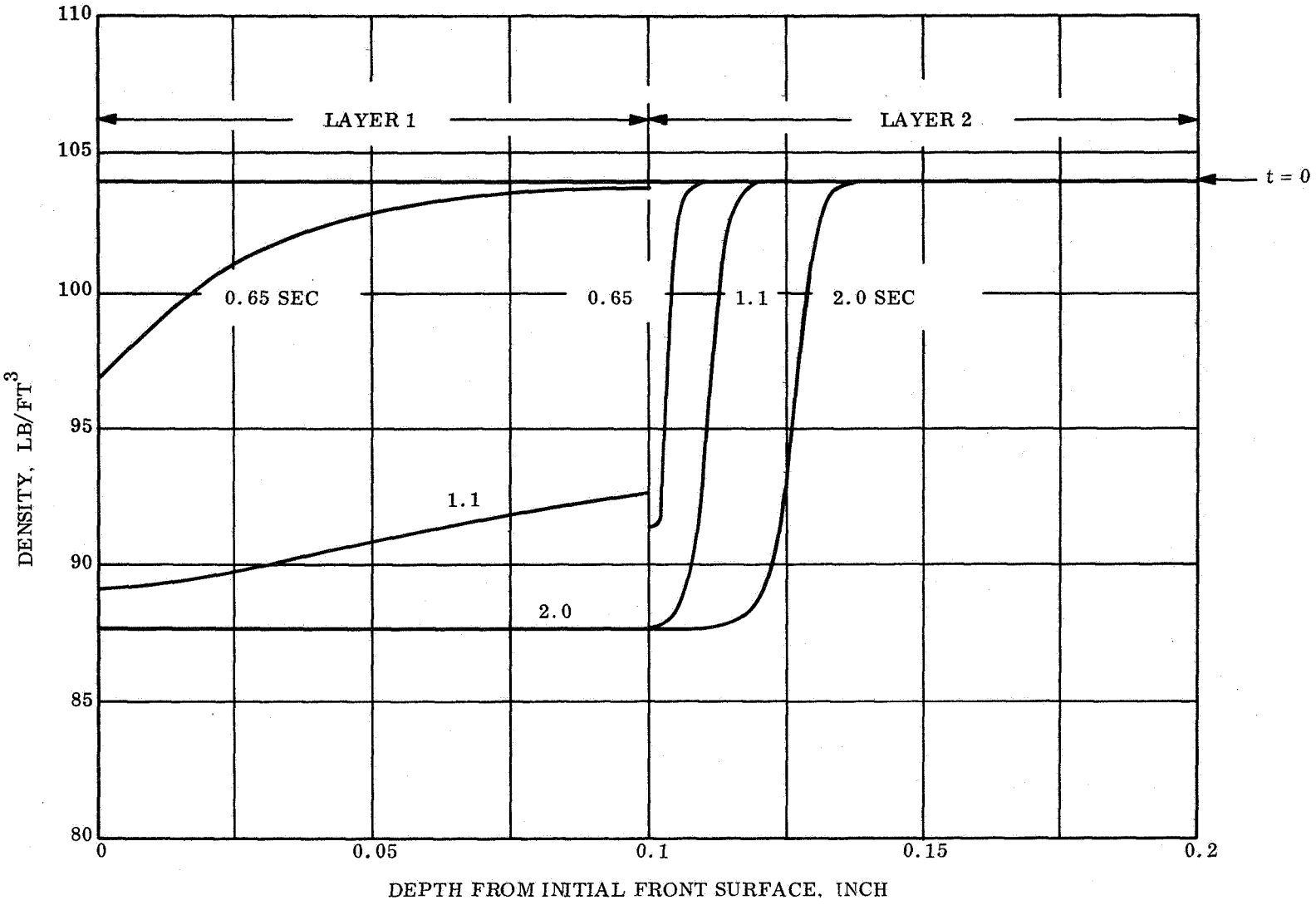

Figure 11. Density History - Two Charring Layers

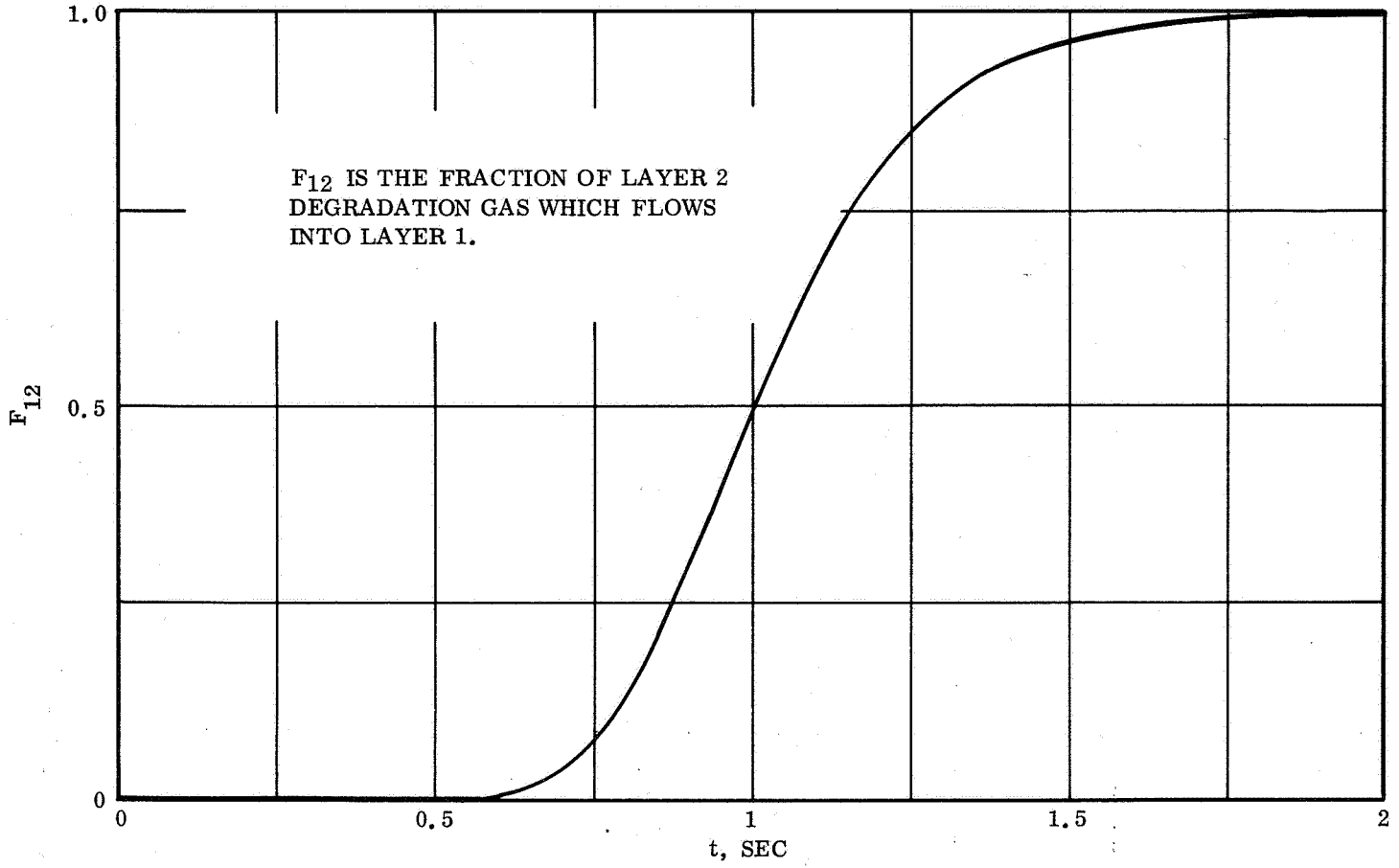

Figure 12. Inter-Layer Gas Flow - Two Charring Layers

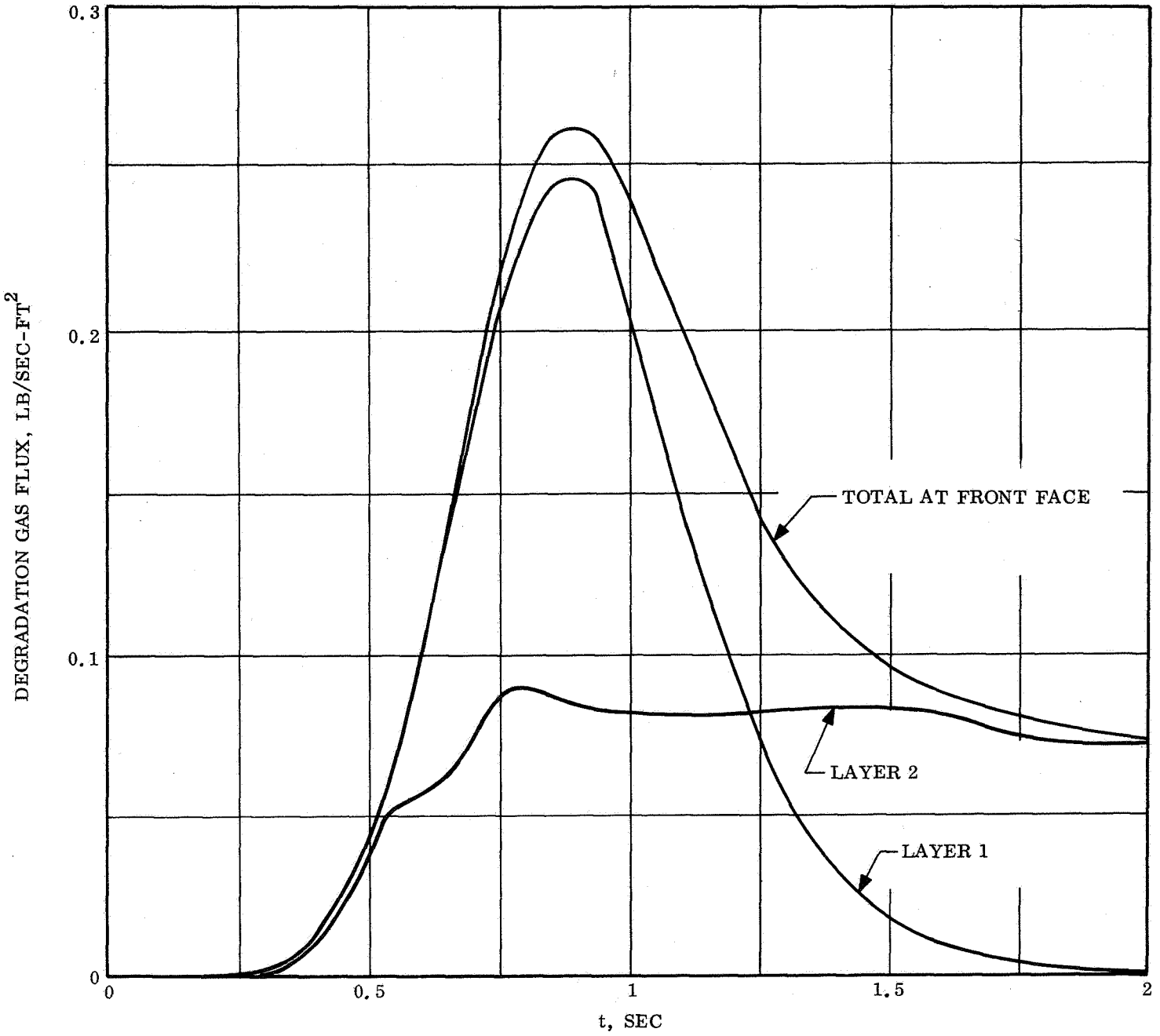

Figure 13. Degradation Gas Flux - Two Charring Layers

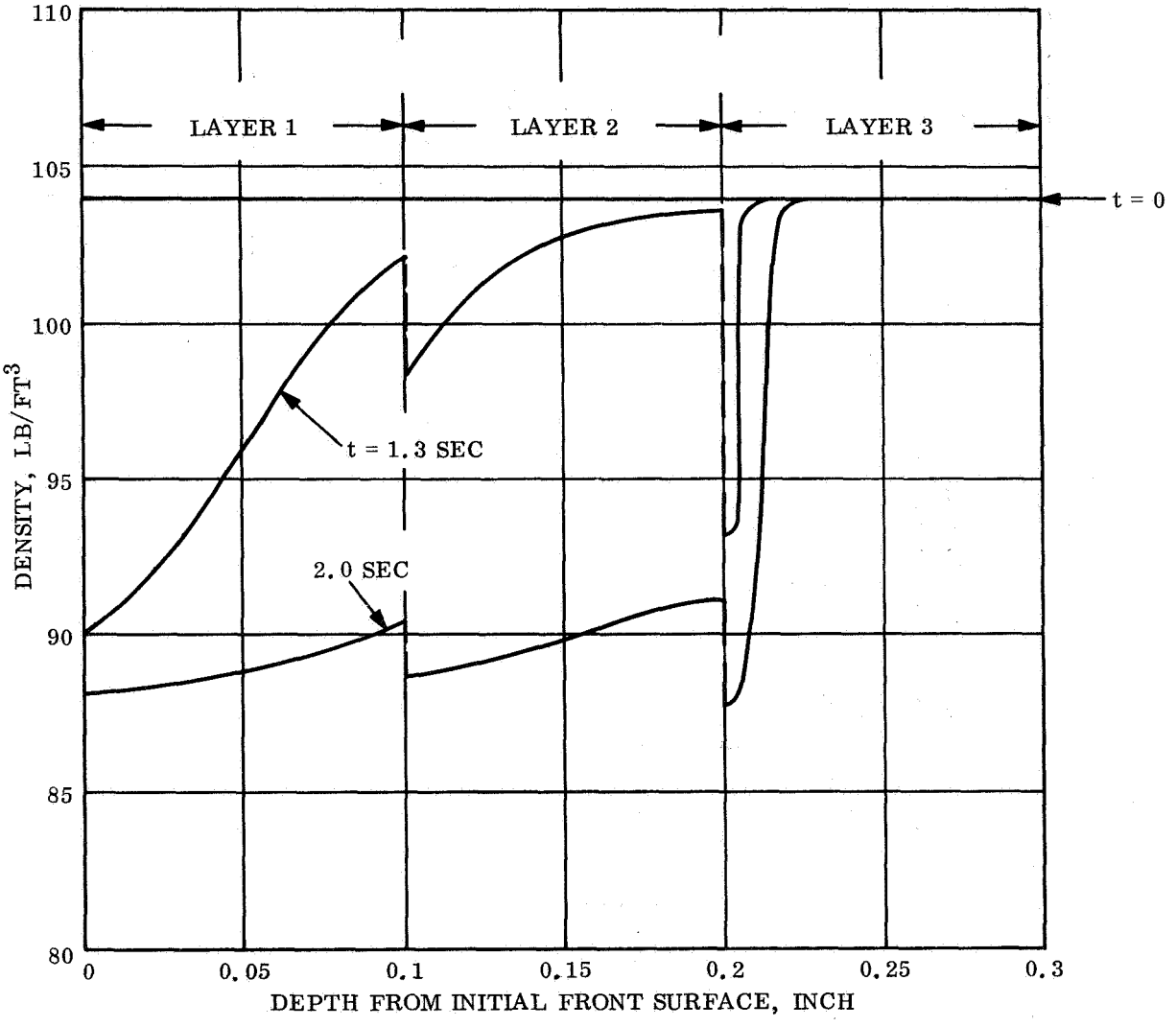

Figure 14. Density History - Three Charring Layers

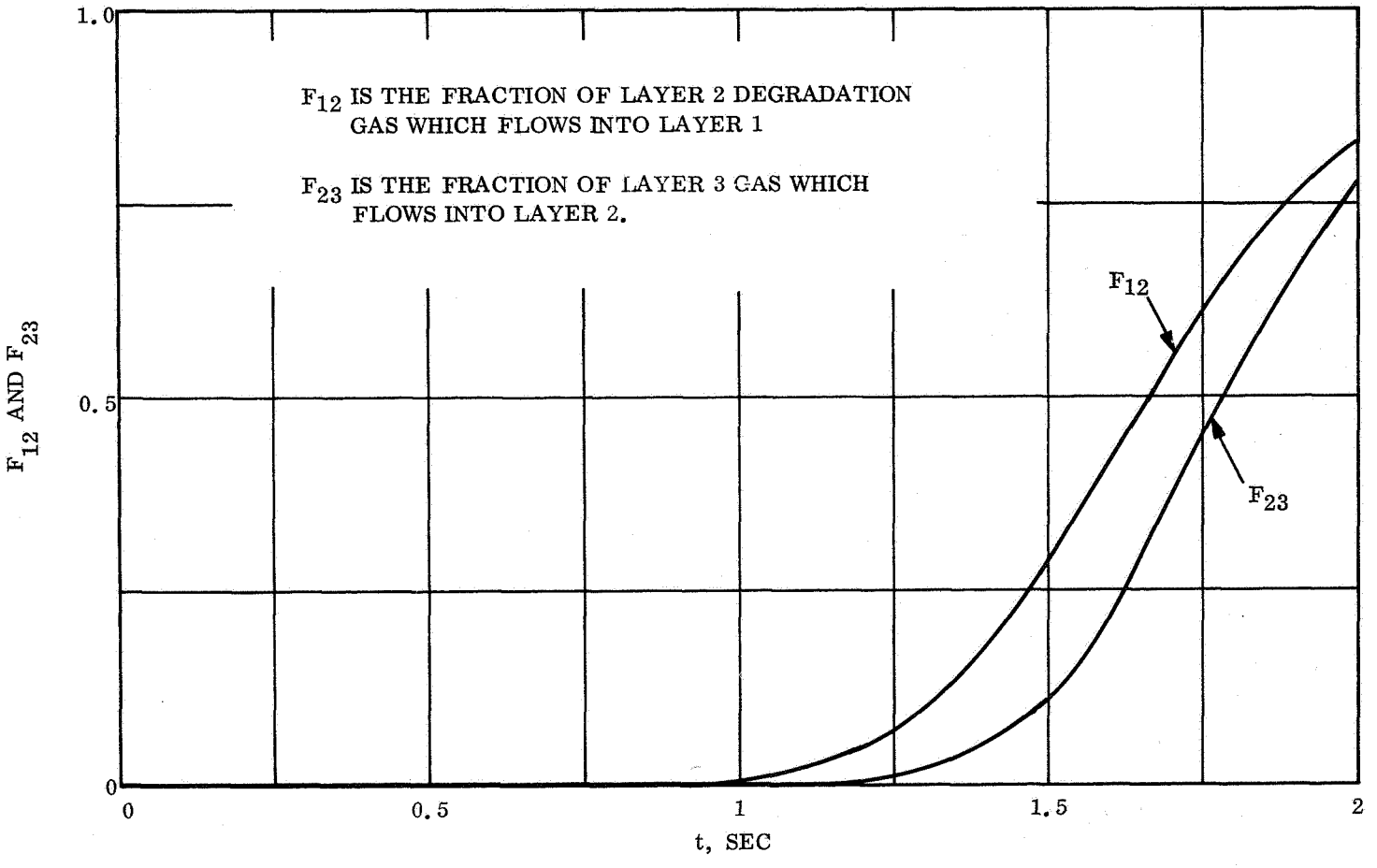

Figure 15. Inter-Layer Gas Flow - Three Charring Layers

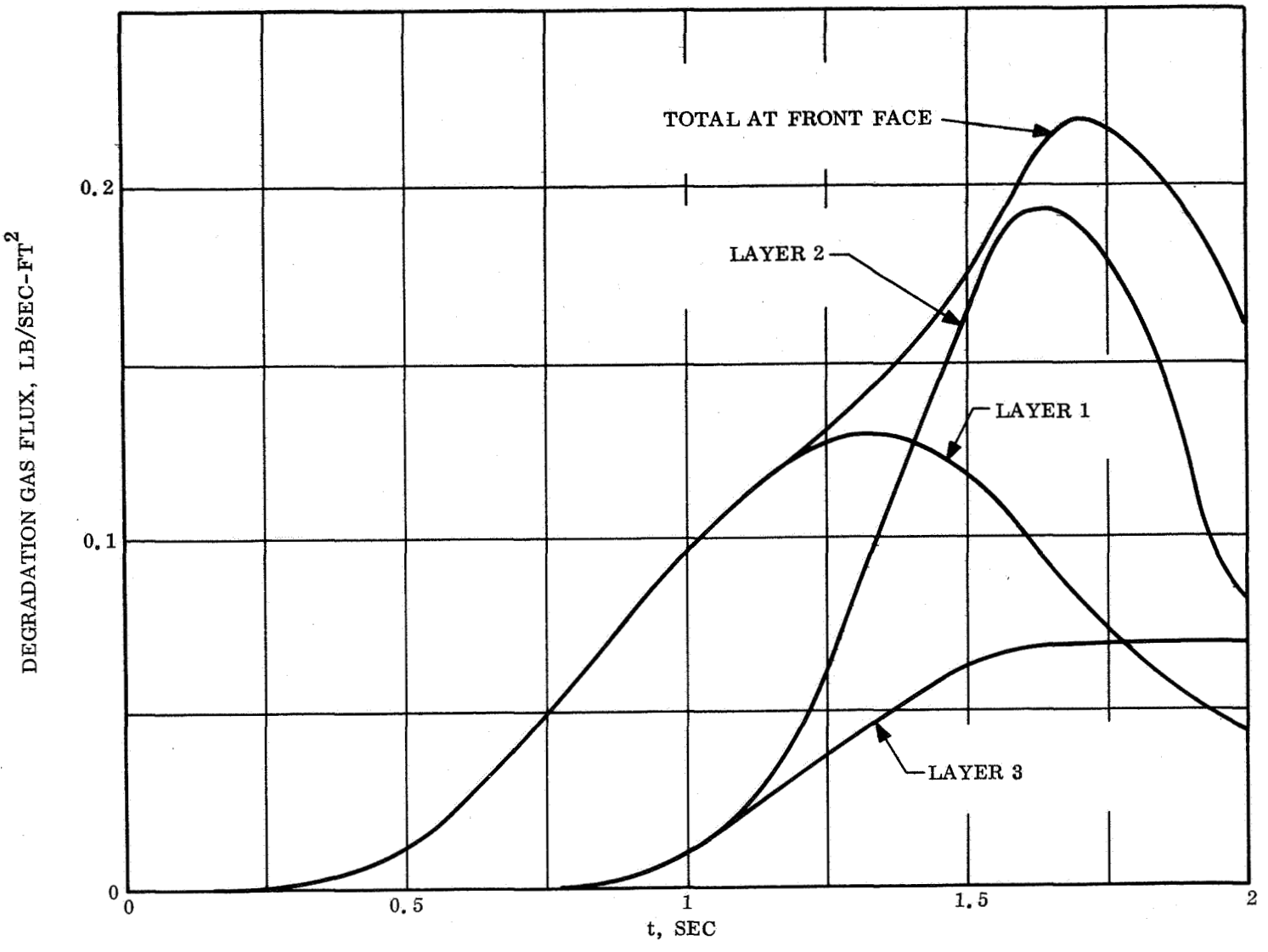

Figure 16. Degradation Gas Flux - Three Charring Layers

APPENDIX A

MATHEMATICAL DESCRIPTION OF THE REACTION KINETICS ABLATION PROGRAM

TABLE OF CONTENTS

1.0 INTRODUCTION

In this appendix, a thermal ablation model is derived for a thermosetting plastic. Consideration is given first to the general three-dimensional case. Simplifications are then introduced to obtain an equation which reasonably satisfies the physical model.

The philosophy of this derivation is to start from fundamental physical principles and to utilize the concepts of continuum mechanics to proceed in a step-by-step fashion, listing all assumptions.

Figure A-1 shows a cross-section of the ablation model. Initially, the outer boundary coincides with the broken line as indicated. The ambient temperature is low enough so that no chemical reactions occur within the plastic. Furthermore, the outer boundary is at the same temperature as its surroundings and, therefore, radiation to or from the front face is zero.

Convective and radiative heat fluxes (arbitrary with time) are impressed on the outer boundary. As a consequence of thermal conduction, laminates of the plastic near the outer boundary increase in temperature and the front face begins to radiate heat. In time, the hotter laminates undergo a chemical reaction which converts the virgin plastic into hydrocarbon gas and a porous char residue.

The gas pressure within the porous char increases as the virgin material undergoes chemical reaction. As a consequence, a pressure profile is established throughout the porous region causing the gas to flow to adjacent pores of lower pressure. In general, the gas flow will be to the outer boundary and result in thermal energy being introduced due to friction. Heat transfer will occur between char and gas if their respective temperatures are different. Varying temperature or pressure changes, or any combination of these two conditions, can result in chemical changes in the gas (cracking or recombination), which will absorb or generate thermal energy. As the gas passes the outer boundary, a portion of the convective heat flux is blocked. As more and more heat enters the front face, reaction laminates will completely degas, thus forming a char layer while moving the reaction zone deeper into the body. And, of course, the outer boundary moves as a result of structural failure, oxidation, or both. If the outer boundary temperature becomes high enough, the char layer will either melt (as in the case of a material having silica fibers), or undergo surface reaction with the boundary layer gases (as for the graphite materials).

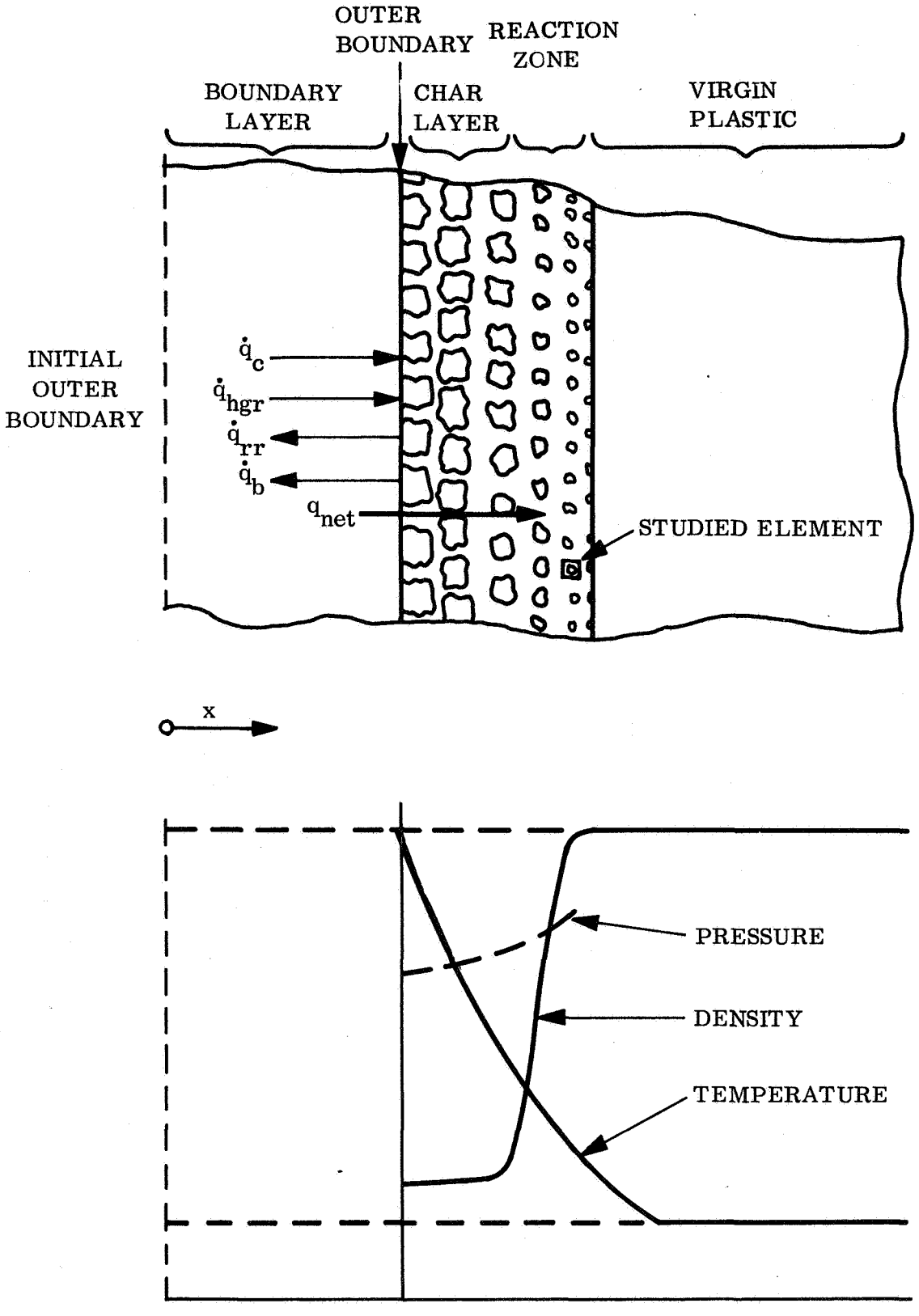

Figure A-1. Schematic of a Degrading Plastic and Corresponding Profiles

2.0 PHYSICAL MODEL

The physical model is that of a multicomponent flow of chemically reacting gases through a porous medium which is itself undergoing chemical reactions. The ablation material consists of unreacted solid (denoted by subscript p), which decomposes to a porous solid (subscript C) and gaseous products of reaction (subscript g). The decomposition process can be schematically represented as:

$$P(S) \rightarrow C(S) + G(g)$$

Before decomposition begins, the ablation material consists solely of unreacted solid. After the process has gone to completion, only solid and gaseous products of reaction exist.

All densities are based on the same unit reference volume of the mixture (solid and gas). Consequently, as the decomposition proceeds at a given location, ρ_p decreases from some initial value to zero while ρ_c is simultaneously increasing from zero to some final value.

The gaseous ablation products are formed by the decomposition of the unreacted solid material. They are a mixture of many different chemical species which flow and diffuse through the porous solid. The various species may react with one another in the gas phase resulting in the familiar "cracking" effect. They may also react with the surrounding solid material, causing a reduction (or increase) in solid density.

In order to validly apply continuum theory to a porous medium, all quantities are presumed to be suitably averaged over an area which is small with respect to the macroscopic dimensions of the material but large with respect to pore size. It is assumed that the ratio of pore area to total area is the same as that of pore volume to total volume, the latter ratio being the definition of porosity.

The solid species remain stationary because the displacements due to thermal expansion, a stress field and/or changes in molecular structure are generally negligible. All species are considered to be pure substances. External body forces (e.g. gravity) have been neglected because they are small for most practical applications.

3.0 EQUATIONS OF STATE

The caloric equation of state for each solid specie is assumed to be of the form:

$$e_p = e_p(T) \qquad \text{and} \qquad e_c = e_c(T)$$

Thus, for any process:

$$e_p = \int_{T_R}^{T} C_{vp}\, dT + \left(e_{F_p}\right)_{T_R} \tag{1}$$

and

$$e_c = \int_{T_R}^{T} C_{v_c}\, dT \left(e_{F_c}\right)_{T_R} \tag{2}$$

The internal energy accounts for thermal and chemical energy. The solid species do not have a thermal equation of state because densities are determined by the application of non-equilibrium reaction kinetics.

The gaseous products are assumed to be a mixture of chemically reacting perfect gases. Thus, the thermal and caloric equations of state for each specie are:

$$P_i = \rho_i \frac{R}{M_i} T, \tag{3}$$

$$e_i = \int_{T_R}^{T} C_{v_i}\, dT + \left(e_{F_i}\right)_{T_R} \tag{4}$$

and

$$h_i = \int_{T_R}^{T} C_{p_i}\, dT + \left(e_{F_i}\right)_{T_R} \tag{5}$$

Note that P_i and ρ_i are partial quantities which are based on a reference volume of the entire mixture (solid plus gas).

For the gaseous mixture as a whole, we have (assuming Dalton's Law of Partial Pressures is valid):

$$P = \rho \frac{R}{\bar{M}_g} T , \tag{6}$$

$$M_g = \frac{1}{\sum_i \frac{K_i}{M_i}} , \qquad K_i = \frac{\rho_i}{\rho} , \tag{7}$$

$$e_g = \sum_i K_i e_i \quad \text{and} \tag{8}$$

$$h_g = \sum_i K_i h_i \tag{9}$$

Note that these assumptions imply that pressure, stress, chemical reactions, etc. have a negligible effect on the specific internal energy of each specie. Obviously, they do affect the amount of each specie present at a given location and thus they do effect the total energy.

4.0 DIFFUSION VELOCITIES

In the flow of multicomponent gases, diffusion currents are generated by gradients in concentration, pressure and temperature. For the present problem, pressure and thermal diffusion effects should be small and so they are neglected. The velocity of the ith species relative to a fixed coordinate system is defined as $\vec{V}_i$. The mass-averaged or observable velocity of the total gas flow is defined as:

$$\vec{V} = \frac{1}{\rho_g} \sum_i \rho_i \vec{V}_i \, .$$

The diffusional velocity of the ith species ($\vec{V}_{d_i}$) is defined as the velocity of the ith specie relative to the mass-averaged velocity:

$$\vec{V}_{d_i} = \vec{V}_i - \vec{V} \, .$$

Note that:

$$\sum_i \rho_i \vec{V}_{d_i} = \sum_i \rho_i \vec{V}_i - \sum_i \rho_i \vec{V} \, .$$

$$\therefore \sum_i \rho_i \vec{V}_{d_i} = \rho_g \vec{V} - \rho_g \vec{V} = 0$$

To summarize, the absolute velocity of the ith species is given by the vector sum of the mean flow velocity and the diffusional velocity of the ith species, and the mass-averaged diffusional velocity is zero:

$$\vec{V}_i = \vec{V} + \vec{V}_{d_i} \quad \text{and}$$

$$\sum_i \rho \vec{V}_{d_i} = 0. \tag{10}$$

For ordinary concentration diffusion in a multicomponent gas, a first order approximation for V_{d_i} is that it depends linearly upon the concentration gradients of all species. For a mixture of perfect gases:

$$\rho_i \vec{V}_{d_i} = \frac{n^2}{\rho_g} \sum_{i \neq j} M_i M_j P_{i_j} \nabla X_j$$

Use of this equation to determine the composition of the mixture results in a formidable mathematical problem. Also, since we are dealing with transport phenomena in a porous medium, its accuracy is not assured. It has been noted by Von Karman (Reference 1) that " ... the process in a multicomponent mixture is so complicated that one mostly uses an approximation by considering the diffusion to be between one appropriately chosen component and the mixture of the rest replaced by a homogeneous gas of average characteristics", i.e., an effective binary mixture insofar as diffusion is concerned.

With this approximation, the diffusion velocity is related to the mass concentration by Fick's Law:

$$\rho_i \vec{V}_{d_i} = -\rho_g D_{12} \nabla K_i \qquad (11)$$

The concept of an effective binary mixture would be a useful starting point in accounting for the effects of diffusion. The largest error in this approximation probably results from the assumption that the diffusion coefficient for all species are the same.

5.0 MOMENTUM EQUATION

Experimental evidence for the flow of a gas through a porous medium indicates that the usual momentum equation of fluid mechanics does not apply (e.g. Reference 2). Consequently, it must be replaced by an empirical relationship between velocity and pressure. For the flow of a homogeneous gas through a porous medium at low velocities, Darcy's Law is reasonably accurate (Reference 2). Very little is known about the present case of chemically reacting flow through a medium of variable porosity. It will be assumed that Darcy's Law gives an adequate representation for the present problem, although other forms could be used if desired. Thus:

$$\vec{V} = - \nabla \frac{k}{\mu} P . \qquad (12)$$

where k is the permeability of the charring material and μ is the viscosity of the ablation gases. These quantities are normally determined by experiment.

6.0 CONTINUITY EQUATIONS

The principal of conservation of mass as applied to the ith gaseous specie within a stationary control volume says that the rate at which mass is accumulated within the volume equals the rate at which mass is transported out by convection and diffusion plus the net rate of production due to chemical reaction. The mathematical statement of this is:

$$\frac{d}{dt}\int_V \rho_i \, dV = -\int_A \rho_i \left(\vec{V} + \vec{V}_{d_i}\right) \cdot \vec{\eta} \, dA + \int_V \dot{W}_i \, dV. \qquad (13)$$

Here $\dot{W}_i$ is the net amount of specie i produced per unit volume per unit time. Note that $\dot{W}_i$ includes the rate of formation of the species from the unreacted solid as well as from any further gas phase or gas-solid phase reactions that might occur.

The surface integral involved in (13) can be transformed into a volume integral by means of the Divergence Theorem*:

$$\int_A \rho_i \left(\vec{V} + \vec{V}_{d_i}\right) \cdot \vec{\eta} \, dA = \int_V \nabla \cdot \rho_i \left(\vec{V} + \vec{V}_{d_i}\right) dV.$$

The order of integration and differentiation can be interchanged* so that:

$$\frac{d}{dt}\int_V \rho_i \, dV = \int_V \frac{\partial \rho_i}{\partial t} \, dV.$$

*It is assumed that all functions are continuous and continuously differentiable and that the region is simply connected (Reference 3).

Substituting these relations into (13) yields:

$$\int_V \left[\frac{\partial \rho_i}{\partial t} + \nabla \cdot \rho_i \left(\vec{V} + \vec{V}_{d_i} \right) - \dot{W}_i \right] dV = 0.$$

Since the volume is arbitrary the integrand must be identically zero. Thus the species continuity equation is:

$$\frac{\partial \rho_i}{\partial t} + \nabla \cdot \rho_i \left(\vec{V} + \vec{V}_{d_i} \right) = \dot{W}_i . \tag{14}$$

Summing this equation over all gaseous species and noting that

$$\sum_i \rho_i \vec{V}_{d_i} = 0: \sum_i \rho_i = \rho_g : \sum_i \dot{W}_i = \dot{W}_g$$

results in the continuity equation for the gas:

$$\frac{\partial \rho_g}{\partial t} + \nabla \cdot \rho_g \vec{V} = \dot{W}_g . \tag{15}$$

Now, gas phase reactions do not change the total mass of gas present; rather, they redistribute the species. Therefore, $\dot{W}_g = \sum_i \dot{W}_i$ is the total rate at which gas is being produced by the decomposition of the unreacted material and by gas-solid phase reactions.

The continuity equations for the solid species are:

$$\frac{\partial \rho_p}{\partial t} = \dot{W}_p \quad \text{and} \tag{16}$$

$$\frac{\partial \rho_c}{\partial t} = \dot{W}_c \tag{17}$$

$\dot{W}_p$ is the rate of depletion of the unreacted material due to decomposition. For charring ablation materials, the decomposition is irreversible and the rate at which it proceeds is generally limited by chemical kinetics. $\dot{W}_p$ is deduced from TGA (thermogravimetric analysis) experiments and is often expressed analytically as a single nth order reaction with an Arrhenius "rate constant."

$$\dot{W}_p = -A (\rho_p)^n,$$

$$A = A_o \exp\left(-\frac{E}{RT}\right) .$$

$\dot{W}_c$ is the rate at which char is formed from the decomposition of the unreacted material (generally a known fraction of W_p) and from gas-solid phase reactions. There is no overall production of mass so that:

$$\dot{W}_p + \dot{W}_c + \dot{W}_g = 0 . \tag{18}$$

It is useful to separate out the mass production rates due to the decomposition, the gas phase reactions, and the gas-solid phase reactions. This can be done by introducing some new quantities.

$$\dot{W}_c = - f_c \dot{W}_p + \dot{W}_c'' \quad \text{and} \tag{19}$$

$$\dot{W}_g = - (1 - f_c) \dot{W}_p + \dot{W}_g'' . \tag{20}$$

Here f_c denotes the fraction of unreacted material which forms char (not necessarily constant) and the superscript double prime denotes gas-solid phase reactions only. The first part of these equations states that char and gas are produced from the decomposition of the unreacted material, while the second part accounts for additional formation due to gas-solid phase reactions. Note that

$$\dot{W}_g'' = - \dot{W}_c'' \tag{21}$$

which follows from (18).

Finally, the species continuity equation can be expressed in terms of gas phase reactions only. Using $\rho_i = K_i \rho_g$ and the chain rule on (14) yields:

$$K_i \left[\frac{\partial \rho_g}{\partial t} + \nabla \cdot \rho_g \vec{V} \right] + \rho_g \left[\frac{\partial K_i}{\partial t} + V \cdot \nabla K_i \right] + \nabla \cdot \left(\rho_g \vec{V}_{d_i} K_i \right) = \dot{W}_i .$$

The first term in brackets equals $\dot{W}_g$ by virture of (15) and so:

$$\rho_g \left[\frac{\partial K_i}{\partial t} + V \cdot \nabla K_i \right] + \nabla \cdot \left(\rho_g K_i \vec{V}_{d_i} \right) = \dot{W}_i' \tag{22}$$

Where:

$$\dot{W}_i' = \dot{W}_i - K_i \dot{W}_g . \tag{23}$$

$\dot{W}_i'$ is the net rate of production of the ith species minus the amount of the ith species formed by the decomposition of the unreacted material plus gas-solid phase reactions. Consequently, $\dot{W}_i'$ is the net rate of production due to gas phase reactions only. Note that:

$$\sum_i \dot{W}_i' = 0.$$

In general, the $\dot{W}_i'$ are functions of temperature, pressure and composition and are determined from a knowledge of the exact chemical reactions which occur. For very slow reactions in the gas phase (i.e., "frozen-flow"), the $\dot{W}_i' = 0$. For very fast reactions, the flow will be in local thermochemical equilibrium and the $\dot{W}_i'$ are determined by imposing constraints on the composition (i.e., equilibrium "constants").

7.0 ENERGY EQUATION

The energy equation is derived by applying the First Law of Thermodynamics to a stationary control volume within the material. This means that the time rate of change of the total energy within the volume equals the rate at which energy is transported into the volume minus the rate at which energy is being convected out plus the rate at which work is being done on the volume. The mathematical expression is

$$\frac{d}{dt}\int_V \left[\rho_p e_p + \rho_c e_c + \sum_i \rho_i \left(e_i + \frac{\vec{V}\cdot\vec{V}}{2}\right)\right] dV = -\int_A \vec{Q}\cdot\vec{n}\, dA$$

$$-\int_A \left[\sum_{i'} \rho_i \vec{V}\left(e_i + \frac{\vec{V}\cdot\vec{V}}{2}\right)\cdot\vec{n}\right] dA + \int_A \vec{P}\cdot\vec{V}\, dA. \qquad (24)$$

The energy flux vector Q may be expressed in terms of contributions due to heat conduction, thermal radiation and diffusion (References 4, 5 and 6):

$$\vec{Q} = \vec{q}_c + \vec{q}_R + \sum_i \rho_i \vec{V}_{d_i} h_i. \qquad (25)$$

It now remains to relate the heat flux vectors and the surface force per unit area to the variables of the problem. Since the solid and the gas are in intimate contact, it is assumed that the temperature of the gas equals that of the solid. The conduction heat flux vector is approximately linearly dependent upon the temperature gradients. For an isotropic material this implies that

$$\vec{q}_c = -K \nabla T$$

which is Fourier's Law.

For anisotropic material, the heat flux depends upon temperature gradients through a second order conductivity tensor. In rectangular cartesian coordinates, this is

$$\vec{q}_c = K_{i_j} \frac{\partial T}{\partial X_j} \vec{e}_i.$$

For the purposes of the present analysis, the material will be considered isotropic although it is noted that it would be easy to include (25) in the analysis should sufficient data be available to justify it. Thus, the conduction heat flux vector is related to the temperature by:

$$\vec{q}_c = -K \nabla T. \qquad (26)$$

Note that the conductivity will be a weighted average of the conductivities of all species that are present, both solid and gas.

In general, the radiation heat flux vector accounts for the net effect of emission, absorption and scattering of thermal radiation of all wavelengths within the material. It is usually assumed that scattering is negligible, the material is isotropic and that the optical properties do not depend on the wavelength. Even with these drastic assumptions, the calculation of $\vec{q}_R$ is quite complex. Thus, for practical calculations, $\vec{q}_R$ is usually neglected and the transport of thermal radiation is approximately accounted for by an increase in thermal conductivity with temperature.

The surface force per unit area can be related to the stresses by considering the forces acting on a small tetrahedron (p. 101, Reference 7).

$$\vec{P} = \vec{n} \cdot \underset{\sim}{T} .$$

$\vec{n}$ is an outward unit normal and $\underset{\sim}{T}$ is a second order stress tensor whose components are σ_{ij}.
Note that this is a dot product of a vector with a tensor and the result is a vector which is different from $\vec{n}$, both in magnitude and direction. Using indicial notation, the surface force would be expressed as:

$$\vec{P} = \sigma_{ij} n_i \vec{e}_j .$$

The required work term is:

$$\vec{P} \cdot \vec{V} = (\vec{V} \cdot \underset{\sim}{T}) \cdot \vec{n} .$$

The stress tensor may be separated into a hydrostatic pressure component (a scalar) and a viscous stress tensor:

$$\underset{\sim}{T} = - P + \underset{\sim}{\tau}$$

For a linear isotropic fluid, the viscous stresses are linearly related to the velocity gradients. For the purposes of this analysis, the viscous stresses will be retained in the general form of $\underset{\sim}{\tau}$. The final form of the work term is then:

$$\vec{P} \cdot \vec{V} = - (p \vec{V}) \cdot \vec{n} + (\vec{V} \cdot \underset{\sim}{\tau}) \cdot \vec{n} . \qquad (27)$$

Substituting (25), (26) and (27) into (24) and following exactly the same procedure as with the species continuity equation results in the differential energy equation:

$$\frac{\partial}{\partial t}\left[\rho_p e_p + \rho_c p_c + \sum_i \rho_i \left(e_i + \frac{\vec{V}\cdot\vec{V}}{2}\right)\right] + \nabla\cdot\left[\sum_i \rho_i \vec{V}\left(e_i + \frac{\vec{V}\cdot\vec{V}}{2}\right)\right]$$
$$+ \nabla\cdot\left[\sum_i \rho_i \vec{V}_{d_i} h_i\right] = \nabla\cdot K\nabla T - \nabla\cdot\vec{q}_R - \nabla\cdot p\vec{V} + \nabla\cdot(\vec{V}\cdot\underset{\sim}{\tau}) \qquad (28)$$

The various terms of the energy equation can be expanded and rearranged to a more convenient form. Adding the term $\partial p/\partial t + \nabla\cdot p\vec{V}$ to both sides of (28) and using Dalton's Law gives:

$$\frac{\partial}{\partial t}\left[\rho_p e_p + \rho_c e_c + \sum_i \rho_i \left(e_i + \frac{p_i}{\rho_i} + \frac{\vec{V}\cdot\vec{V}}{2}\right)\right]$$
$$+ \nabla\cdot\left[\sum_i \rho_i \vec{V}\left(e_i + \frac{p_i}{\rho_i} + \frac{\vec{V}\cdot\vec{V}}{2}\right)\right] + \nabla\cdot\left[\sum_i \rho_i \vec{V}_{d_i} h_i\right] \qquad (29)$$
$$= \nabla\cdot K\nabla T - \nabla\cdot\vec{q}_R + \frac{\partial p}{\partial t} + \nabla\cdot(\vec{V}\cdot\underset{\sim}{\tau}).$$

Noting that

$$h_i = e_i + \frac{p_i}{\rho_i} \quad ; \quad \rho_g = \sum_i \rho_i$$

and using the chain rule, (29) can be expanded to:

$$\left[\rho_p \frac{\partial e_p}{\partial t} + e_{v_p}\frac{\partial \rho_p}{\partial t} + \rho_c \frac{\partial e_c}{\partial t} + e_c \frac{\partial \rho_c}{\partial t} + \sum_i\left(\rho_i \frac{\partial h_i}{\partial t} + h_i \frac{\partial \rho_i}{\partial t}\right)\right.$$
$$\left. + \frac{\partial}{\partial t}\left(\rho_g \frac{V\cdot V}{2}\right)\right] + \left[\sum_i\left(\rho_i\left(\vec{V} + \vec{V}_{d_i}\right)\cdot\nabla h_i + h_i \nabla\cdot\rho_i\left(\vec{V} + \vec{V}_{d_i}\right)\right)\right. \qquad (30)$$
$$\left. + \nabla\cdot\rho_g \vec{V}\frac{\vec{V}\cdot\vec{V}}{2}\right] = \nabla\cdot K\nabla T - \nabla\cdot\vec{q}_R + \frac{\partial p}{\partial t} + \nabla\cdot(\vec{V}\cdot\underset{\sim}{\tau}).$$

Noting that the temperature of the gas equals that of the solid, differentiating the caloric equations of state, (1), (2) and (5) yields:

$$\frac{\partial e_p}{\partial t} = C_{v_p} \frac{\partial T}{\partial t}, \qquad \frac{\partial h_i}{\partial t} = C_{p_i} \frac{\partial T}{\partial t}, \text{ and}$$

$$\frac{\partial e_c}{\partial t} = C_{v_c} \frac{\partial T}{\partial t}, \qquad \nabla h_i = C_{p_i} \nabla T.$$

Substituting these relations into (30) and rearranging terms gives

$$\left[\rho_p C_{v_p} + \rho_c C_{v_c} + \sum_i \rho_i C_{p_i}\right] \frac{\partial T}{\partial t} + \left[e_p \frac{\partial \rho_p}{\partial t} + e_c \frac{\partial \rho_c}{\partial t} + \sum_i h_i \left(\frac{\partial \rho_i}{\partial t} + \nabla \cdot \rho_i \left(\vec{V} + \vec{V}_{d_i}\right)\right)\right] + \left[\sum_i \rho_i C_{p_i} \left(\vec{V} + \vec{V}_{d_i}\right)\right] \cdot \nabla T = \nabla \cdot K \nabla T - \nabla \cdot \vec{q}_R \quad (31)$$
$$+ \frac{\partial \rho}{\partial t} + \nabla \cdot (\vec{V} \cdot \tau) - \left[\frac{\partial}{\partial t}\left(\rho_g \frac{\vec{V} \cdot \vec{V}}{2}\right) + \nabla \cdot \left(\rho_g \vec{V} \frac{\vec{V} \cdot \vec{V}}{2}\right)\right]$$

The second and eighth terms can be simplified by use of the continuity equations. Using (14), (16) and (17), the second term becomes

$$[\cdots] = e_p \dot{W}_p + e_c \dot{W}_c + \sum_i h_i \dot{W}_i.$$

Using (23), this last term is:

$$\sum_i \dot{W}_i h_i = \sum_i \dot{W}_i' h_i + \dot{W}_g h_g.$$

From (19), (20), and (21) we have:

$$\dot{W}_c = -f_c \dot{W}_p + \dot{W}_c'',$$

$$\dot{W}_g = -(1 - f_c)\,\dot{W}_p + \dot{W}_g''$$

and $\dot{W}_g'' = -\dot{W}_c''$.

Combining these relations, the final form of the second term of (31) is:

$$[\cdots] = -\dot{W}_p \left[(1 - f_c)\, h_g + f_c\, e_c - e_{vp}\right] + \sum_i \dot{W}_i'\, h_i - \dot{W}_c''\,(h_g - e_v) \qquad (32)$$

The eighth term of (31) can be expanded to:

$$[\cdots] = \frac{\vec{V}\cdot\vec{V}}{2}\left[\frac{\partial \rho_g}{\partial t} + \nabla\cdot\rho_g\vec{V}\right] + \rho_g\left[\frac{\partial}{\partial t}\left(\frac{\vec{V}\cdot\vec{V}}{2}\right) + \vec{V}\cdot\nabla\left(\frac{\vec{V}\cdot\vec{V}}{2}\right)\right].$$

Using (15), the final form of the eighth term is:

$$[\cdots] = \frac{\vec{V}\cdot\vec{V}}{2}\,\dot{W}_g + \rho_g\left[\frac{\partial}{\partial t}\left(\frac{\vec{V}\cdot\vec{V}}{2}\right) + V\cdot\nabla\left(\frac{\vec{V}\cdot\vec{V}}{2}\right)\right]. \qquad (33)$$

Substituting (32) and (33) into (31) yields a final form of the energy equation:

I. Storage

$$\left(\rho_p C_{v_p} + \rho_c C_{v_p} + \rho_g \bar{C}_{p_g}\right) \frac{\partial T}{\partial t}$$

II. Decomposition

$$- \dot{W}_p \left[(1 - f_c) h_g + f_c e_c - e_p\right]$$

III. Cracking

$$+ \sum \dot{W}_i h_i$$

IV. Gas-solid phase reaction

$$- \dot{W}_c'' (h_g - e_c)$$

V. Convection

$$+ \rho_g \bar{C}_{p_g} \vec{V} \cdot \nabla T$$

VI. Diffusion

$$+ \sum_i \rho_i C_{p_i} \vec{V}_{d_i} \cdot \nabla T$$

VII. Heat Conduction

$$= \nabla \cdot K \nabla T$$

VIII. Thermal Radiation

$$- \nabla \cdot \vec{q}_R$$

IX. Pressure

$$+ \frac{\partial P}{\partial t}$$

X. Kinetic Energy

$$+ \frac{\vec{V} \cdot \vec{V}}{2} \dot{W}_g$$

XI. Viscous Stresses

$$+ \left[\nabla \cdot (\vec{V} \cdot \underset{\sim}{\tau}) - \rho_g \left\{ \frac{\partial}{\partial t} \left(\frac{\vec{V} \cdot \vec{V}}{2}\right) + \vec{V} \cdot \nabla \left(\frac{\vec{V} \cdot \vec{V}}{2}\right) \right\}\right]. \qquad (34)$$

8.0 SUMMARY OF EQUATIONS

Energy Equation

$$\left(\rho_p C_{v_p} + \rho_c C_{v_c} + \rho_g \bar{C}_{p_g}\right)\frac{\partial T}{\partial t} - \dot{W}_p \left[(1 - f_c) h_g + f_c e_c - e_p\right]$$

$$+ \sum_i \dot{W}_i' h_i - \dot{W}_c'' (h_g - e_c) + \rho_g C_{p_g} \vec{V} \cdot \nabla T + \sum_i \rho_i \vec{V}_{d_i} h_i \cdot \nabla T \qquad (35)$$

$$= \nabla \cdot K \nabla T - \nabla \cdot \vec{q}_R + \frac{\partial P}{\partial t} + \frac{\vec{V} \cdot \vec{V}}{2} \dot{W}_g + \nabla \cdot (\vec{V} \cdot \underset{\sim}{\tau})$$

$$- \rho_g \left\{ \frac{\partial}{\partial t} \left(\frac{\vec{V} \cdot \vec{V}}{2} \right) + \vec{V} \cdot \nabla \left(\frac{\vec{V} \cdot \vec{V}}{2} \right) \right\} .$$

Species Continuity

$$\rho_g \left(\frac{\partial K_i}{\partial t} + \vec{V} \cdot \nabla K_i \right) + \nabla \cdot \left(\rho_i \vec{V}_{d_i} \right) = \dot{W}_i' . \qquad (36)$$

Continuity

$$\frac{\partial \rho_g}{\partial t} + \nabla \cdot \rho_g \vec{V} = - (1 - f_c) \dot{W}_p - \dot{W}_c'' , \qquad (37)$$

$$\frac{\partial \rho_p}{\partial t} = \dot{W}_p \quad \text{and} \qquad (38)$$

$$\frac{\partial \rho_c}{\partial t} = - f_c \dot{W}_p + \dot{W}_c'' . \qquad (39)$$

The various terms of this equation are identified as:

I	energy storage
II	energy absorbed due to the decomposition of the solid
III	energy absorbed due to gas phase reactions (i.e. cracking)
IV	energy absorbed due to gas-solid phase reactions
V	energy transfer due to convection
VI	energy transfer due to diffusion
VII	energy transfer due to heat conduction
VIII	energy transfer due to thermal radiation
IX	rate of work associated with the pressure
X	kinetic energy associated with gas formation
XI	rate of work associated with the viscous stresses and kinetic energy

The "heat of decomposition" appears in term II:

$$h_{gf} = (1 - f_c)\, h_g + f_c\, e_c - e_{v_p}$$

If the usual momentum equation could be used to simplify term XI, it would reduce to the familiar work of pressure forces plus the work of viscous forces (i.e. $V \cdot \nabla_p + \Phi$ where Φ is the dissipation function).

State

$$P = \rho_g \frac{R}{M_g} T. \tag{40}$$

Momentum

$$\vec{V} = -\frac{k}{\mu} \nabla P. \tag{41}$$

Diffusion (binary mixture approximation)

$$\rho_i \vec{V}_{d_i} = -\rho_g D_{12} \nabla K_i \,. \tag{42}$$

Neglecting $\underset{\sim}{\tau}$ and q_r, there are 6+2 (N - 1) equations for the following physical variables (N is the total number of gaseous species):

$$T,\ \rho_p,\ \rho_c,\ \rho_g,\ P,\ \vec{V},\ \vec{V}_{d_i},\ K_i$$

These equations require that the following material properties (10 + 4N in all) be known functions of the variables:

$$C_{v_p},\ e_p,\ \dot{W}_p$$

$$C_{v_c},\ e_c,\ f_c,\ \dot{W}_c''$$

$$C_{p_i},\ h_i,\ \dot{W}_i',\ M_i$$

$$K,\ \frac{k}{\mu},\ D_{12}$$

9.0 DISCUSSION

The equations developed so far represent a quite general physical model of charring ablation. They account for the simultaneous transfer of energy and mass within a solid material of variable porosity which is decomposing. The ablation gases may be flowing, diffusing, reacting with themselves or reacting with the char and they are not necessarily in local thermochemical equilibrium.

It is generally desirable to invoke further physical assumptions in order to simplify the mathematical analysis and to reduce the number of required material properties, which are often not known. Several of these assumptions will now be discussed.

Two approaches will be described for the simplification of the general equations derived above. One approach to the problem is to simplify the gas chemistry while retaining the gas dynamical features. The ultimate end in this approach is to assume that the gas contains only a single specie. Note that this assumption does not exclude gas-solid phase reactions. Thus, we have $\vec{V}_{d_i} = 0$, $\dot{W}_i' = 0$ and the species continuity equation is superfluous. Neglecting the radiant flux and using the definitions of $\dot{W}_c$ (19) and $\dot{W}_g$ (20), equations (35) - (39) simplify to:

Energy

$$\left(\rho_p C_{vp} + e_c C_{vc} + \rho_g C_{p_g}\right)\frac{\partial T}{\partial t} + \left(\dot{W}_p e_p + \dot{W}_c e_c + \dot{W}_h h_g\right) + (\rho_g C_{p_g} \vec{V}) \cdot \nabla T \tag{43}$$

$$= \nabla \cdot K \nabla T + \frac{\partial P}{\partial t} + \frac{\vec{V} \cdot \vec{V}}{2}\dot{W}_g + \nabla \cdot (\vec{V} \cdot \underset{\sim}{\tau}) - e_g\left[\frac{\partial}{\partial t}\left(\frac{\vec{V} \cdot \vec{V}}{2}\right) + \vec{V} \cdot \nabla\left(\frac{\vec{V} \cdot \vec{V}}{2}\right)\right].$$

Continuity

$$\frac{\partial \rho_g}{\partial t} + \nabla \cdot e_g \vec{V} = \dot{W}_g. \tag{44}$$

$$\frac{\partial \rho_p}{\partial t} = \dot{W}_p. \tag{45}$$

$$\frac{\partial \rho_c}{\partial t} = \dot{W}_c. \tag{46}$$

$$\dot{W}_p + \dot{W}_c + \dot{W}_g = 0. \tag{47}$$

State

$$P = \rho \frac{R}{M} T. \tag{48}$$

Momentum

$$\vec{V} = - \nabla \frac{k}{\mu} P. \tag{49}$$

The gas density used in the derivation of the equations described here is the weight of the gas in a given solid-gas volume divided by that volume. The gas density referred to within the REKAP program is the above density divided by the porosity of the material. Porosity is defined as:

$$\epsilon = \frac{\text{Actual Gas Volume}}{\text{Total Volume}} = \frac{\text{Void Volume}}{\text{Total Volume}}$$

The porosity is calculated at each step by:

$$\epsilon = 1 - \tilde{\rho}_c \left(\frac{1}{\tilde{\rho}_c} - \frac{1}{\tilde{\rho}_{vp}} \right) - \frac{\rho_s}{\tilde{\rho}_{vp}}$$

The thermal conductivity of the gas (k_g) and thermal conductivity of the solid (K_S) are each based on their respective areas.

$\tilde{\rho}_c$ is the final density of the char based on the volume of the char (i.e. if the char is carbon then $\tilde{\rho}_c$ is equal to the density of carbon) and $\tilde{\rho}_{vp}$ is the initial density of the virgin plastic before heating or any charring has taken place.

Now simplifying the equations it will be assumed that the gas is in local thermochemical equilibrium and that diffusion is negligible. This means that the gas composition is a known function of temperature and pressure. Finally, it is assumed that radiation can be accounted for as an increase in effective conductivity and that the mechanical work terms are negligible compared to the thermal terms in the energy equation. All of these are reasonably plausible engineering assumptions.

In the absence of diffusion, the species continuity equation (22) is:

$$\rho_g \left[\frac{\partial K_i}{\partial t} + \vec{V} \cdot \nabla K_i \right] = \dot{W}_i'.$$

Since the composition is a known function of temperature and pressure, this implies:

$$\dot{W}_i' = \rho_g \left(\frac{\partial K_i}{\partial T}\right)\left[\frac{\partial T}{\partial t} + \vec{V}\cdot\nabla T\right] + \rho_g \left(\frac{\partial K_i}{\partial P}\right)\left[\frac{\partial P}{\partial t} + \vec{V}\cdot\nabla P\right].$$

Substituting this into the energy equation (34) and neglecting diffusion, radiation, and mechanical work terms we get:

$$\left(\rho_P C_{v_p} + \rho_c C_{v_c} + \rho_g \overline{C}_{p_g}\right)\frac{\partial T}{\partial t} - \dot{W}_p\left[(1-f_c)\,h_g + f_c e_c - e_p\right]$$

$$+\rho_g\left(\sum_i h_i \frac{\partial K_i}{\partial T}\right)\left[\frac{\partial T}{\partial t} + \vec{V}\cdot\nabla T\right] + \rho_g\left(\sum_i h_i \frac{\partial K_i}{\partial P}\right)\left[\frac{\partial P}{\partial t} + \vec{V}\cdot\nabla P\right] \quad (50)$$

$$-\dot{W}_c''(h_g - e_c) + \left(\rho_g \overline{C}_{p_g}\vec{V}\right)\cdot\nabla T = \nabla\cdot K\nabla T.$$

The continuity equations (34) - (39), thermal equation of state (40) and the momentum equation (41) remain unchanged.

It is possible to simplify (50) even further by neglecting the gas density in comparison with the solid density, while retaining the mass flow rate term. This implies that as $\rho_g \to 0$, $\rho_g V$ remains finite so that $\vec{V} \to \infty$, i.e., the "residence time" is negligible. This means that the equation of state and the momentum equation are superfluous. The pressure is assumed to be uniform at its ambient value, which is not necessarily steady. The continuity equations remain unchanged except the time derivative of the gas density in (37) is dropped. The energy equation (50) becomes:

$$\left(\rho_p C_{v_p} + \rho_c C_{v_c}\right)\frac{\partial T}{\partial t} + \rho_g \vec{V}\left(\overline{C}_{p_g} + \sum_i h_i \frac{\partial K_i}{\partial T}\right)\cdot\nabla T = \nabla\cdot K\nabla T$$

$$+ \dot{W}_p\left[(1-f_c)\,h_g + f_c e_c - e_p\right] + \dot{W}_c''(h_g - e_i). \quad (51)$$

This equation in one dimension is the equation solved in the REKAP program. Neglecting the gas-solid phase reactions and combining equations (37) - (39) and (51), the following equations result:

Energy:

$$\left(\rho_p C_{v_p} + \rho_c C_{v_c}\right) \frac{\partial T}{\partial t} + \rho_g V \left(\overline{C_{p_g}} + \sum_i h_i \frac{\partial K_i}{\partial T}\right) \frac{\partial T}{\partial X}$$

$$= \frac{\partial}{\partial X}\left(K \frac{\partial T}{\partial X}\right) + \left[\frac{\partial}{\partial t}\left(\rho_P + \rho_c\right)\right] \cdot \left[h_g + \frac{f_c}{1 - f_c} e_c - \frac{1}{1 - f_c} e_p\right].$$

Continuity:

$$\rho_g V = - \int_{X_{BF}}^{X_{FF}} \frac{\partial}{\partial t} (\rho_p + \rho_c) \, dX$$

Density:

$$\frac{\partial}{\partial t}(\rho_p + \rho_c) = - (1 - f_c) \dot{W}_p$$

Some of the nomenclature used above is re-defined for use in the REKAP program. These changes are summarized below.

Derivation	REKAP Program
$\rho_p + \rho_c$	ρ
$\dfrac{\rho_p C_{v_p} + \rho_c C_{v_c}}{\rho_p + \rho_c}$	C_p
$\rho_g V$	$\dot{M}_g$

Derivation	REKAP Program
$\sum_i h_i \frac{\partial K_i}{\partial T}$	H_{cg}
$h_g + \frac{f_c}{1 - f_c} e_c - \frac{1}{1 - f_c} e_p$	H_{gf}
$(1 - f_c) \dot{W}_p$	$\rho_{vp}\left(\frac{\rho - \rho_c}{\rho_{vp}}\right)^{n_1} Z e^{-E/RT}$

10.0 SUMMARY OF REKAP EQUATIONS

Energy:

$$\rho C_p \frac{\partial T}{\partial t} = \frac{\partial}{\partial X}\left(K \frac{\partial T}{\partial t}\right) + M_g\left(\overline{C}_{p_g} + H_{c_g}\right)\frac{\partial T}{\partial X} + H_{gf} \frac{\partial \rho}{\partial t}$$

Continuity:

$$\dot{M}_g = - \int_{X_{FF}}^{X_{BF}} \frac{\partial \rho}{\partial t} \, dX$$

Density:

$$\frac{\partial \rho}{\rho t} = - \rho_{vp}\left(\frac{\rho - \rho_c}{\rho_{vp}}\right)^n Z e^{- E/RT}$$

11.0 ENERGY EQUATION BOUNDARY CONDITIONS

The boundary conditions of present interest are those which describe the heat input or removal from the front and back face of a body and the surface recession at the front face.

11.1 Heat Input to the Body

The heat input to the front face of a body may be specified in any one of three ways: wall temperature (T_W), heat flux ($\dot{q}_c$ and/or $\dot{q}_{HGR}$) or convective heat transfer coefficient ($\dot{q}_c/\Delta h$). Each of these quantities may be time dependent. The heat transfer to or from the back face of the last layer may also be specified as a time dependent quantity.

In order to evaluate the rate of heat conduction ($K\,\partial T/\partial X$) into a body front surface, an energy flux balance is performed according to the following equation:

$$\dot{q}_{NET} = \dot{q}_c + \dot{q}_{HGR} - \dot{q}_{BLK} - \dot{q}_{RR} - \dot{q}_{VAP} .$$

$\dot{q}_c$ and $\dot{q}_{HGR}$ respectively designate the convective and radiative heat fluxes from the external environment to the front surface of the first layer (the surface at which recession occurs). $\dot{q}_{RR}$ denotes the radiative heat flux from the front surface to the surroundings. $\dot{q}_{VAP}$ represents the rate of heat absorption due to vaporization (e.g., sublimation) per unit surface area.

The "blocking" term in the heat balance equation, $\dot{q}_{BLK}$, represents the portion of the convective heat flux which is absorbed due to the injection of degradation gases into the boundary layer. If all of the first three layers of a body char, it is possible for degradation gases from all three layers to flow to the surface of the first layer. The blocking equations which were used in the previous version of the REKAP program are retained in the present version:

$$\dot{q}_{BLK} = \dot{q}_c \left[0.69 \left(\frac{M_{BL}}{M_{AB}} \right)^{1/3} \frac{\varphi_o}{Pr^{1/3}} \right] \quad \text{for a laminar boundary layer,}$$

and

$$\dot{q}_{BLK} = \dot{q}_c \left[1 - e^{-0.38\, C_T \varphi_o} \right] \quad \text{for a turbulent boundary layer}$$

where

$$\varphi_o = \dot{m}_g \frac{1}{\dot{q}_c / \Delta h} .$$

Therefore, $\dot{m}_g$ has been re-defined to mean the total mass flux of gases which originate in all the charring layers and which arrive at the front face of the first layer.

For three charring layers

$$\varphi_o = \left(\dot{m}_{g_1} + F_{12} \cdot m_{g_2} + F_{12} \cdot F_{23} \cdot \dot{m}_{g_3}\right) \frac{1}{\dot{q}_c / \Delta h} \cdot$$

M_{BL}/M_{AB}, Pr and C_T are input to the program for each charring layer (see Appendix B, User's Manual) and the corresponding properties for the gas mixture at the front face of layer one are calculated on a mass-averaged basis as follows (for three charring layers):

$$\left(\frac{M_{BL}}{M_{AB}}\right)_{AVG} = \frac{\left(\frac{M_{BL}}{M_{AB}}\right)_1 \dot{m}_{g_1} + F_{12}\left(\frac{M_{BL}}{M_{AB}}\right)_2 \dot{m}_{g_2} + F_{12} \cdot F_{23} \cdot \left(\frac{M_{BL}}{M_{AB}}\right) \dot{m}_{g_3}}{\dot{m}_{g_1} + F_{12} \cdot \dot{m}_{g_2} + F_{12} \cdot F_{23} \cdot \dot{m}_{g_3}}$$

$$(Pr)_{AVG} = \frac{P_{r_1} \cdot m_{g_1} + F_{12} \cdot P_{r_2} \cdot \dot{m}_{g_2} + F_{12} \cdot F_{23} \cdot P_{r_3} \cdot \dot{m}_{g_3}}{\dot{m}_{g_1} + F_{12} \cdot \dot{m}_{g_2} + F_{12} \cdot F_{23} \cdot \dot{m}_{g_3}}$$

and

$$(C_T)_{AVG} = \frac{C_{T_1} \cdot \dot{m}_{g_1} + F_{12} \cdot C_{T_2} \cdot \dot{m}_{g_2} + F_{12} \cdot F_{23} \cdot C_{T_3} \cdot \dot{m}_{g_3}}{\dot{m}_{g_1} + F_{12} \cdot \dot{m}_{g_2} + F_{12} \cdot F_{23} \cdot \dot{m}_{g_3}}$$

F_{12} and F_{23} have been defined previously (equations 7 and 8):

$$F_{12} = \frac{\rho_{VP_1} - \rho_{LN_1}}{\rho_{VP_1} - \rho_{c_1}} \quad \text{and}$$

$$F_{23} = \frac{\rho_{VP_2} - \rho_{LN_2}}{\rho_{VP_2} - \rho_{c_2}}$$

For fewer than three charring layers the above blocking equations become simplified according to the values of $\dot{m}_{g_1}$, $\dot{m}_{g_2}$, $\dot{m}_{g_3}$, F_{12} and F_{23}.

11.2 Surface Recession

The rate of surface recession due to aerothermochemical action is computed according to any one of five analytical models: no recession, specified char depth, graphite oxidation/sublimation, fixed ablation temperature and the refrasil model. Recession is confined to the first material layer.

The "no recession" model permits no body dimensional change and allows all of the incoming convective and radiative heat to be conducted into the body, except that which is re-radiated from the surface.

With the "specified char depth" option no recession occurs until the char depth equals a specified maximum. Char depth is arbitrarily defined as the distance from the front surface to the point at which the density is ninety-seven percent of the virgin (uncharred) material density. After the char depth attains it maximum, the surface recedes according to:

$$\dot{S}_m = \frac{\dot{m}_{g_{FF}}}{\rho_{VP} - \rho_c}$$

in which

$$\dot{m}_{g_{FF}} = -\int_{X_{FF}}^{X_{BF}} \left(\frac{\partial \rho}{\partial t}\right) \, dx.$$

The equation for $\dot{m}_{g_{FF}}$ states that the mass flux of degradation gas at a layer front face is equal to the solid material decomposition rate integrated across the layer. For a composite material, the binder material (e.g., resin) gasifies during the decomposition process. The density of the binder is approximately given by $(\rho_{VP} - \rho_c)$. Therefore, $\dot{S}_m$ in the above equation is a measure of the rate at which the decomposition reaction zone moves through the material.

The "graphite oxidation/sublimation" recession computation is based on the theoretical model for the mass removal of graphite in an air boundary layer as derived by Scala (Reference 8) and by Scala and Gilbert (Reference 9). The rate of surface recession is given by:

$$\dot{S}_m = \frac{1}{\rho_{SURF}} \left[\frac{\dot{q}_c}{K_1 + K_2 (H_R - C_{p_{BL}} T_W)}\right] \left[1 + 2.64 \times 10^9 \, P_e^{-0.67} \, e^{-\frac{11.05 \times 10^4}{T_W}}\right].$$

The first bracketed term in this equation represents $\dot{m}_D$, the mass loss rate for the "diffusion-controlled regime". This term controls $\dot{S}_m$ over the wall temperature range for which the dominating mechanism of mass removal is the diffusion of oxygen-bearing species across the boundary layer to the surface. The second bracketed term accounts for recession due to sublimation. The REKAP program employs the assumption that graphite surface recession is negligible in the "reaction rate-controlled regime".

Figures A-2 and A-3 illustrate the wall temperature dependence of the various mechanisms of graphite ablation.

With the "fixed ablation temperature" model no recession occurs until a specified surface temperature is attained. The recession rate is expressed as follows:

$$\dot{S}_m = \frac{\dot{q}_{NET} + \left(K\frac{\partial T}{\partial X}\right)_{SURF.}}{\Gamma \rho_c L},$$

where

$$\dot{q}_{NET} = \dot{q}_c + \dot{q}_{HGR} - \dot{q}_{RR} - \dot{q}_{BLK.}$$

The numerator of the equation for $\dot{S}_m$ represents the heat available for melting or vaporizing material at the surface. The denominator equals the heat absorbed per unit volume in the melting or vaporization process. The term Γ may be interpreted as:

$$\Gamma = \frac{(\dot{S}_c)_{M,V}}{(\dot{S}_c)_{M,V} + (\dot{S}_c)_{MECH}}$$

in which $(\dot{S}_c)_{M,V}$ is the rate of char recession due to melting or vaporization and $(\dot{S}_c)_{MECH.}$ is the recession rate due to mechanical action (e.g., aerodynamic shear or char "pop-off"). The value of Γ is determined empirically.

The "refrasil option" was originally developed to predict the surface recession of phenolic refrasil. However, with the proper choice of β_1, β_2 and β_3 in the following equation it may be successfully applied to many other materials. Surface recession is computed according to:

$$\dot{S}_m = \beta_1 T_W^{\beta_2} e^{-\beta_3/T_W}.$$

The values of β_1, β_2, and β_3 must be experimentally measured for the material of interest.

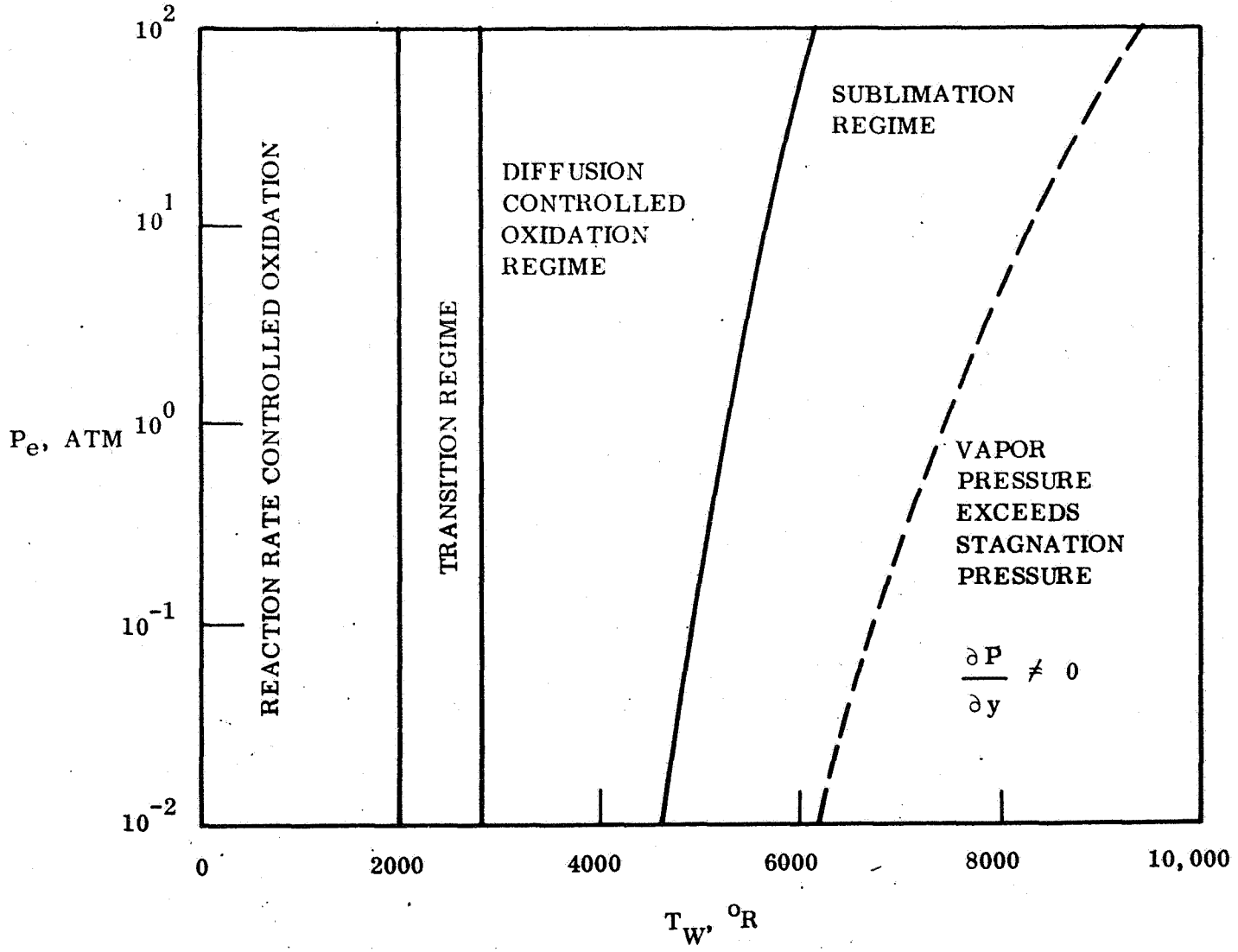

Figure A-2. Mass Transfer Regimes for Ablating Graphite

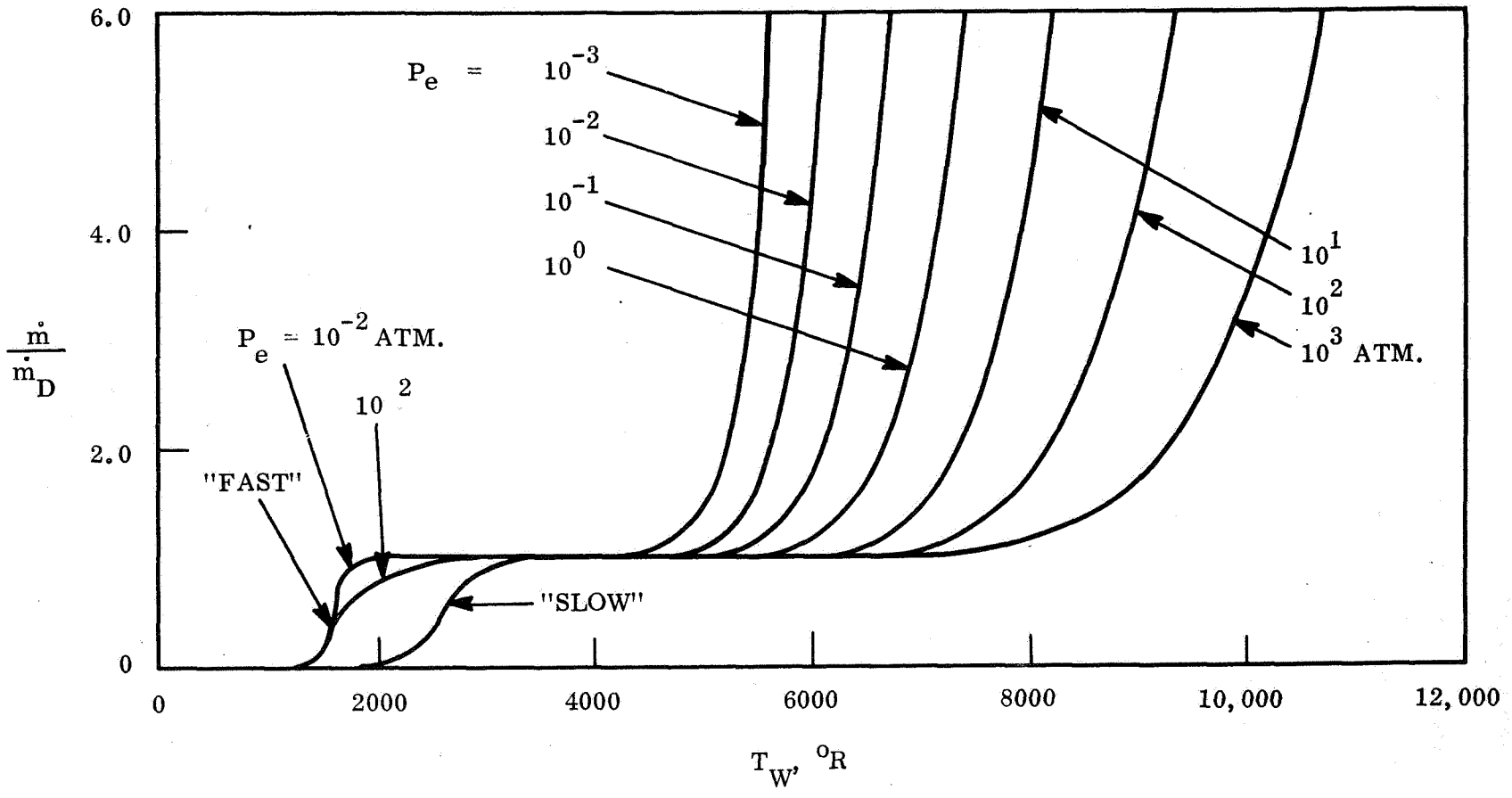

Figure A-3. Normalized Ablation Rate of Graphite Over the Entire Range of Surface Temperature

12.0 NOMENCLATURE

A	surface area	ft^2
C_v	specific heat at constant volume	BTU/lbm^oR
C_p	specific heat at constant pressure	BTU/lbm^oR
$\overline{C_{pg}}$	$\Sigma_i K_i C_{pi}$	BTU/lbm^oR
$C_{p_{bl}}$	specific heat of the boundary layer gases	BTU/lb
C_T	Dimensionless constant used in turbulent blocking calculation	
D_{i_j}	multicomponent diffusion coefficient	ft^2/sec
D_{12}	binary diffusion coefficient	ft^2/sec
e	specific internal energy	BTU/lbm
e_F	energy of formation	BTU/lbm
$\vec{e}$	unit base vector	
f_c	fraction of unreacted material that forms char	
H_r	recovery enthalpy	BTU/lb
h_{FF}	boundary layer gas enthalpy at wall temperature	BTU/lb
k	permeability	ft^2
K	Thermal conductivity	BTU/ft-sec^oR
K_i	$\frac{\rho_i}{\rho}$ = mass concentration	
K_{i_j}	conductivity tensor	BTU/ft-sec^oR
K_1	quantity used in the graphite diffusion regime mass loss equation	BTU/lb
K_2	dimensionless quantity used in graphite diffusion regime mass loss equation	lb/lb-mole
L	latent heat of fusion or vaporization	BTU/lb
$\dot{m}_g$	degradation gas mass flux	lb/ft^2-sec.

M	$\dfrac{1}{\sum \dfrac{K_i}{M_i}}$ = average molecular weight	lbm/mole
n	total number of moles per unit volume; degradation reaction order	$moles/ft^3$
p	pressure	lbf/ft^2
$\vec{P}$	surface force per unit area	lbf/ft^2
P_e	boundary layer edge pressure	lb/ft^2
Pr	Prandtl number of the boundary layer gases	
ϵ	porosity	
$\tilde{\rho}_c$	final density of the char based on the volume of the char	lbf/ft^3
$\tilde{\rho}_{vp}$ or ρ_{vp}	initial density of the virgin plastic	lbf/ft^3
$\dot{q}_c$	convective heat flux	BTU/ft^2-sec
$\dot{q}_{HGR}$	heat flux due to hot gas radiation	BTU/ft^2-sec
$\dot{q}_{RR}$	reradiative heat flux	BTU/ft^2-sec
$\dot{q}_{BLK}$	convective heat flux blocked due to mass injection	BTU/ft^2-sec
$\vec{qc}$ or $\vec{q}_c$	conduction heat flux vector	BTU/ft^2-sec
$\vec{qR}$ or $\vec{q}_R$	radiant heat flux vector	BTU/ft^2-sec
R	universal gas constant	lbf ft/lbm mole^oR
$\dot{S}_m$	rate of surface recession,	ft/sec
T	temperature	^oR
T_r	recovery temperature	^oR
T_w	wall temperature	^oR
T_{bf}	temperature of backface	^oR
$\underset{\sim}{T}$	stress tensor	lbf/ft^2

V	volume	ft^3
$\vec{V}_i$	absolute velocity of ith species	ft/sec
$\vec{V}_{d_i}$	diffusion velocity of ith species	ft/sec
$\vec{V}$	mass averaged velocity	ft/sec
$\dot{W}_i$ or ω_i	net rate of production of the ith gaseous species due to all chemical reactions	lbm/ft^3
$\dot{W}_i'$ or $\dot{\omega}_i'$	net rate of production of ith species due to gas phase reactions	lbm/ft^3
$\dot{W}_g''$ or $\dot{\omega}''_g$	rate of production of gas due to gas-solid phase reactions	lbm/ft^3
X	mole fraction	
$\vec{\eta}$	outward unit normal	
ρ	density	lbm/ft^3
σ_{i_j}	component of the stress tensor	lbf/ft^2
$\underset{\sim}{\tau}$	viscous stress tensor	lbf/ft^2
μ	gas viscosity	$lbf\text{-}sec/ft^2$
σ	Stefan-Boltzmann constant (0.476×10^{-12} BTU/sec-$ft^2\,{}^oR^4$)	
Γ	gasification ratio	
φ_o	dimensionless ratio used in blocking calculation	

SUBSCRIPTS

AB	Ablative material
BL	Boundary layer
c	Char
g	Gas
p	Virgin plastic

13.0 REFERENCES

1. Von Karman, T., "Fundamental Equations in Aerothermochemistry" Proc. 2nd AGARD Combustion Collog., Liege, Belgium, Dec. 1955.

2. Muskat, M., The Flow of Homogeneous Fluids Through Porous Media, J.W. Edwards Inc., 1946.

3. Sokolnikoff, I.S. and Redheffer, R.M., Mathematics of Physics and Modern Engineering, McGraw Hill, 1958.

4. Scala, S.M., "The Equations of Motion in a Multicomponent Chemically Reacting Gas," General Electric Co. Missile and Ordnance Systems Dept., Doc. No. R58SD205, Dec. 1957.

5. Hirschfelder, J.D., Curtiss, C.F. and Bird, R.B., Molecular Theory of Gases and Liquids, John Wiley and Sons, 1954.

6. Bird, R.B., Stewart, W.E., and Lightfoot, E.N., Transport Phenomena, John Wiley and Sons, 1960.

7. Aris, R.A., Vectors, Tensors and The Basic Equations of Fluid Mechanics Prentice Hall, 1962.

8. Scala, S.M., "The Ablation of Graphite in Dissociated Air, Part I - Theory", IAS Paper No. 62-154, Thirtieth National Summer Meeting, June 1962; also G.E. Co., MSD, TIS R62SD72, September 1962.

9. Scala, S.M., and Gilbert, L.M., "Aerothermochemical Behavior of Graphite at Elevated Temperatures," G.E. Co., MSD, TIS R63SD89, November, 1963.

14.0 BIBLIOGRAPHY

1. Von Karman, T., "Fundamental Equations in Aerothermochemistry" Proc. 2nd AGARD Combustion Collog., Liege, Belgium, Dec. 1955.

2. Scala, S.M., "The Equations of Motion in a Multicomponent Chemically Reacting Gas," General Electric Co. Missile and Ordnance Systems Dept., Doc. No. R58SD205, Dec. 1957.

3. Hirschfelder, J.D., Curtiss, C.F. and Bird, R.B., Molecular Theory of Gases and Liquids, John Wiley and Sons, 1954.

4. Bird, R.B., Stewart, W.E., and Lightfoot, E.N., Transport Phenomena, John Wiley and Sons, 1960.

5. Hayday, A.A., "Governing Equations of Multicomponent Fluid Continua with Chemical Reactions," University of Illinois, Technical Report No. ILL-6-P (Project SQUID), April 1962.

6. Sokolnikoff, I.S. and Redheffer, R.M., Mathematics of Physics and Modern Engineering, McGraw Hill, 1958.

7. Carslaw, H.S. and Jaeger, J.C., Conduction of Heat in Solids, Oxford Press 1959.

8. Aris, R.A., Vectors, Tensors and The Basic Equations of Fluid Mechanics Prentice Hall, 1962.

9. Muskat, M., The Flow of Homogeneous Fluids Through Porous Media, J.W. Edwards Inc., 1946.

10. Kratsch, K.M., Hearne, L.F. and McChesney, H.R., "Thermal Performance of Heat Shield Composites During Planetary Entry," paper presented at the AIAA-NASA National Meeting, Palo Alto, Calif., Oct. 1963.

11. Lafazan, S., and Welsh, W.E., Jr., "The Charring Ablator Concept: Application to Lifting Orbital and Superorbital Entry," paper presented at the Symposium on Dynamics of Manned, Lifting Planetary Entry, Philadelphia, Pa., 1963.

12. Munson, T.R. and Spindler, R.J., "Transient Thermal Behavior of Decomposing Materials, Part I: General Theory and Application to Convective Heating," paper presented at IAS 30th Annual Meeting, New York, N.Y. Jan. 1962.

13. Wells, P.B., "A Method for Predicting the Thermal Response of Charring Ablation Materials," The Boeing Co., Aero Space Div., Doc. No. D2-23256, June, 1964.

14. Pappas, C.C. and Okuno, A.F., "Measurements of Skin Friction of the Compressible Turbulent Boundary Layer on a Cone with Foreign Gas Injection", Journal of the Aerospace Sciences, May 1960.

15. Tewfik, O.E., Jurewicz, L.S., and Eckert, E.R.G., "Measurements of Heat Transfer from a Cylinder with Air Injection into a Turbulent Boundary Layer," ASME Paper No. 63-HT-45, August 1963.

16. Bartle, E.R. and Leadon, B.M., "The Effectiveness as a Universal Measure of Mass Transfer Cooling for a Turbulent Boundary Layer," Proceedings of the 1962 Heat Transfer and Fluid Mechanics Institute, Stanford Univ. Press, June, 1962.

17. Leadon, B.M. and Scott, C.J., "Measurement of Recovery Factors and Heat Transfer Coefficients with Transpiration Cooling in a Turbulent Boundary Layer at M = 3 Using Air and Helium as Coolants," Rosemount Aero. Lab. Research Report Number 126, February 1956.

18. Gross, Hartnett, Masson, and Gazley: "A Review of Binary Laminar Boundary Layer Characteristics" - International Journal of Heat and Mass Transfer, 3,3, pages 198 to 221, October 1961.

19. Baron: "The Binary Boundary Layer Associated with Mass Transfer Cooling at High Speed" - MIT Naval Supersonic Lab Report 160 (1956).

20. Eckert, Schenider, Hayday and Larson: "Mass Transfer Cooling of a Laminar Boundary Layer by Injection of a Light Weight Gas" - Rand Symposium on Mass Transfer Cooling for Hypersonic Flight.

21. Sziklas and Banas: "Mass Transfer Cooling in Compressible Laminar Flow" - Rand Symposium on Mass Transfer Cooling for Hypersonic Flight.

22. Hartnett and Eckert: "Mass Transfer Cooling in a Laminar Boundary Layer with Constant Fluid Properties: - Trans. ASME, 79, 247 (1957).

23. Eckert: "Engineering Relations for Heat Transfer and Skin Friction in High Velocity Laminar and Turbulent Boundary Layer Flow over Surfaces with Constant Pressure and Temperature" - Trans. ASME 78, 1273 (1956).

24. Gross: "The Laminar Binary Boundary Layer" - RM-1915 - The Rand Corporation, September 1956.

25. Spalding: "Mass Transfer through Laminar Boundary Layers - 1. The Velocity Boundary Layer" Int. J. Ht. Mass Transfer, 3, Nos. 1 and 2, Pg. 15, March 1961.

26. Faulders: "Heat Transfer in the Laminar Boundary Layer with Ablation of Vapor of Arbitrary Molecular Weight" - J. Aero. Sci 29, 1, 76, Jan. 1962.

27. Eckert, Hayday and Minkowycz: "Heat Transfer, Temperature Recovery, and Skin Friction on a Flat Plate with Hydrogen Release into a Laminar Boundary Layer" - Int. J. Ht. Mass Trans. 4, Page 17, Dec. 1961.

28. Emmons and Leigh: "Tabulation of the Blasius Function with Blowing and Sunction" Harvard Report: Combustion Aero Lab Int. Tech. Rpt. #9 (1953).

29. Lew and Fanucci: "The Laminar Compressible Boundary Layers Over a Flat Plate with Sunction or Injection" - J. Aeron. Sci. 22, 9, pg. 589-597, September 1955.

30. Brown: "Tables of Exact Laminar Boundary Layer Solutions when the Wall is Porous and Fluid Properties are Variable" - NACA TN 2479 - September 1951.

31. Eschenroeder: "The Compressible Laminar Boundary Layer with Constant Injected Mass Flux at the Surface" - Jour. Aero - Space Sceinces, 26, 11, Pg. 762 (1959).

32. Mickley, Ross, Squyers, & Stewart: "Heat, Mass and Momentum Transfer for Flow Over a Flat Plate with Blowing and Sunction" - NACA TN 3208 (1954).

33. Stewart: "Transpiration Cooling: An Engineering Approach" - General Electric Missile and Space Vehicle Department Report R59SD338 - May 1, 1959.

34. Schlichting: "Boundary Layer Theory", Pergamon Press (1955).

35. Nestler, D.E., "The Effects of Liquid Layers on Ablation Performance" - General Electric Co., RSD, Thermodynamics Fund. Memo No. 022, TFM-8151-022, December, 1963.

36. Scala, S.M., "The Ablation of Graphite in Dissociated Air, Part I - Theory", IAS Paper No. 62-154, Thirtieth National Summer Meeting, June 1962; also G.E. Co., MSD, TIS R62SD72, September 1962.

37. Scala, S.M., and Gilbert, L.M., "Aerothermochemical Behavior of Graphite at Elevated Temperatures," G.E. Co., MSD, TIS R63SD89, November, 1963.

APPENDIX B

USER'S MANUAL FOR THE ONE-DIMENSIONAL THREE CHARRING LAYER REKAP PROGRAM

TABLE OF CONTENTS

1.0 APPLICABILITY OF THE PROGRAM

The Reaction Kinetics Ablation Program (REKAP) is used to predict the performance of an externally heated composite slab of ablative material. The surface recession and in-depth temperature and density histories are computed. The program is primarily directed to problems in which a hot gaseous boundary layer (as exists in a rocket nozzle or adjacent to a re-entry vehicle) heats an ablative material which thermally degrades ("chars") in depth. Of course, the program readily handles the simpler problem of heat conduction in non-charring materials.

2.0 KEY ENGINEERING FEATURES OF THE PROGRAM

The REKAP program is written in the FORTRAN IV language for either the IBM 7094 or for the General Electric 635 computer. A brief description of the engineering capability of the program is presented below.

2.1 Energy Equation

The main function of the REKAP program is to compute solutions of an equation which describes the conservation of thermal energy in a charring material. This equation may be written as follows (see Nomenclature):

$$\rho C_P \frac{\partial T}{\partial t} = \frac{\partial}{\partial X}\left(K \frac{\partial T}{\partial X}\right) + H_{g_f} \frac{\partial \rho}{\partial t} + \overline{C}_{P_g} \dot{m}_{g_T} \frac{\partial T}{\partial X} + H_{c_g} \dot{m}_{g_T} \frac{\partial T}{\partial X} \qquad \text{(B-1)}$$

1 2 3 4 5

STORAGE CONDUCTION DECOMP. CONVECTION CHEMICAL REACTION

Equation (B-1) states that over a given time interval the net rate of heat being stored within a volume of ablative material is equal to the algebraic sum of four other rates of energy exchange: the rate of heat conduction into the volume, the rate of heat absorption due to decomposition of the solid material into gas, the rate of convective cooling by the degradation gases as they flow through the volume (made porous by the decomposition process) and the rate of heat transfer to the solid material due to chemical reactions among the degradation gases. For a non-charring material, terms 3, 4, and 5 of equation (B-1) equal zero.

2.2 Thermal Degradation

For a charring material REKAP computes the rate of thermal degradation (i.e., density change) according to the following relation:

$$\frac{\partial \rho}{\partial t} = -\rho_{vp} \left(\frac{\rho - \rho_c}{\rho_{vp}}\right)^{\eta} Ze^{-E/RT} \qquad \text{(B-2)}$$

in which Z and E may be density dependent. For many materials Z and E are chiefly dependent on temperature regime and equation (B-2) takes the form:

$$\frac{\partial \rho}{\partial t} = - \rho_{vp} \left(\frac{\rho - \rho_c}{\rho_{vp}} \right)^{\eta} \left(Z_1 e^{-E_1/RT} + Z_2 e^{-E_2/RT} + \ldots Z_n e^{-E_n/RT} \right) \quad \text{(B-3)}$$

in which each Z, E pair dominates for a particular temperature range.

2.3 Body Configuration

The program may be applied to a body composed of ten material layers. Any combination of charring or non-charring materials may be used in the first three layers.

Any sub-layer may be a gas gap, across which heat is transferred by conduction and radiation. The radiative transfer across the gap is computed according to the following equation:

$$\dot{q}_{R_{GAP}} = \sigma F_e F_a (T_1^4 - T_2^4) \quad \text{(B-4)}$$

in which the factor F_e may be interpreted as follows:

$$F_e = \frac{1}{\frac{1}{\epsilon_1} + \frac{1}{\epsilon_2} - 1} \quad \text{(B-5)}$$

ϵ_1 and ϵ_2 are respectively equal to the emissivity of the solid material at the front and at the back of the gas gap. F_a is the radiation view factor.

If it is recognized that the temperature difference across a layer is negligibly small, the calculation may be simplified by instructing the program to compute only one temperature for such a layer. One of these "thermal capacitance" layers may be inserted behind each of the ten "normal layers" (making twenty layers in all).

2.4 Coordinate Systems

A Cartesian, cylindrical or spherical coordinate system may be used. Each layer is divided into "nodes" with initial spacing specified by the program user. By definition, all properties (e.g. T and ρ) are invariant with distance across a node.

The program automatically makes a coordinate transformation to allow the first layer nodes to shrink as the layer thickness decreases due to ablation.

Time-dependent node squeezing toward the front face of layer one may be employed. By this means the nodes are made close together near the front face and progressively farther apart toward the back face according to an exponential function. This feature is especially useful for cases in which a steep temperature gradient exists near the front face for only a portion of the total time span of interest.

2.5 Material Properties

The values of all material properties used in the program may be temperature-dependent. For charring materials the thermal conductivity and the specific heat are considered to be functions of both temperature and density according to:

$$K = \left[K\,(T)\right]\left[1-C_1 + C_1\left(\frac{\rho-\rho_c}{\rho_{vp}-\rho_c}\right)^{N_1}\right] \quad \text{and} \qquad \text{(B-4)}$$

$$C_P = \left[C_P(T)\right]\left[1-C_2 + C_2\left(\frac{\rho-\rho_c}{\rho_{vp}-\rho_c}\right)^{N_2}\right]. \qquad \text{(B-5)}$$

K(T) and $C_P(T)$ are the temperature dependent values which are input to the program. C_1, N_1, C_2 and N_2 are empirically determined input constants, while ρ is the instantaneous computed value of density for a particular node and computation time step.

2.6 Heating Environment

The time-dependent radiative and/or convective front surface heating are included in the program input data.

In some cases it is advantageous to use an approximate analytical solution (semi-infinite slab) to compute the temperature response during initial heating. The REKAP program provides two of these solutions: one for constant heating for an initial time increment, the other for heating which increases linearly with time from zero at time zero to a desired value at the end of a specified time interval.

The time-dependent heating (or cooling) rate at the back face of the last layer may be specified.

Surface cooling mechanisms include re-radiation, heat absorption due to melting or vaporization, the "blocking" of convective heating due to outgassing of the decomposition gases at the surface, and heat conduction into the body. The portion of the laminar convective heat flux which is "blocked" is expressed as a function of the mass flux, molecular weight and Prandtl number of the decomposition gases:

$$\dot{q}_{BLK} = \dot{q}_c \left[0.69 \left(\frac{M_{BL}}{M_{AB}} \right)^{1/3} \frac{\varphi_o}{Pr^{1/3}} \right] , \text{ in which} \qquad \text{(B-6)}$$

$$\varphi_o = \dot{m}_{g_T} \frac{1}{\dot{q}_c/\Delta h} . \qquad \text{(B-7)}$$

$\dot{m}_{g_T}$ is the total mass flux of the decomposition gases at the frontface. For a turbulent boundary layer,

$$\dot{q}_{BLK} = \dot{q}_c \left(1 - e^{-0.38\, C_T \varphi_o}\right) . \qquad \text{(B-8)}$$

The value of C_T is empirically determined and depends on the composition of the charring material and on the properties of the boundary layer gases.

2.7 Surface Recession

The rate of surface recession due to aerothermochemical action is computed according to any one of five analytical models: no recession, specified char depth, graphite oxidation/sublimation, fixed ablation temperature and the refrasil model. Recession is confined to the first material layer.

The "no recession" model permits no body dimensional change and allows all of the incoming convective and radiative heat to be conducted into the body, except that which is re-radiated from the surface.

With the "maximum char thickness" option no recession occurs until the char depth equals a specified maximum. Char depth is arbitrarily defined as the distance from the front surface to the point at which the density is ninety-seven percent of the virgin (un-charred) material density. After the char depth attains its maximum, the surface recedes according to:

$$\dot{S}_m = \frac{\dot{m}_{g_{FF}}}{\rho_{vp} - \rho_c} \quad \text{in which} \tag{B-9}$$

$$\dot{m}_{g_{FF}} = - \int_{X_{FF}}^{X_{BF}} \left(\frac{\partial \rho}{\partial t}\right) dx. \tag{B-10}$$

Equation (B-10) states that the mass flux of degradation gas at a layer front face is equal to the solid material decomposition rate integrated across the layer. For a composite material, the binder material (e.g. resin) gasifies during the decomposition process. The density of the binder is approximately given by $(\rho_{vp} - \rho_c)$. Therefore, $\dot{S}_m$ in equation (B-9) is a measure of the rate at which the decomposition reaction zone moves through the material.

The graphite oxidation/sublimation recession computation is based on the theoretical model for the mass removal of graphite in an air boundary layer as derived by Scala (Reference 1) and by Scala and Gilbert (Reference 2). The rate of surface recession is given by:

$$\dot{S}_m = \frac{1}{\rho_{SURF.}} \left[\frac{\dot{q}_c}{K_1 + K_2\left(H_R - C_{P_{BL}} T_W\right)}\right] \left[1 + 2.64 \times 10^9 P_e^{-0.67} e^{-\frac{11.05 \times 10^4}{T_W}}\right]. \tag{B-11}$$

The first bracketed term in equation (B-11) represents the mass loss rate for the "diffusion-controlled regime". This term dominates over the wall temperature range for which the dominating mechanism for mass removal is the diffusion of oxygen-bearing species across the boundary layer to the surface. The second bracketed term accounts for recession due to sublimation.

With the fixed ablation temperature model no recession occurs until a specified surface temperature is attained. The recession rate is expressed as follows:

$$\dot{S}_m = \frac{\dot{q}_{NET} + \left(K \frac{\partial T}{\partial X}\right)_{SURF.}}{\Gamma \rho_c L} \text{, where} \tag{B-12}$$

$$\dot{q}_{NET} = \dot{q}_c + \dot{q}_{HGR} - \dot{q}_{RR} - \dot{q}_{BLK.} \qquad \text{(B-13)}$$

The numerator of equation (B-12) represents the heat flux available for melting or vaporizing material at the surface. The denominator equals the heat absorbed per unit volume in the melting or vaporization process. The term Γ may be interpreted as:

$$\Gamma = \frac{(\dot{S}_c)_{M,V}}{(\dot{S}_c)_{M,V} + (\dot{S}_c)_{MECH.}} \quad \text{in which } (\dot{S}_c)_{M,V} \text{ is} \qquad \text{(B-14)}$$

the rate of char recession due to melting or vaporization and $(\dot{S}_c)_{MECH.}$ is the recession rate due to mechanical action (e.g. aerodynamic shear or char "popoff"). The value of Γ is determined empirically.

The "refrasil option" was originally developed to predict the surface recession of phenolic refrasil. However, with the proper choice of constants (equation B-15) it may be successfully applied to many other materials. Surface recession is computed according to:

$$\dot{S}_m = \beta_1 T_W^{\beta_2} e^{-\beta_3/T_W} . \qquad \text{(B-15)}$$

The values of β_1, β_2, and β_3 must be experimentally measured for the material of interest.

2.8 Simplifications for Successive Computer Runs

If REKAP computer runs are to be made for a group of similar problems the entire set of runs may be submitted simultaneously. For example, it may be desirable to evaluate the performance of a particular ablative rocket nozzle throat insert in two different rocket flow environments. The two computer runs could be made "back-to-back", so that the only input data required for the second case would be the different boundary layer information (heat transfer coefficient, etc.). The Program would be loaded into the computer only once. This scheme typically saves about two minutes of machine time per run.

An initial in-depth distribution of temperature and density may be employed. In this case, tables of T and ρ versus x are included in the program input data.

3.0 GENERAL DESCRIPTION OF PROGRAM INPUT

Except for the Hollerith identification card all of the input data must be in table form.

The magnitudes of quantities contained in the independent tables must be in ascending order.

The dependent tables may contain one value, two values or an entire table. If one value is used, the program fills the table with that value according to the number of entries in the corresponding independent table. If two values are entered into a dependent table, the program linearly interpolates to fill the table.

The input tables may be arranged in any order. If a table occupies more than one card, then the cards for that particular table must be in consecutive order.

With the exception of initial temperature-density distribution problems, successive cases may be submitted simultaneously with input data consisting only of that which differs from the first case of the set.

3.1 Preparation of Punched Card Input

The following description of the REKAP program input applies to the system used at the NASA Lewis Research Center. Some modifications may be required for program operation at other computer facilities.

The first input data card must be a Hollerith alphanumeric identification card. Card columns 1 through 72 may be used. This is the only card for which card column 1 may be used.

The second input card must contain $REKAP with the $ in column 2.

All of the input data tables follow the $REKAP card. These tables may be arranged in any order. If a table occupies more than one card, then the cards for that particular table must be in consecutive order. A comma "," must be placed at the end of each table.

GENRL TABLE

This table may contain 20 values. Not all of these locations are used at present.

GENRL(1) = Start time in seconds.

GENRL(2) = Stop time in seconds.

GENRL(3) =
- $-\Delta t$ in seconds: use approximate (semi-infinite slab) solution assuming constant heat flux from t = GENRL(1) to t = GENRL(1) $+\Delta t$. Heat flux is entered in the TTABL table.
- 0: normal REKAP solution
- Δt in seconds: use approximate (semi-infinite slab) solution assuming heat flux = 0 at t = GENRL(1) with flux increasing linearly with t from t = GENRL(1) until t = GENRL(1) + Δt. The value of heat flux at t = GENRL(1) + Δt is entered in the TTABL table.

GENRL(4) = Initial temperature throughout body, in degrees R. except if an initial distribution of T and ρ vs. X is desired, GENRL(4) must be zero. In this case the T and ρ distribution is entered in the XFØRT, TMT, XFØRDN and TMDENS tables.

GENRL(5) =
- 0: first TTABL table is convective heat flux, $\dot{q}_c$.
- 1: first TTABL table is film coefficient, $\dot{q}_c/\Delta h$.
- -1: first TTABL table is front face temperature, T_W.

GENRL(6) = Number of layers

GENRL(7) =
- 0: fifth TTABL table is $\dot{q}$ at back face of last layer
- 1: fifth TTABL table is T at back face of last layer

GENRL(8) = 0

GENRL(9) =
- 0: Cartesian coordinate system
- r: Radius of curvature in feet for innermost surface in cylindrical coordinate system (see sketch)
- -r: Radius of curvature in feet for innermost surface in spherical coordinate system (see sketch)

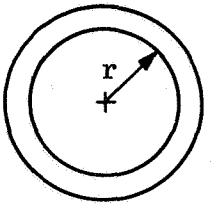

GENRL(10) =

0: Heat flow direction is nominally from the front surface toward the back surface; for cylindrical or spherical coordinates heat flow is from the outside toward the center of curvature (layer 1 is the outside layer).

1: Heat flow direction is nominally from the back surface toward the front surface; for cylindrical or spherical coordinates heat flow is from the inside away from the center of curvature (layer 1 is the outside layer).

GENRL(11) =

0: output lengths in feet

1: output lengths in inches

GENRL(12) =

0: Either there is no ZORET table (therefore no in-depth thermal decomposition) or the Z and E values in the ZORET table are density dependent (which requires a TDENS table).

1: The ZORET table contains one pair of Z and E values for each charring (decomposing) layer and the Z and E values are not density dependent (there is no TDENS table).

2: Same as 1 above except that ZORET contains two Z and E pairs for each charring layer.

3: Same as 1 above except that ZORET contains three Z and E pairs for each charring layer.

Sample Problem

The interior of a 3-layer ablative rocket nozzle throat insert is exposed to a constant heat flux from time 20 seconds to time 80 seconds at which the heat flux drops to zero and cool-down occurs until time 300 seconds. It is desired to make a REKAP run for the full 280 second firing-cool-down cycle. It is estimated that the semi-infinite slab constant heat flux solution (see Section 2.6 of this Appendix) may be used for the first 0.1 seconds of heating. The throat insert is initially at 540 degrees R. The convective heat input to the insert is expressed in terms of a heat transfer coefficient $\dot{q}_c/\Delta h$ (to be entered in the TTABL table). The nozzle throat radius is one inch (0.08333 ft.). The outermost (i.e. farthest from the center of curvature) surface of the third material layer is to be cooled at a rate which will be entered into the fifth TTABL table. The second material layer decomposes according to a reaction which is described by 3 pairs of Z and E values which will be entered into the ZORET table. No density dependence of Z and E is desired (there is no TDENS table). The lengths which appear in the REKAP output are to be in inches (e.g. surface recession rate is to be in inches/sec. and temperature profile is to be given as T versus X in inches). The GENRL input table for this problem is:

```
GENRL  =  20,300 -.1,540,1,3,0,0,.08333,1,1,3,
```

card column 2

THIKN Table

This table gives the body layer thicknesses (in feet) for as many as 10 layers (including a gas gap).

Sample Problem

For 5 layers with thicknesses of 0.1, 0.2, 0.2, 0.5 and 0.1 inches, the THIKN table is:

THIKN = .00833, .01667, .01667, .04167, .00833,

or

THIKN = .00833, 2*.01667, .04167, .00833,
(See note at bottom of this page)

DENSE Table

This table contains the initial densities (in lb/ft^3) for the layers. If one of the layers is a gas gap enter the gas specific heat, C_p, in BTU/lb-deg. R. instead of the density in this table.

Sample Problems

(1) For 3 layers with initial densities of 104, 96 and 96 lb/ft^3, the DENSE table is:

DENSE = 104, 96, 96,

or

DENSE = 104, 2*96,

(2) For a case similar except that layer 2 is a gas gap having a specific heat of 0.24 BTU/lb-deg. R., the DENSE table is:

DENSE = 104, .24, 96,

NOTE: If n consecutive entries in any of the input tables are of equal value V, the format n*V may be used (e.g., the 2*.01667 in the THIKN table sample problem).

WARM Table

This is the independent table of temperatures (in degrees R.) for all of the temperature-dependent tables (PRØPT, CTABL, HTABL and GASPR). This table may contain a maximum of 20 values, which must be in ascending order. The program will linearly interpolate for intermediate temperature values but will not extrapolate. Therefore, the table should span a somewhat wider temperature range than that which could exist in the REKAP solution for the problem at hand.

Sample Problem

The temperature dependence of the quantities in the HTABL, CTABL and GASPR tables can be adequately described using only 3 temperature values (1000, 2000 and 5000 degrees R.). However, the thermal conductivity (entered in the PRØPT table) for one of the materials in the body has an irregular temperature dependence which requires specification of the conductivity at 1050, 1100, 1500, 2500 and 4000 degrees R. The WARM table for this problem is:

```
WARM  =  1000, 1050, 1100, 1500, 2000, 2500, 4000, 5000,
```

NWARM Table

This table contains the number of entries in the WARM table. The NWARM table corresponding to the WARM Table sample problem is:

```
NWARM  =  8,
```

PRØPT Table

This temperature dependent composite table (made up of several sub-tables) contains the initial values of specific heat, C_P (in BTU/lb-deg. R), thermal conductivity, K (in BTU/sec-deg. R. -ft) and the derivative of thermal conductivity with respect to temperature, dK/dT (in BTU/sec-deg. R^2-ft) for all of the material layers (except for a gas gap layer). There must be a value given for each of these properties for every temperature in the WARM table, with the following exceptions: (a) if a zero is entered for dK/dT the Program will compute dK/dT from the K and T values given in the PRØPT and WARM tables respectively, (b) for a gas gap layer the density (in lb/ft^3) must be entered in the position where the specific heat would be placed for a solid material layer and (c) for a gas gap layer enter a zero for the thermal conductivity (see AGPTB table).

The property values must be in the following order:

C_P values for layer 1, K values for layer 1, dK/dT values for layer 1,

C_P values for layer 2, K values for layer 2, dK/dT values for layer 2,

C_P values for layer 3, K values for layer 3, dK/dT values for layer 3, etc.

Every value in the PRØPT table must be followed by a comma.

Sample Problem

The WARM table contains 3 temperatures: 500, 1000 and 5000 degrees R. The body of interest consists of 3 layers of which the second layer is a gas gap. It is desired to have the Program compute the values of dK/dT. The C_P and K for the layers are given in the table below.

Layer	T deg. R.	C_P BTU/lb-deg. R.	K BTU/sec-deg. R. -ft	Density $lb/ft.^3$
1	500	0.1	0.016	(in DENSE table)
	1000	.25	.010	(in DENSE table)
	5000	.38	.007	(in DENSE table)
2	500	(in DENSE table)	(in AGPTB table)	0.09
	1000	(in DENSE table)	(in AGPTB table)	0.04
	5000	(in DENSE table)	(in AGPTB table)	.008
3	500	0.3	0.7×10^{-5}	(in DENSE table)
	1000	.3	2.0×10^{-5}	(in DENSE table)
	5000	.3	2.0×10^{-5}	(in DENSE table)

The PRØPT Table for this problem is:

Layer 1

PRØPT = .1, .25, .38, .016, .01, .007, 0,

(C_P: .1, .25, .38; K: .016, .01, .007; dK/dT control: 0)

Layer 2

.09, .04, .008, 0, 0,

(C_P: .09, .04, .008; K: 0; dK/dT control: 0)

Layer 3

.3, .7E-5, 2*2.E-5, 0,

(C_P: .3; K: .7E-5, 2*2.E-5; dK/dT control: 0)

Note that if one value is entered for a dependent table the Program automatically fills the table with the number of values in the corresponding independent table. For the above sample problem there are 3 values in the independent table (WARM). Therefore, the Program fills the layer 3 C_P table with three values (.3, .3, .3).

NPRØPT Table

This table states the number of entries in each of the PROPT sub-tables as shown in the following table:

NPRØPT Position	Description
1	Number of C_P values for layer 1 in PRØPT Table
2	Number of K values for layer 1 in PRØPT Table
3	" " dK/dT " " " " " " " "
4	" " C_P " " " 2 " " "
5	" " K " " " " " " "
6	" " dK/dT " " " " " " "
etc.	etc.

For the PRØPT table sample problem given above the corresponding NPRØPT table is:

NPRØPT = 3, 3, 1, 3, 3*1, 3, 1,

HTABL Table

This is a composite dependent table which gives the values of boundary layer gas specific heat at constant pressure, $C_{P_{BL}}$ in BTU/lb-deg.R., and the front face emissivity, ϵ_{FF}. The $C_{P_{BL}}$ and ϵ values depend on the temperatures in the WARM table.

Sample Problem

The WARM table contains 3 temperatures: 500, 1000 and 5000 degrees R. The $C_{P_{BL}}$ and ϵ_{FF} values are shown in the following table:

T deg. R.	$C_{P_{BL}}$ BTU/lb-deg.R.	ϵ_{FF}
500	0.24	0.8
1000	.24	.8
5000	.31	.8

The HTABL for this problem is:

HTABL = .24, .24, .31, .8,

NHTABL Table

This table gives the number of entries in each of the sub-tables in the HTABL table. For the preceding sample problem the NHTABL table is:

NHTABL = 3, 1,

CTABL Table

This is a composite temperature dependent table of values of $\rho C_p L$ (density x specific heat x thickness) in BTU/ft^2-deg. R. which is optionally used in cases for which there is a negligible temperature difference across a non-charring sub-layer (i.e. other than layer 1) throughout the time span of interest. The CTABL values depend on the temperatures in the WARM table.

CTABL "layers" are not counted as layers in the REKAP conduction solution. Therefore, GENRL (5) and the THIKN, DENSE, PRØPT and PTSIN tables do not include values for CTABL layers.

The first CTABL sub-table applies to a "layer" which is sandwiched between layers 1 and 2. The second CTABL sub-table applies to a "layer" between layers 2 and 3.

The CTABL may contain 10 sub-tables, each of which corresponds to a "layer" behind one of the 10 "true" layers.

If no CTABL layer is used behind layer n, enter a zero in the n^{th} CTABL sub-table.

The Program sets the temperature of a CTABL "layer" equal to the back face temperature of the immediately preceding "true" layer. Heat is stored within the CTABL "layer" according to the $\rho C_p L$ value entered in the CTABL table.

Sample Problem

A body consists of 5 layers. It is determined that there will be a negligible temperature difference across layers 2 and 5. If the CTABL solution is used layers 2 and 5 become CTABL "layers" and layers 1, 3 and 4 are "true" layers. The following sketches of temperature profile illustrate the CTABL simplification:

ACTUAL TEMPERATURE PROFILE

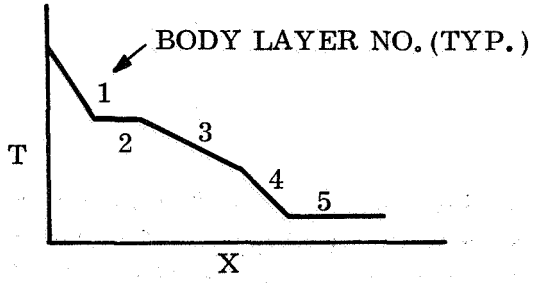

REKAP CTABL SOLUTION

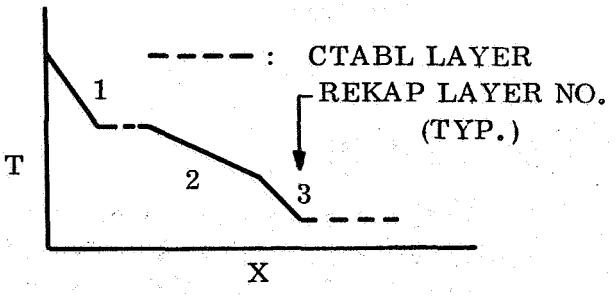

The WARM table contains 3 temperatures: 500, 1000 and 5000 degrees R. The $\rho C_p L$ values for body layers 2 and 5 are given in the following table:

Body Layer	T deg. R.	$C_p L$ BTU/ft^2-deg. R.
2	500	0.30
	1000	.35
	5000	.42
5	500	1.49
	1000	1.76
	5000	2.11

The CTABL for this problem is:

CTABL = .3, .35, .42, 0, 1.49, 1.76, 2.11,

↑ no CTABL behind REKAP layer 2

NCTABL Table

This table gives the number of entries in each of the sub-tables in the CTABL table. For the preceding sample problem the NCTABL table is:

NCTABL = 3, 1, 3,

GASPR Table

This is a composite temperature dependent table of values which is used only for cases in which at least one of the first 3 material layers chars (decreases in density with time). The GASPR table contains the values of heat of decomposition, H_{g_f} in BTU/lb, decomposition gas specific heat at constant pressure, C_{P_g} in BTU/lb-deg.R., heat of gas phase chemical reaction, H_{c_g} in BTU/lb-deg.R. and decomposition gas molecular weight, M for the first 3 layers. The fifth sub-table for each layer is un-used and must contain a zero. For a non-charring layer enter a zero for all the GASPR properties. The GASPR table values depend on the temperatures in the WARM table.

The GASPR sub-tables must be in the following order:

H_{g_f}, C_{P_g}, H_{c_g}, M and 0 (unused) for layer 1,
" " " " " " " " " 2 and
" " " " " " " " " 3.

Sample Problem

A body is composed of 4 layers. Only layers 2 and 3 char. There are 3 values in the WARM table: 500, 1000 and 5000 degrees R. The GASPR properties are given in the following table:

Layer	T deg.R.	H_{g_f} BTU/lb	C_{P_g} BTU/lb.deg.R.	H_{c_g} BTU/lb-deg.R.	M
2	500	300	0.24	0	30
	1000	300	.25	0	30
	5000	300	.25	0	30
3	500	400	0.4	100	20
	1000	350	.5	100	20
	5000	350	.6	100	20

The GASPR table for this problem is:

Layer 1 Layer 2 Layer 3

GASPR = 5*0, 300, .24, .25, .35, 0, 30, 0, 400, 2*350, .4, .5, .6, 100, 20, 0,

(H_{g_f} C_{P_g} H_{c_g} M) (H_{g_f} C_{P_g} H_{c_g} M)

unused location unused location

NGASPR Table

This table gives the number of entries in each of the sub-tables in the GASPR table. For the sample problem under GASPR the NGASPR table is:

Layer 1 Layer 2 Layer 3

NGASPR = 1, 1, 1, 1, 1, 1, 3, 1, 1, 1, 3, 3, 1, 1, 1,

or NGASPR = 6*1, 3, 3*1, 2*3, 3*1,

CHART1 Table

This table contains (a) char properties for the first material layer and (b) the boundary layer transition time. If the first layer does not char and TMELT $\neq 2$ (see TMELT table description), the CHART1 table is not used.

CHART1 (1) = 1: First layer chars

CHART1 (2) = ρ_c, char density in lb/ft^3 for layer 1.

CHART1 (3) = η, decomposition reaction order (in equation B-2)

CHART1 (4) = Boundary layer transition time, t_t, in seconds.

CHART1 (4) sec.	Laminar Boundary Layer Time Span	Turbulent Boundary Layer Time Span
t_t	GENRL (1) $\leq t \leq t_t$	$t_t \leq t \leq$ GENRL (2)
0	- - -	GENRL(1) $\leq t \leq$ GENRL (2)
$-t_t$	$t_t \leq t \leq$ GENRL (2)	GENRL(1) $\leq t \leq t_t$

CHART1 (4) is used in two ways: (a) to determine whether equation (B-6) or (B-8) should be used in the $\dot{q}_{BLK}$ computation and (b) to determine the value of graphite sublimation energy when TMELT = 2.

CHART1 (5) = N_1 in equation (B-4) for layer 1

CHART1 (6) = C_1 in equation (B-4) for layer 1

CHART1 (7) = N_2 in equation (B-5) for layer 1

CHART1 (8) = C_2 in equation (B-5) for layer 1

Sample Problems

(1) The first layer of a multi-layered body chars. The boundary layer is turbulent throughout the time interval of interest. The char properties are as follows:

ρ_c	= 30 lb/ft^3	C_2	= 0.744
η	= 2	M_{BL}/M_{AB}	= 0.5
N_1	= 1	Pr	= 0.7
C_1	= 0.192	C_T	= 1
N_2	= 1		

The CHART1 table for this problem is:

CHART1 = 1, 30, 2, 0.1, .192, 1, .744, .5, .7, 1,

no space between T and 1

(2) A body contains no charring layers. The first layer is graphite and the graphite oxidation/sublimation surface recession option is to be used (TMELT = 2). The boundary layer is to be laminar for the entire REKAP computer run. Therefore, t_t for transition from a laminar to a turbulent boundary layer is considered to be any time greater than GENRL(2). For GENRL(2) = 30 the CHART1 table may be:

CHART1 = 3*0, 31, 7*0,

or CHART1 (4) = 31, (The Program assumes that all the other CHART1 values are zero)

CHART1 (9) = M_{BL}/M_{AB} in equation (B-6) for layer 1 degradation gases.

CHART1 (10) = Pr in equation (B-6) for layer 1 degradation gases.

CHART1 (11) = C_T in equation (B-8) for layer 1 degradation gases.

CHART2 Table

This table contains char properties for the second material layer and should be deleted if the second layer does not char.

CHART2 (1) = 1: Second layer chars.

CHART2 (2) = ρ_c, char density for layer 2

CHART2 (3) = η, decomposition reaction order for layer 2 (in equation B-2)

CHART2 (4) = 0, unused location

CHART2 (5) = N_1 in equation (B-4) for layer 2,

CHART2 (6) = C_1 in equation (B-4) for layer 2,

CHART2 (7) = N_2 in equation (B-5) for layer 2,

CHART2 (8) = C_2 in equation (B-5) for layer 2,

CHART2 (9) = M_{BL}/M_{AB} in equation (B-6) for layer 2 degradation gases.

CHART2 (10) = Pr in equation (B-6) for layer 2 degradation gases.

CHART2 (11) = C_T in equation (B-8) for layer 2 degradation gases.

CHART3 Table

This table contains char properties for the third material layer and should be deleted if the third layer does not char.

CHART3 (1) = 1: Third layer chars

CHART3 (2) = ρ_c, char density for layer 3

CHART3 (3) = η, decomposition reaction order for layer 3 (in equation B-2)

CHART3 (4) = 0, unused location

CHART3 (5) = N_1 in equation (B-4) for layer 3

CHART3 (6) = C_1 in equation (B-4) for layer 3

CHART3 (7) = N_2 in equation (B-5) for layer 3

CHART3 (8) = C_2 in equation (B-5) for layer 3

CHART3 (9) = M_{BL}/M_{AB} in equation (B-6) for layer 3 degradation gases

CHART3 (10) = Pr in equation (B-6) for layer 3 degradation gases

CHART3 (11) = C_T in equation (B-6) for layer 3 degradation gases

ZØRET and TDENS Tables

ZØRET is a composite table which contains the values of Z (pre-exponential constant in 1/sec.) and E (activation energy in BTU/lb-mole) for all the charring layers (see equations B-2 and B-3).

The format of the ZØRET table depends on which form of decomposition equation is used, equation (B-2) or (B-3).

Equation (B-2) Decomposition (density dependent Z and E)

With equation (B-2) one pair of Z and E values is used for each node at each computation time step, with the Z and E values dependent on the current density of each node. In this case the ZØRET sub-tables must be in the following order:

Z values for layer 1, E values for layer 1,

Z values for layer 2, E values for layer 2,

Z values for layer 3, E values for layer 3.

The values of density upon which Z and E depend are entered in the TDENS table. For every charring layer Z and E values must be specified at every density in the TDENS table.

TDENS Table

This is the independent table of densities (in lb/ft^3) which is used only when the ZØRET values are density dependent. This table may contain a maximum of 20 values, which must be in ascending order. The Program linearly interpolates for intermediate density values but will not extrapolate. Therefore, the largest TDENS value should be slightly larger than the highest density which could exist throughout the charring layers and the smallest TDENS value should be slightly smaller than the lowest density which could exist in any charring layer (to allow for possible computer round-off error).

Sample Problem

Layer 2 of a 5 layer body does not char. Layers 1 and 3 char according to the following density dependent values of Z and E (Equation B-2):

Layer	Density lb/ft^3	Z 1/sec	E BTU/lb mode
1	100	1000	12000
	90	900	20000
	70	800	20000
2	Does not char		-
3	75	850	20000
	50	850	27000
	40	850	40000

The maximum and minimum densities which could exist in the REKAP solution for layers 1 and 3 are 100 and 40 lb/ft^3 respectively. For this problem the TDENS table is:

TDENS = 39.9, 40, 50, 70, 75, 90, 100, 100.1,

For every charring layer Z and E values must be specified at all 8 densities in the TDENS table. Therefore, the ZØRET table for this problem is:

Layer 1 Layer 2 Layer 3

ZØRET = 4*800,825,900,2*1000,6*2.E4,2*1.2E4,0,0,850,2*4.E4,2.7E4,3*2.E4,2*1.2E4,

Z E Z E Z E

Linear interpolation was used to determine the value of Z at 75 lb/ft^3 density in the first layer.

Equation (B-3) Decomposition (Multiple Reaction)

With equation (B-3) one, two or three pairs of constant Z and E values are used for each node at each computation time step. For every charring layer the same number of Z, E pairs must be entered in the ZØRET table (if necessary use zeroes to equalize the number of Z, E pairs for all the charring layers). In this case the ZØRET sub-tables must be in the following order:

Z_1, E_1, Z_2, E_2, Z_3, E_3 for layer 1,

Z_1, E_1, Z_2, E_2, Z_3, E_3 for layer 2, and

Z_1, E_1, Z_2, E_2, Z_3, E_3 for layer 3.

Sample Problem

Layer 1 of a 4 layer body does not char. The decomposition process in layer 2 is described by Equation (B-3) according to the following Z and E values:

Layer	Z_1, Z_2, Z_3 1/sec.	E_1, E_2, E_3 BTU/lb-mole
1	Does not char	-
2	10^{-4}, 1300, 10^{6}	1200, 33500, 56040
3	83.4	25200

The ZØRET table for this problem is:

Layer 1 Layer 2 Layer 3

ZØRET = 0, .0001, 1200, 1300, 33500, 1.E6, 56040, 83.4, 25200, 4*0,

NTDENS Table

This table states the number of entries in the TDENS table. For the TDENS table used in the sample problem above under "Equation (B-2) Decomposition (density dependent Z and E)" the NTDENS table is:

NTDENS = 8,

NZØRET Table

This table states the number of entries in each of the ZØRET sub-tables. For the ZØRET table used above in the sample problem under "Equation (B-2) Decomposition (density dependent Z and E)" the NZØRET table is:

NZØRET = 8, 8, 1, 1, 1, 8, or NZØRET = 8, 8, 3*1, 8,

For the ZØRET table given above in the sample problem under "Equation (B-3) Decomposition (Multiple Reaction)" the NZØRET table is:

NZØRET = 1, 6, 6,

TMELT Table

The TMELT table entries control the surface recession model to be used.

TMELT (1) = 0: Use "no recession" model.

= 1: Use "specified char depth" model (equation B-9).

= 2: Use "graphite oxidation/sublimation" model (equation B-11).

= 3: Use "refrasil" model (equation B-15).

= 4: Not used at present.

= 5: Use "fixed ablation temperature" model (equation B-12).

TMELT (2) = Not used if TMELT (1) = 0, 1 or 2.

= β_1 in ft/sec - (deg. R.)^2 if TMELT (1) = 3 (equation B-15).

= ablation temperature in degrees R. if TMELT (1) = 5.

TMELT (3) : Not used if TMELT (1) = 0, 1, 2 or 5.

= β_2 (dimensionless) if TMELT (1) = 3 (equation B-15).

TMELT (4) : Not used if TMELT (1) = 0, 1, 2 or 5.

= β_3 in degrees R. if TMELT (1) = 3 (equation B-15).

Sample Problems

(1) The "refrasil" surface recession model is to be used. The values of β_1, β_2 and β_3 (equation B-15) are respectively equal to 0.00917 ft/sec - (deg. R.)^2, 2.0 and 1×10^5 deg. R. The TMELT table for this problem is:

TMELT = 3, .00917, 2.0, 1.E5,

(2) The surface of a body maintains an essentially constant temperature of 5000 deg. R. during recession. The REKAP "fixed ablation temperature" model is to be used. The TMELT table for this problem is:

TMELT = 5, 5000,

(3) The surface of a body recedes according to the "graphite oxidation/sublimation" model. The TMELT table is:

TMELT = 2,

HØRA Table

This is the independent table of times (in seconds) upon which the TTABL entries depend. The HØRA table may contain a maximum of 50 values, which must be in ascending order.

Sample Problem

The values in the TTABL table are specified at the following times: 0, .1, .5, 1, 10 and 50 seconds. The HØRA table for this problem is:

HØRA = 0, .1, .5, 1, 10, 50,

NHORA Table

This table states the number of entries in the HØRA table. For the HØRA table sample problem given above the NHØRA table is:

NHØRA = 6,

TTABL Table

This time dependent composite table contains the quantities which describe the body heating environment. The definitions of the entries in the TTABL depend on the values of TMELT (1), GENRL (5), and GENRL (7). The values in the TTABL depend on the times given in the HØRA table. The TTABL entries are described in the following table:

TTABL Table Entries

TMELT(1)	Surface Recession Model	TTABL(1)	TTABL(2)	TTABL(3)	TTABL(4)	TTABL(5)	TTABL(6)	TTABL(7)	TTABL(8)
0	No Recession	T_W if GENRL(5) = -1 $\dot{q}_c$ if GENRL(5) = 0 $\dot{q}_c/\Delta h$ if GENRL(5) = 1	h_R	$\dot{q}_{HGR}$	0	$\dot{q}_{BF}$ if GENRL(7) = 0* T_{BF} if GENRL(7) = 1	0	0	0
1	Specified Char Depth	T_W if GENRL(5) = -1 $\dot{q}_c$ if GENRL(5) = 0 $-\dot{q}_c/\Delta h$ if GENRL(5) = 1	h_R	$\dot{q}_{HGR}$	0	$\dot{q}_{BF}$ if GENRL(7) = 0* T_{BF} if GENRL(7) = 1	0	S_{c_m}	$\dot{S}_{c_m}$
2	Graphite Oxidation/ Sublimation	T_W if GENRL(5) = -1 $\dot{q}_c$ if GENRL(5) = 0 $\dot{q}_c/\Delta h$ if GENRL(5) = 1	h_R	$\dot{q}_{HGR}$	p_e	$\dot{q}_{BF}$ if GENRL(7) = 0* T_{BF} if GENRL(7) = 1	0	K_1	K_2
3	Refrasil	T_W if GENRL(5) = -1 $\dot{q}_c$ if GENRL(5) = 0 $\dot{q}_c/\Delta h$ if GENRL(5) = 1	h_R	$\dot{q}_{HGR}$	0	$\dot{q}_{BF}$ if GENRL(7) = 0* T_{BF} if GENRL(7) = 1	ρL	0	0
4	Not Used								
5	Fixed Ablation Temperature	T_W if GENRL(5) = -1 $\dot{q}_c$ if GENRL(5) = 0 $\dot{q}_c/\Delta h$ if GENRL(5) = 1	h_R	$\dot{q}_{HGR}$	0	$\dot{q}_{BF}$ if GENRL(7) = 0* T_{BF} if GENRL(7) = 1	ρL	Γ	0

*For back face cooling enter a positive quantity for $\dot{q}_{BF}$.

For back face heating enter a negative quantity for $\dot{q}_{BF}$.

Sample Problem

The graphite oxidation/sublimation surface recession model is to be used so that TMELT (1) = 2. The HØRA table contains 3 entries: 0, 20 and 50 seconds. The values which describe the heating environment are summarized in the following table:

Time sec.	$\dot{q}_c/\Delta h$ lb/ft^2 sec	h_R BTU/lb	$\dot{q}_{HGR}$ BTU/ft^2 sec	p_e lb/ft^2	$\dot{q}_{BF}$ BTU/ft^2 sec	K_1 BTU/lb	K_2
0	0	0	0	0	0	0	0
1	0.22	6000	0	8000	-200	0	5.9
20	0.27	6000	0	9000	-300	1000	5.9
50	0.35	7000	0	10000	-400	2000	5.9

Front face heating is specified in terms of the heat transfer coefficient $\dot{q}_c/\Delta h$. Therefore, GENRL (5) = 1. Back face heating is given as a flux, so that GENRL (7) = 1. The TTABL table for this problem is:

$\dot{q}_c/\Delta h$ $\quad$ h_R $\quad$ $\dot{q}_{HGR}$ $\quad$ p_e

TTABL = 0, .22, .27, .35, 0, 2* 6000, 7000, 0, 0, 8.E3, 9.E3, 1.E4,

$\dot{q}_{BF}$ $\quad$ K_1 $\quad$ K_2

0, -200, -300, -400, 0, 2* 0, 1.E3, 2.E3, 0, 3* 5.9,

NTTABL Table

This table gives the number of entries in each of the TTABL sub-tables. For the TTABL sample problem given above the NTTABL table is:

NTTABL = 4, 4, 1, 4, 4, 1, 4, 4,

AGPTB Table

This table is used only when one body layer is a gas gap.

AGPTB(1) = gas gap layer number

AGPTB(2) = emissivity factor F_e in equations (B-4) and (B-5)

AGPTB(3) = radiation view factor F_a in equation (B-4)

AGPTB(4) = thermal conductivity of gas in gap in BTU/sec-ft-deg. R.

Note that if an AGPTB table is used the gas gap density must be entered in the PROPT table in the normal location for C_P (the first PROPT sub-table) so that the density can be temperature dependent.

The gas gap C_P must be entered in the DENSE table. Typically, C_P is weakly dependent on temperature for a likely gas gap temperature range.

Sample Problem

Layer 3 of a 5 layer body is a gas gap. The emissivity of the back face of layer 2 is 0.8. The front face of layer 4 has a emissivity of 0.2. The radiation view factor is approximately equal to 1. The mean conductivity of the gas in the gap is 1.0×10^{-5} BTU/sec-ft-deg. R. Equation (B-5) is used to calculate F_e:

$$F_e = \frac{1}{\frac{1}{\epsilon_1} + \frac{1}{\epsilon_2} - 1} = \frac{1}{\frac{1}{0.8} + \frac{1}{0.2} - 1} = 0.190.$$

The AGPTB table for this problem is:

AGPTB = 3, .19, 1, 1.E-5,

Initial Distribution of Temperature and Density

It may be advantageous to input an initial temperature and density profile across the body. In order to use this program option it is required that GENRL(4) = 0 and that all of the following tables be included in the program input: XFØRT, NXT, TMT, NT, XFØRP, NXP, TMP, NP, XFØRDN, NXD, TMDENS, ND.

XFØRT Table

This is the independent table of distances, X (in feet) upon which the initial temperatures depend. The maximum number of XFØRT entries is 145.

For a Cartesian coordinate system X is measured from the surface of layer 1 (the surface at which surface recession occurs).

For a cylindrical or spherical coordinate system X is always measured from the center of curvature, regardless of the direction of heat flow or the location of the ablating surface. With a cylindrical or spherical coordinate system the first XFØRT entry should apply to the innermost surface (closest to the center of curvature).

The Program linearly interpolates between XFØRT values but will not extrapolate. Therefore, the last XFØRT entry should be slightly larger than the sum of all the THIKN table values plus (for cylindrical or spherical coordinates) the radius of curvature of the innermost surface.

The XFØRT entries must be in ascending order.

NXT Table

This table gives the number of entries in the XFØRT table.

TMT Table

This is the table of temperatures (in degrees R.) which depend on the distances given in the XFØRT table.

NT Table

This table states the number of entries in the TMT table.

XFØRP Table

This is the independent table of distance, X (in feet) upon which an initial pressure profile depends. In the present version of the REKAP program, in-depth pressure is not calculated. However, the XFØRP table must contain at least 2 entries: one X value less than or equal to the smallest X in the body and the other greater than the largest X in the body. X is measured in the same way as that described above under "XFØRT".

NXP Table

This table gives the number of entries in the XFØRP table.

TMP Table

This is the table of pressures (in lb/ft^2) which depend on the distances given in the XFØRP table. For the present version of the Program any number except zero may be entered in the TMP table.

NP Table

This table states the number of entries in the TMP table.

XFORDN Table

This is the independent table of distances, X (in feet) upon which the initial density profile depends. The maximum number of XFØRDN entries is 145.

X is measured in the same way as that described above under "XFØRT".

If a discontinuity in the density profile occurs at an interface between layers n and n+1, it may be necessary to use rather close node spacing for layer n+1 in order to assure that the program uses a relatively accurate density profile near the interface. Nodal spacing for all the layers is controlled by the values in the PTSIN table.

NXD Table

This table gives the number of entries in the XFØRDN table.

TMDENS Table

This is the table of densities (in lb/ft^3) which depend on the distances given in the XFØRDN table.

ND Table

This table states the number of entries in the TMDENS table.

Sample Problem

A REKAP computer run is made to determine the thermal response of a 3-layer body over a 30-second heating period. It is decided to alter the heating environment for the final 10 seconds of this period. In this case, the temperature and density profiles which exist at t = 20 seconds can be used as initial conditions for a second REKAP run which will compute the thermal response for $20 \leq t \leq 30$ seconds. A sketch of the body, tables giving the temperature and density profiles at t = 20 seconds and the proper input table values are shown below.

t = 20 sec.			t = 20 sec.		
Layer	X ft.	T deg. R.	Layer	X ft.	ρ lb/ft^3
1	.050	4750	1	.050	190
	.052	4600		.060	190
	.056	4490			
	.060	4400	2	.060	92.4
				.0624	93.1
2	.060	4400		.064	96.0
	.061	3700		.0656	98.1
	.062	3200		.0672	99.4
	.064	2600		.0696	100.3
	.067	2000		.072	100.4
	.072	1600			
			3	.072	120
3	.072	1600		.080	120
	.075	900			
	.080	600			

Layers 1 and 3 do not char. The initial distribution tables for this problem are:

XFØRT = .05, .052, .056, .060, .061, .062, .064, .067, .072, .075, .08001,

TMT = 4750, 4600, 4490, 4400, 3700, 3200, 2600, 2000, 1600, 900, 600,

NXT = 11, NT = 11,

XFØRP = .05, .09, NXP = 2, TMP = 1, NP = 1,

XFORDN = .05, .06, .06001, .0624, .064, .0656, .0672, .0696, .072, .07201, .08001,

NXD = 11, ND = 11,

TMDENS = 190, 190, 92.4, 93.1, 96, 98.1, 99.4, 100.3, 100.4, 120, 120,

Also, GENRL(4) = 0.

PTSIN Table

This table gives the number of interior nodal points for all the layers. Except for a gas gap layer every PTSIN value must be an odd number equal to or greater than 3. For a gas gap layer enter a zero in the PTSIN table. For each layer, the Program automatically assigns a front and a back face node. The total number of nodes (front face nodes and back face nodes and the sum of all of the PTSIN values) may not exceed 150.

Sample Problem

Layers 1, 2 and 4 of a four layer body are to have 11, 21 and 5 interior nodes. Layer 3 is a gas gap. The PTSIN table for this problem is:

PTSIN = 11, 21, 0, 5,

SPACE Table

This table is used to control the nodal mesh size in the first layer. If a constant mesh size is adequate, delete the SPACE table.

The entries in the SPACE table indicate the degree of squeezing of nodal points toward the front face of layer 1.

The degree of mesh squeezing at the front face is approximately proportional to the SPACE table squeezing factor entry. The nodal points are progressively farther apart toward the back face of layer 1 according to an exponential relation.

Different degrees of squeezing may be specified at the initial time, t = GENRL(1) at an intermediate time and at the final time, t = GENRL(2).

The SPACE table entries are described as follows:

SPACE(1) = 1: indicates that the SPACE table is to be used.

SPACE(2) = Squeezing factor at t = GENRL(1).

SPACE(3) = Squeezing factor at t = SPACE(5).

SPACE(4) = Squeezing factor at t = GENRL(2).

SPACE(5) = Time in seconds for squeezing factor SPACE(3) to take effect.

If constant squeezing is desired for the entire run, enter the squeezing factor in SPACE(2) and delete SPACE(3), (4) and (5).

SPACE(2) must be less than or greater than SPACE (3).

A complete discussion of the REKAP nodal squeezing is included in Section VII of "Analysis of the One-Dimensional Heat Conduction Computer Program," General Electric Company Missile and Space Division Report R66SD10, March 1966.

Sample Problem

It is estimated that for $0 < t < 10$ seconds the temperature gradient increases relatively gradually at front surface of a body. For $10 < t < 15$ seconds the gradient increases sharply after which it gradually decreases until t = 30 seconds. GENRL(1) = 0 and GENRL(2) = 30. A satisfactory SPACE table for this problem is:

SPACE = 1, 1, 5, 1,

DTIME Table

This table gives the values of computation time step (in seconds). A maximum of 10 different values of time step may be used.

DTIME(1) = Δt_1 = Computation time step for GENRL(1) < t < DTIME(2).

DTIME(2) = Cut-off time for Δt_1.

DTIME(3) = Δt_2 = Computation time step for DTIME(2) < t < DTIME(4).

DTIME(4) = Cut-off time for Δt_2.

DTIME(5) = Δt_3 = Computation time step for DTIME(4) < t < DTIME(6).

DTIME(6) = Cut-off time for Δt_3.

. .

. .

. .

DTIME(19) = Δt_{10} = Computation time step for DTIME(18) < t < DTIME(20).

DTIME(20) = Cut-off time for Δt_{10}.

Sample Problem

The computation time steps for a REKAP run are summarized in the following table:

t, sec.	0 → 0.01	0.01 → 0.1	0.1 → 1.0	1.0 → 10	10.0 → 10.1	10.1 → 30
Δt, sec.	0.001	0.01	0.1	0.2	0.01	0.5

The DTIME table for this problem is: DTIME = .001, .01, .1, 1, .2, 10, .01, 10.1, .5, 30,

ØUTTB Table

This table controls the frequency of print-out of computed results. The time interval between print-outs may have a maximum of 9 values during one computer run.

If the ØUTTB table is deleted, computed results are printed out for every computation time step.

ØUTTB(1) = Time interval (in seconds) between print-outs for GENRL(1) < t < ØUTTB(2).

ØUTTB(2) = Cut-off time for print-out interval = ØUTTB(1).

ØUTTB(3) = Time interval between print-outs for ØUTTB(2) < t < ØUTTB(4).

ØUTTB(4) = Cut-off time for print-out interval = ØUTTB(3).

ØUTTB(5) = Time interval between print-outs for ØUTTB(4) < t < ØUTTB(6).

ØUTTB(6) = Cut-off time for print-out interval = ØUTTB(5).

. .

. .

. .

ØUTTB(17) = Time interval between print-outs for ØUTTB(16) < t < ØUTTB(18).

ØUTTB(18) = Cut-off time for print-out interval = ØUTTB(17).

The values of the cut-off times must be in ascending order.

Sample Problem

The results of the REKAP run are to be printed out at every 0.1 second for the initial 5 seconds and at every 1 second thereafter. GENRL(1) = 0 and GENRL(2) = 30. The ØUTTB table for this problem is:

ØUTTB = .1, 5, 1, 30,

END Table

If a single REKAP run is made the input data must include the following table:

END = 1,

If successive ("back-to-back") runs are made this table must be deleted.

Last Physical Card

The last item in the REKAP input must be a $ in any card column except column 1.

3.2 Procedure for Successive Computer Runs

It may be necessary to make two or more computer runs which have only slightly differing input data. If desired, the input data for all of the runs can be submitted simultaneously in a greatly simplified form.

If this procedure is used, the computer will load the program only once for the complete package of cases. This scheme saves approximately two minutes of IBM 7094 time for each additional case.

3.2.1 Preparation of Input Data Deck for Successive Runs

1. Assemble the input data deck as usual for Case #1 except delete the END = 1 card.

2. Insert a Hollerith alphanumeric identification card for Case #2 immediately behind the Case #1 $ card.

3. Insert a $REKAP card ($ in card column 2) immediately behind the Case #2 Hollerith identification card.

4. Immediately following the $REKAP card insert the Case #2 input data which differs from the Case #1 input data.*

5. If Case #2 is the final case include an END = 1 card in the Case #2 input data. If Case #2 is not the final case, delete the END = 1 card.

6. Place a $ at the end of the Case #2 input data. If Case #2 is the final case, the $ is the last item required in the input data deck.

7. If Case #2 is not the final case, the Case #2 $ card must be followed by a Hollerith identification card for Case #3.

8. The Case #3 identification card must be immediately followed by a $REKAP card ($ in card column 2).

Etc.

*If an initial distribution of temperature and density is used for successive cases, all of the initial distribution tables (XFØRT, NXT, TMT, NT, XFØRP, NXP, TMP, NP, XFØRDN, NXD, TMDENS and ND) must be included for every initial distribution case, whether or not the distribution of T and ρ is identical for successive cases.

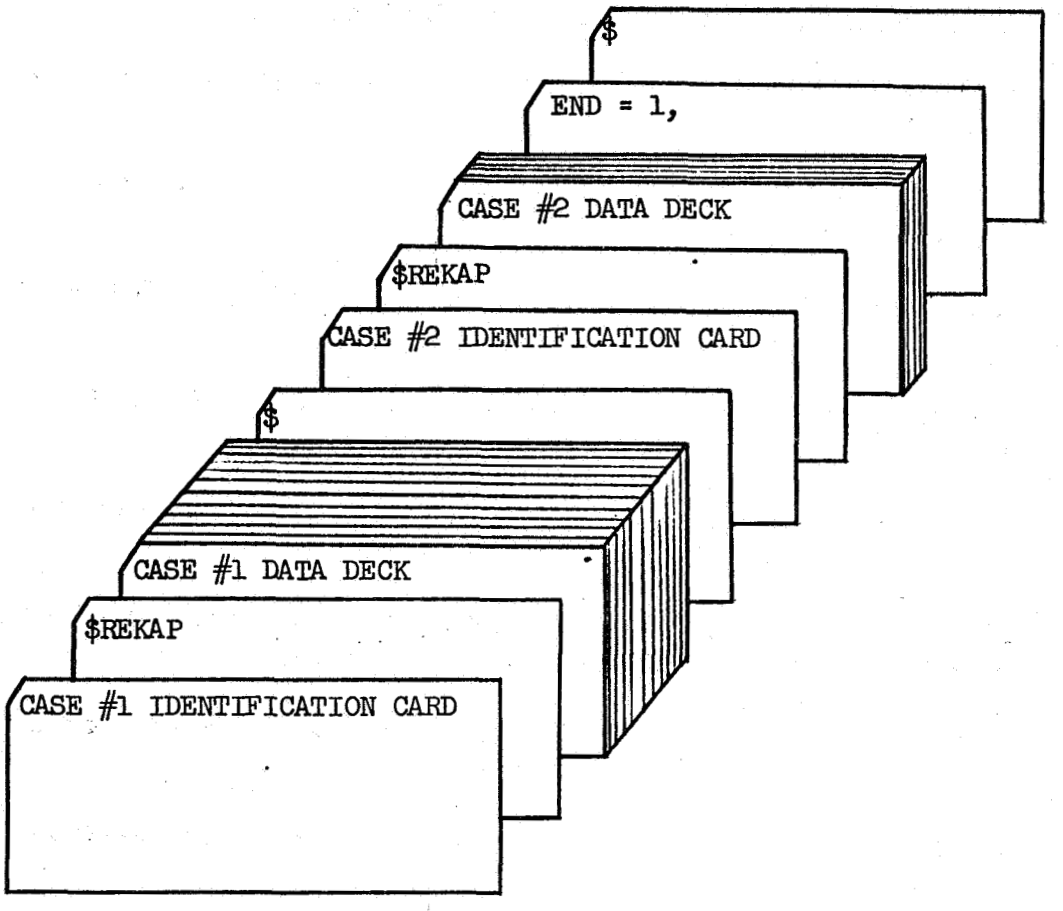

Figure 1-B. Schematic of Input Data Deck for Two Successive Cases

4.0 NOMENCLATURE

C_1	Constant used in expression for density dependent K
C_2	Constant used in expression for density dependent C_P
C_P	Specific heat, BTU/lb-deg. R.
C_T	Constant used in turbulent blocking-equation (Appendix A)
E	Activation energy, BTU/lb
F_a	Radiation view factor across gas gap
F_e	Emissivity factor used in equation for radiation across gas gap
F_{12}	Fraction of layer 2 degradation gases which flow into layer 1
F_{23}	Fraction of layer 3 degradation gases which flow into layer 2
H_{c_g}	Heat of gas phase chemical reaction, BTU/lb
H_{g_f}	Heat of decomposition, BTU/lb
H_r	Recovery enthalpy, BTU/lb
ierfc	Integral of the complementary error function
K	Thermal conductivity, BTU/sec ft^2deg. R./ft
K_1	Quantity used in the graphite diffusion regime mass loss equation, BTU/lb
K_2	Dimensionless quantity used in the graphite diffusion regime mass loss equation
L	Latent heat of fusion or vaporization, BTU/lb
M	Molecular weight, lb/lb-mole
$\dot{m}_g$	Gas mass flux, lb/sec-ft^2
N_1	Constant used in expression for density dependent K
N_2	Constant used in expression for density dependent C_P
P_e	Boundary layer edge pressure, lb/ft^2
Pr	Prandtl number

$\dot{q}_c$	Convective heating rate, BTU/sec-ft^2
R	Universal gas constant, BTU/lb mole-deg. R.
$\dot{S}_c$	Rate of charring, ft/sec
$\dot{S}_m$	Rate of surface recession, ft/sec
T	Temperature, deg. R.
t	Time, sec.
X	Distance from front face, ft.
Z	Pre-exponential factor in equation (2)
Δh	Boundary layer recovery enthalpy minus wall enthalpy, BTU/lb
Δt	Computation time step, sec.
β_1	Constant used in refrasil recession model ft/sec-(deg. R.^{2})
β_2	Dimensionless constant used in refrasil recession model
$\beta 3$	Constant used in refrasil recession model, deg. R.
Γ	Dimensionless constant used in fixed ablation temperature recession model
ϵ	Emissivity
η	Order of thermal degradation reaction
ρ	Density, lb/ft^3
φ_o	Dimensionless ratio used in "blocking" calculation

SUBSCRIPTS

AB	Ablative material
AMB	Ambient
BF	Back face
BL	Boundary layer
BLK	Blocking
c	Char
FF	Front face
g	Gas
HGR	Hot gas radiation
LN	Last node, i.e. node nearest back face
M, V	Melting or vaporization
MECH	Mechanical
RR	Re-radiated
SURF.	Surface
T	Total
VP	Virgin (un-degraded) material
W	Wall
1	First layer, i.e. layer adjacent to front face
2	Second layer
3	Third layer

DISTRIBUTION LIST
EXTERNAL

National Aeronautics and Space Administration
Lewis Research Center
21000 Brookpark Road
Cleveland, Ohio 44135
Attention: Contracting Officer, MS 500-313 (1)
Liquid Rocket Technology Branch, MS 500-209 (8)
Technical Report Control Office, MS 5-5 (1)
Technology Utilization Office, MS 3-16 (1)
AFSC Liaison Office, MS 4-1 (2)
Library (2)
Office of Reliability & Quality Assurance, MS 500-203 (1)
E.W. Conrad, MS 100-1 (1)

National Aeronautics and Space Administration
Washington, D.C. 20546
Attention: Code MT (1)
RPX (2)
RPL (2)
SV (1)

Scientific and Technical Information Facility
P.O. Box 33
College Park, Maryland 20740
Attention: NASA Representative
Code CRT (6)

National Aeronautics and Space Administration
Ames Research Center
Moffett Field, California 94035
Attention: Library (1)

Jet Propulsion Laboratory
4800 Oak Grove Drive
Pasadena, California 91103
Attention: Library (1)
Robert G. Nagler (1)

National Aeronautics and Space Administration
Flight Research Center
P.O. Box 273
Edwards, California 93523
Attention: Library (1)

National Aeronautics and Space Administration
Goddard Space Flight Center
Greenbelt, Maryland 20771
Attention: Library (1)

National Aeronautics and Space Administration
John F. Kennedy Space Center
Cocoa Beach, Florida 32931
Attention: Library (1)

National Aeronautics and Space Administration
Langley Research Center
Langley Station
Hampton, Virginia 23365
Attention: Library (1)

National Aeronautics and Space Administration
Manned Spacecraft Center
Houston, Texas 77001
Attention: Library (1)
Donald Curry (1)

National Aeronautics and Space Administration
George C. Marshall Space Flight Center
Huntsville, Alabama 35812
Attention: Library (1)
Keith Chandler, R-P & VE-PA (1)

Office of the Director of Defense
Research & Engineering
Washington, D.C. 20301

Attention: Dr. H.W. Schulz,
Office of Asst. Dir.
(Chem. Technology) (1)

Defense Documentation Center
Cameron Station
Alexandria, Virginia 22314 (1)

Arnold Engineering Development Center
Air Force Systems Command
Tullahoma, Tennessee 37389

Attention: AEOIM (1)

Advanced Research Projects Agency
Washington, D.C. 20525

Attention: D.E. Mock (1)

Aeronautical Systems Division
Air Force Systems Command
Wright-Patterson Air Force Base,
Dayton, Ohio

Attention: D.L. Schmidt,
Code ASRCNC-2 (1)

Air Force Missile Test Center
Patrick Air Force Base, Florida

Attention: L.J. Ullian (1)

Air Force Systems (SCLT/
Capt. S.W. Bowen) (1)
Andrews Air Force Base
Washington, D.C. 20332

Air Force Rocket Propulsion
Laboratory (RPR)
Edwards, California 93523 (RPREE) (1)
(Capt. Clyde McLaughlin) (1)

Air Force Rocket
Propulsion Laboratory (RPM) (1)
Edwards, California 93523 (1)

Air Force FTC (FTAT-2)
Edwards Air Force Base, California 93523

Attention: Col. J.M. Silk (1)

Air Force Office of Scientific Research
Washington, D.C. 20333

Attention: SREP, Dr. J.F. Masi (1)

Office of Research Analyses (OAR)
Holloman Air Force Base, New Mexico 88330

Attention: RRRT (1)
Maj. R.E. Brocken,
Code MDGRT (1)

U.S. Air Force
Washington 25, D.C.

Attention: Col. C.K. Stambaugh,
Code AFRST (1)

Commanding Officer
U.S. Army Research Office (Durham)
Box CM, Duke Station
Durham, North Carolina 27706 (1)

U.S. Army Missile Command
Redstone Scientific Information Center
Redstone Arsenal, Alabama 35808

Attention: Chief, Document Section (1)
Dr. W. Wharton (1)

Bureau of Naval Weapons
Department of the Navy
Washington, D.C.

Attention: J. Kay, Code
RTMS-41 (1)

Commander
U.S. Naval Missile Center
Point Mugu, California 93041

Attention: Technical Library (1)

Commander
U.S. Naval Ordnance Test Station
China Lake, California 93557
Attention: Code 45 (1)
Code 753 (1)
W.F. Thorm, Code 4562 (1)

Commanding Officer
Office of Naval Research
1030 E. Green Street
Pasadena, California 91101 (1)

Director (Code 6180)
U.S. Naval Research Laboratory
Washington, D.C. 20390

Attention: H.W. Carhart (1)

Picatinny Arsenal
Dover, New Jersey

Attention: I. Forsten, Chief (1)
Liquid Propulsion
Laboratory

Air Force Aero Propulsion Laboratory
Research & Technology Division
Air Force Systems Command
United States Air Force
Wright-Patterson AFB, Ohio 45433

Attention: APRP (C.M. Donaldson) (1)

Aerojet-General Corporation
P.O. Box 296
Azusa, California 91703

Attention: Librarian (1)

Aerojet-General Corporation
11711 South Woodruff Avenue
Downey, California 90241

Attention: F.M. West,
Chief Librarian (1)

Aerojet-General Corporation
P.O. Box 1947
Sacramento, California 95809

Attention: Technical Library
2484-2015A (1)
R.D. Glauz (1)

Aeronutronic Division of
Philco Corporation
Ford Road
Newport Beach, California 92600

Attention: Technical Information
Department (1)

Aerospace Corporation
P.O. Box 95085
Los Angeles, California 90045

Attention: W.P. Herbig (1)
Library-Documents (1)

Aerotherm Corp.
485 Clyde Ave.
Mountainview, Calif.

Attention: Roald Rindal (1)

Astropower, Inc.
Subs. of Douglas Aircraft Company
2968 Randolph Avenue
Costa Mesa, California

Attention: Dr. George Moc
Director, Research (1)

ARO, Incorporated
Arnold Engineering Development Center
Arnold AF Station, Tennessee 37389

Attention: Dr. B.H. Goethert
Chief Scientist (1)

Atlantic Research Corporation
Shirley Highway & Edsall Road
Alexandria, Virginia 22314

Attention: Security Office
for Library (1)

AVCO Corp.
Space Systems Division
Industrial Park
Lowell, Mass. 01851

Attention: Donald Crowley (1)

Battelle Memorial Institute
505 King Avenue
Columbus, Ohio 43201

Attention: Report Library, Room 6A (1)

Bell Aerosystems, Inc.
Box 1
Buffalo, New York 14205

Attention: W. M. Smith (1)

Fiberite Corp.
512 W. Third Street
Winona, Minn. 55987

Attention: D. Schmanski (1)

Lockheed Missiles & Space Company
P. O. Box 504
Sunnyvale, California

Attention: Technical Information Center (1)

The Boeing Company
Aero Space Division
P. O. Box 3707
Seattle, Washington 98124

Attention: Ruth E. Peerenboom (1190) (1)

Chemical Propulsion Information Agency (1)
Applied Physics Laboratory
8621 Georgia Avenue
Silver Spring, Maryland 20910

Chrysler Corporation
Missile Division
Warren, Michigan

Attention: John Gates (1)

Curtiss-Wright Corporation
Wright Aeronautical Division
Woodridge, New Jersey

Attention: G. Kelley (1)

University of Denver
Denver Research Institute
P. O. Box 10127
Denver, Colorado 80210

Attention: Security Office (1)

Douglas Aircraft Company, Inc.
Santa Monica Division
3000 Ocean Park Blvd.,
Santa Monica, California 90405

Attention: J. L. Waisman (1)
R. W. Hallet (1)
G. W. Burge (1)

Fairchild Stratos Corporation
Aircraft Missiles Division
Hagerstown, Maryland

Attention: J. S. Kerr (1)

General Dynamics/Astronautics
P. O. Box 1128
San Diego, California 92112

Attention: Library & Information Services (128-00) (1)

Convair Division
General Dynamics Corporation
P. O. Box 1128
San Diego, California 92112

Attention: Mr. W. Fenning
Centaur Resident
Project Office (1)

W. R. Grace & Co.
Washington Research Center
Clarksville, Maryland 21029

Attention: R. G Rice (1)

Grumman Aircraft Engineering Corporation
Bethpage, Long Island,
New York

Attention: Joseph Gavin (1)

Hercules Inc.
Allegheny Ballistics Laboratory
P.O. Box 210
Cumberland, Maryland 21501

Attention: Library (1)

Houston Research Institute
6001 Gulf Freeway
Houston, Texas 77023

Attention: E.B. Miller (1)

IIT Research Institute
Technology Center
Chicago, Illinois 60616

Attention: C.K. Hersh,
Chemistry Division (1)

Kaman Nuclear
Garden of the Gods Road
Colorado Springs, Colorado 80907

Attention: A.P. Bridges (1)

Kidde Aero-Space Division
Walter Kidde & Company, Inc.
675 Main Street
Belleville, New Jersey

Attention: R.J. Hanville,
Director of Research
Engineering (1)

Leesona Moos Laboratories
Lake Success Park
Community Drive
Great Neck, Long Island, N.Y. 11021

Attention: M. Kaplan (1)

Lockheed-California Company
10445 Glen Oaks Blvd.,
Pacoima, California

Attention: G.D. Brewer (1)

Lockheed Propulsion Company
P.O. Box 111
Redlands, California 92374

Attention: Miss Belle Berlad,
Librarian (1)

Lockheed Missiles & Space Company
Propulsion Engineering Division (D.55-11)
1111 Lockheed Way
Sunnyvale, California 94087 (1)

Marquardt Corporation
16555 Saticoy Street
Box 2013 - South Annex
Van Nuys, California 91404

Attention: Librarian (1)
Cliff Coulbert (1)

Martin-Marietta Corporation
Ablative Heat Shield Section
Mail No. 1631
Denver, Colorado 80201

Attention: D.V. Sallis (1)

McDonnell Douglas Corporation
P.O. Box 6101
Lambert Field, Missouri

Attention: R.A. Herzmark (1)

North American Aviation, Inc.
Space & Information Systems Division
12214 Lakewood Boulevard
Downey, California 90242

Attention: Technical Information Center,
D/096-722 (AJ01) (1)

Northrop Space Laboratories
1001 East Broadway
Hawthorne, California

Attention: Dr. William Howard (1)

Purdue University
Lafayette, Indiana 47907

Attention: Technical Librarian (1)

Republic Aviation Corporation
Farmingdale, Long Island
New York

Attention: Dr. William O'Donnell (1)

Rocket Research Corporation (1)
520 South Portland Street
Seattle, Washington 98108

Rocketdyne Division of
North American Aviation, Inc.
6633 Canoga Avenue
Canoga Park, California 91304

Attention: Library, Department
596-306 (1)

Rohm and Haas Company
Redstone Arsenal Research Division
Huntsville, Alabama 35808

Attention: Librarian (1)

Space-General Corporation
777 Flower Street
Glendale, California

Attention: C.E. Roth (1)

Stanford Research Institute
333 Ravenswood Avenue
Menlo Park, California 94025

Attention: Thor Smith (1)

Thiokol Chemical Corporation
Alpha Division, Huntsville Plant
Huntsville, Alabama 35800

Attention: Technical Director (1)

Thiokol Chemical Corporation
Reaction Motors Division
Denville, New Jersey 07834

Attention: Librarian (1)

Thiokol Chemical Corporation
Redstone Division
Huntsville, Alabama

Attention: John Goodloe (1)

TRW Systems, Incorporated
1 Space Park
Redondo Beach, California 90200

Attention: STL Tech. Lib. Doc.
Acquisitions (1)

TRW, Incorporated
TAPCO Division
23555 Euclid Avenue
Cleveland, Ohio 44117

Attention: P.T. Angell (1)

United Aircraft Corporation
Corporation Library
400 Main Street
East Hartford, Connecticut 06118

Attention: Dr. David Rix (1)
Erle Martin (1)

United Aircraft Corporation
Pratt & Whitney Division
Florida Research & Development Center
P.O. Box 2691
West Palm Beach, Florida 33402

Attention: R.J. Coar (1)
Library (1)

United Aircraft Corporation
United Technology Center
P.O. Box 358
Sunnyvale, California 94088

Attention: Librarian (1)

Vought Astronautics
Box 5907
Dallas 22, Texas

Attention: Warren C. Trent (1)

DISTRIBUTION LIST
NASA CR 72488

INTERNAL

P. Cline	U1217 VFSTC
D. Florence	U1217 VFSTC
C. Dohner	U1217 VFSTC
D. Stevenson	U3041 VFSTC
V. Saffire	U3029 VFSTC
W. Daskin	U7211 VFSTC
R. Farrelly	10035 WSEC
Dr. J. Stewart	3846B Chst
F. Schultz (2)	1016 CCF #1
R. Price (2)	U1217 VFSTC
D. Garner	U1217 VFSTC
R. Ebersole	U1217 VFSTC
E. Hilbert (1)	U1226 VFSTC
P. Andrews (1)	U1226 VFSTC

ALL EXTRA COPIES TO P. CLINE U1217 VFSTC